NOTICE

The quality of this microform is heavily dependent upon the quality of the original thesis submitted for microfilming. Every effort has been made to ensure the highest quality of reproduction possible.

If pages are missing, contact the university which granted the degree.

Some pages may have indistinct print especially if the original pages were typed with a poor typewriter ribbon or if the university sent us an inferior photocopy.

Reproduction in full or in part of this microform is governed by the Canadian Copyright Act, R.S.C. 1970, c. C-30, and subsequent amendments.

AVIS

La qualité de cette microforme dépend grandement de la qualité de la thèse soumise au microfilmage. Nous avons tout fait pour assurer une qualité supérieure de reproduction.

S'il manque des pages, veuillez communiquer avec l'université qui a conféré le grade.

La qualité d'impression de certaines pages peut laisser à désirer, surtout si les pages originales ont été dactylographiées à l'aide d'un ruban usé ou si l'université nous a fait parvenir une photocopie de qualité inférieure.

La reproduction, même partielle, de cette microforme est soumise à la Loi canadienne sur le droit d'auteur, SRC 1970, c. C-30, et ses amendements subséquents.

An Investigation of the Behaviour of Gold in Grinding Circuits

Samad Banisi

A thesis submitted to the Faculty of Graduate Studies and research in partial fulfillment of the requirements for the degree of Master of Engineering

Department of Mining and Metallurgical Engineering

McGill University

Montreal, Canada

ISBN 0-315-67537-3

IN THE NAME OF GOD

THE COMPASSIONATE, THE MERCIFUL

Abstract

A 7.6 cm (3") Knelson concentrator was used to estimate free gold content in samples extracted from industrial grinding and gravity circuits. Its recovery was comparable with that of amalgamation and the Mozley Laboratory Separator (MLS). It was then used for a study on gold grinding and classification behaviour.

Laboratory studies of monosized gold and silica showed that gold produces fewer fines upon grinding: 75% of the mass reports to the next Tyler class, as opposed to 45% for silica. Disappearance from the monosized class (840-1200 μm) follows first order kinetics for both minerals. However, the rate constant of gold was five to six times lower than that of silica, and folding predominated over actual breakage. Folding yields either spherical or cylindrical particles which flatten upon additional impacting.

Smearing of gold onto silica and embedding of silica into gold flakes were observed. It was postulated that gold smearing can lead to metallurgical losses in flotation circuits. A gravity circuit could then increase overall gold recovery.

The Knelson concentrator was used to study the behaviour of gold in the Hemlo mill grinding circuit. The ratio of the selection function of ore to gold increased from 6 at 50-100 μm to 20 at 500-1000 μm. In the primary cyclones, gold's cut size was much finer than the ore, 20 vs. 57 μm.

Résumé

Nous avons utilisé un concentrateur Knelson de 7.6 cm (3") pour estimer la concentration en or libre d'échantillons extraits de circuits industriels de broyage et de concentration gravimétrique. La récupération du Knelson était semblable à celle obtenue par amalgamation ou par séparateur de laboratoire Mozley. Nous avons par la suite utilisé le Knelson pour étudier le comportement de l'or au broyage et à la classification.

En laboratoire, l'or produit moins de fines que la silice lorsqu'on le broie: 75 % du poids qui disparaît de 840-1200 μm se retrouve ainsi dans le 600-840 μm, comparé à 45% pour la silice. Pour les deux minéraux, le broyage suit une cinétique de premier ordre, mais la constante cinétique de la silice est de cinq à six fois plus élevée que celle de l'or, qui a tendance à se plier plus qu'à se briser. Les flocons d'or pliés deviennent soit des sphères, soit des cylindres, qui eux-même s'écrasent lorsque broyés.

Nous avons observé qu'une partie de l'or se gommait à la surface des particules de silice et que des grains de silice s'étaient incrustés dans des particules d'or. Nous postulons que le gommage de l'or à la surface d'autres minéraux plus durs explique en grande partie pourquoi les circuits de récupération d'or par gravité peuvent augmenter la récupération globale de l'or, surtout lorsqu'ils précèdent un circuit de flottation.

Dans le circuit de broyage des Mines Hemlo, le rapport de la fonction de sélection du minerai sur celle de l'or passe de 6 pour le 50-100 μm jusqu'à 20 pour le 500-100 μm. La classification primaire produit un taille de classification (D_{50}) de 57 μm pour le minerai, mais de 20 μm pour l'or. La cinétique de broyage moins élevée et la taille de coupure plus fine d'or contribuent à lui donner une charge circulante élevée, 8600%, comparé à 270% pour le minerai.

Acknowledgements

I would like to thank Professor A.R. Laplante for his interest, encouragement and thoughtful advice throughout this project. Special thanks are given to Professor J.A. Finch for his informative lectures.

I wish to express my appreciation to my friends D. Lin, Y. Shu and M. Leroux for many helpful discussions as well as all of my colleagues in the McGill mineral processing group.

I am grateful to the Ministry of Culture and Higher Education of the Islamic Republic of Iran for providing me a fellowship.

I also wish to thank Hemlo Gold Mines for access to their plant and technical support, Les Mines Camchib Inc. for providing the gold flakes, and Le Centre de Recherches Minérales du Québec for performing amalgamation tests. Financial support from the Natural Science and Engineering Research Council of Canada is also acknowledged.

Last but not least, my sincere and heartfelt thanks to my wife for her patience and understanding.

Table of Contents

List of Figures

List of Tables

Chapter 1

Introduction

1.1 General Introduction

Gravity concentration of gold has been used since antiquity [Adamson, 1972]. Its importance, however, has decreased since the turn of the century, when the cyanide process was developed. This is not entirely true for the small gold projects in Latin America, Southeast Asia and to a lesser extent in North America for which cyanidation may not be the choice of initial process [Bradford, 1987].

Dorr and Bosqui (1950) emphasize the importance of the removal of gold from

the grinding circuit and advocate gravity concentration, especially for those ores in which a significant proportion of the gold is associated with base metal sulphides. An investigation of Witwaterstands ores in South Africa suggested that the use of gravity concentration ahead of cyanidation can improve overall gold recovery by 0.5 per cent [Douglas, 1961]. This results from reducing soluble losses and gold adsorption on gangue minerals, and recovering large or slow-leaching gold particles that would otherwise be incompletely leached [Loveday, 1982]. Brittan and Van Vuuren (1973) were able to show that the overall recovery of gold was correlated with the recovery of gold by gravity concentration. However, their study did not demonstrate the causality link between the two; it is in fact more likely that the correlation stems from a common cause -- i.e. an increase in coarse gold content yields an increase in both gravity and overall recovery [Splaine, 1982]. The recent introduction of the carbon-in-pulp (CIP) process at some mines has greatly decreased soluble losses (virtually all the gold that is in solution is adsorbed onto the granules of activated carbon) and hence has removed part of the motivation for gravity concentration. However, the removal of some of the gold by gravity could reduce the number of CIP stages and the lock-up of gold in the CIP plant. The recovery of larger slow-leaching gold grains remains a potential benefit of gravity concentration [Loveday, 1982]. In the last few years, gold gravity recovery has been re-evaluated due to the availability of new gravity concentrators and its comparatively small impact on the environment,

compared to cyanidation.

Different gravity systems are used to recover gold in grinding circuits. In South Africa, the endless-belt and the Johnson drum concentrators have been extensively utilized to recover coarse gold [Bath, 1973]. Douglas and Moir (1961) pointed out that 75% of the major plants incorporated gravity concentration followed by cyanidation of the bulk ore. In these plants, up to 73% of gold was recovered by gravity concentration when gold was relatively coarse. Jigs have never gained wide acceptance in the South African gold industry, probably due to the large bulk of concentrate. In North America, they are often used [Hinds, 1989]. The new Canadian centrifugal concentrators, the Knelson and the Falcon, are being operated in some plants in Canada and the United States [Knelson, 1990; McAlister, 1989]. Other gravity devices such as spirals, cones and sluiceboxes are also being used in different plants [Mclean, 1975; Ferree, 1984; Robinson, 1984; Poling, 1985].

Due to the diversity of recovery circuits and gold ore types, different levels of success have been reported. For example, gravity gold recovery in the Homestake mill in the United States has changed an unacceptable overall recovery to acceptable levels and in the OK Tedi project in New Guinea, a one per cent increase in the overall recovery was obtained [Hinds, 1989; Lammers, 1984]. However, eliminating the gravity circuit of Hemlo gold mine did not have any detectable effect on the overall recovery [Larsen, 1989].

Because of its malleability and density, gold accumulates in grinding circuits. This can cause losses due to overgrinding and difficulties in the estimation of the head grade or gold inventory. Gold gravity recovery can be used to alleviate these problems. Even before the economic impact of gravity recovery can be assessed, the optimum gravity circuit must be selected and its effect on metallurgical recovery must be determined. There is only limited work on the subject. Some of the basic questions to be answered are: From which stream of the grinding circuit should gold be recovered? What type of equipment should be used? How much gold is free and can be recovered by gravity? How much gold recovered by gravity would not be recovered at all otherwise and why?

To answer the above questions adequately, what is needed is a methodology to determine free and recoverable gold content. This has traditionally been obtained by amalgamation; more recently, gravity, with the Mozley Laboratory Separator (MLS), and flotation, with a laboratory Denver cell (0.033 m^3) have been used [Graham, 1989; Laplante et al., 1990]. In this study, the rationale for using a 7.6 cm Knelson concentrator to estimate free gold content is presented. This novel approach is first compared to other estimators of free gold content and then demonstrated with an industrial case study.

1.2 Objectives of the Study

The objectives of the study are as follows:

1- To compare the Knelson concentrator with alternative means of measuring free gold content (i.e. amalgamation and the MLS)

2- To evaluate the behaviour and morphology of gold in grinding circuits

3- To evaluate the performance of the Hemlo mill grinding circuit with the 7.6 cm (3") Knelson concentrator

1.3 Thesis Structure

Chapter two compares the efficiency of the Knelson concentrator in recovering free gold with amalgamation and the MLS. The basic principles of the Knelson and amalgamation are also discussed. Tests are performed on samples from the Meston and Hemlo mill grinding circuits.

Chapter three investigates in a laboratory mill the grinding behaviour of gold by means of breakage and selection functions and contrasts it with silica. Grinding is performed on samples of gold flake and silica in the size class 850-1200 μm. The variation of flake weight and the evolution of flake shape with decreasing flake diameter are discussed. The relationship between the malleability

of gold and its effect on grinding are described. Chapter three also discusses the implications of the embedding of silica in gold flakes and the smearing of gold onto silica on the efficiency of mineral separation systems.

The evaluation of the grinding circuit of Hemlo gold mine is presented in chapter four. It contains a sampling survey of the grinding circuit which was performed in August 1989. Gold and 'free' gold size-by-size distributions, cyclone classification efficiency and sub-sieve analysis are discussed. The selection and breakage functions of gold and silica in the plant and laboratory are also compared.

In chapter five, the general conclusions and suggestions for future work are addressed.

Chapter 2

Determining Free Gold Content

Introduction

The conventional method of assessing free or liberated gold content is amalgamation, but its use is hazardous and time consuming. Further, since the objective of such work is to assess the feasibility of gravity recovery, amalgamation may yield erroneous results. For example, very thin flakes of gold that would be refractory to gravity recovery will be readily amalgamated; gravity recovery may then over-predicted. Amalgamation can also underpredict recovery,

as gravity-recoverable gold can resist amalgamation, if its surface is coated with a contaminant or is imperfectly liberated. Another shortfall of amalgamation is that the precious metal particles are either completely or partially 'dissolved' in mercury, thus losing their original configuration. This loss of information can be significant, especially in the context of research into gold's behaviour in processing circuits.

In a recent study at McGill University, the Mozley Laboratory Separator (MLS) was used to estimate the free gold content [Liu, 1989]. This procedure consists of wet and dry screening 2-3 kg of material, and processing 75 to 150 g of each size class with the MLS, recovering four different products to generate a grade-yield curve. This approach is safe, but still time consuming and requires a large number of assays to determine recovery yield curves. Results were found not entirely reproducible. A first problem was that results were operator-dependent, as the MLS slope had to be adjusted for each sample to optimize separation. A second problem was the capacity of the MLS. A maximum mass of 150 g can be processed, which, for coarse classes, is clearly insufficient for good statistical reproducibility [Liu, 1989]. Whereas the first problem can be minimized with careful operation, the second is an inherent limitation of the MLS, and a higher throughput separator is needed.

The ability of the large Knelson concentrators (72 cm and 30 cm) to recover free gold has been reported by some investigators [Forssberg, et al., 1987;

Laplante, et al., 1990;]. This suggests that if the laboratory Knelson concentrator (7.6 cm in diameter) can match or surpass the performance of higher capacity Knelson units and recover free gold, it could be a reliable tool to evaluate free gold content in samples extracted from gravity and grinding circuits. In this chapter, the efficiency of this unit in recovering of free gold is compared with that of amalgamation and the MLS.

2.1 The 7.6 cm (3") Knelson Concentrator

2.1.1 Background

Centrifugal concentrators have been in use since the early days of mineral processing, but never extensively; recent innovations may make their use more widespread [Silva, 1986].

Basically, centrifugal concentrators can be categorized into the two types: single walled units and fluidized bed bowl units [Knelson, 1988]. Single walled or unfluidized bed units have been used only to a limited extent in small placer operations. The main advantages of these units are a reduced power consumption and lower water use. On the negative side, however, the recovery of gold can decrease as a result of the compaction of the concentrate in the riffles. Silva

(1986) argues that the availability of more efficient equipment, fluidized bed bowls, limits the widespread use of these concentrators.

2.1.2 General Characteristics

The Knelson concentrator is a centrifugal bowl-type concentrator developed by Lee Mar Industries, Inc., of Burnaby, B.C., Canada (Figure 2.1). The unit is essentially a high speed, ribbed, rotary cone with a drive unit.

The Knelson concentrator utilizes the principles of hindered settling and centrifugal force. Slurry containing 20 to 40% solids is fed through a central tube at the bottom of the unit. Centrifugal forces cause the feed to fill the ribs from bottom to top. In the 7.6 cm unit the central perforated cone rotates at 1700 rpm, generating a force of 60 G (theoretically). Heavy particles are forced out against the walls and are trapped between the ribs. Lighter particles are carried by water to the top of the unit and are ejected against the outer wall of the unit, and then evacuated through an opening at bottom of the unit. The cone is surrounded by a pressurized water jacket that forces water through the holes in the cone to keep the bed of heavy particles fluidized. The water force acts against the centrifugal force of the rotating cone. This counterforce is strong enough to inhibit severe compaction of the collected concentrate. As a result, the mineral grains remain mobile, allowing more heavier particles to penetrate into the bed either by

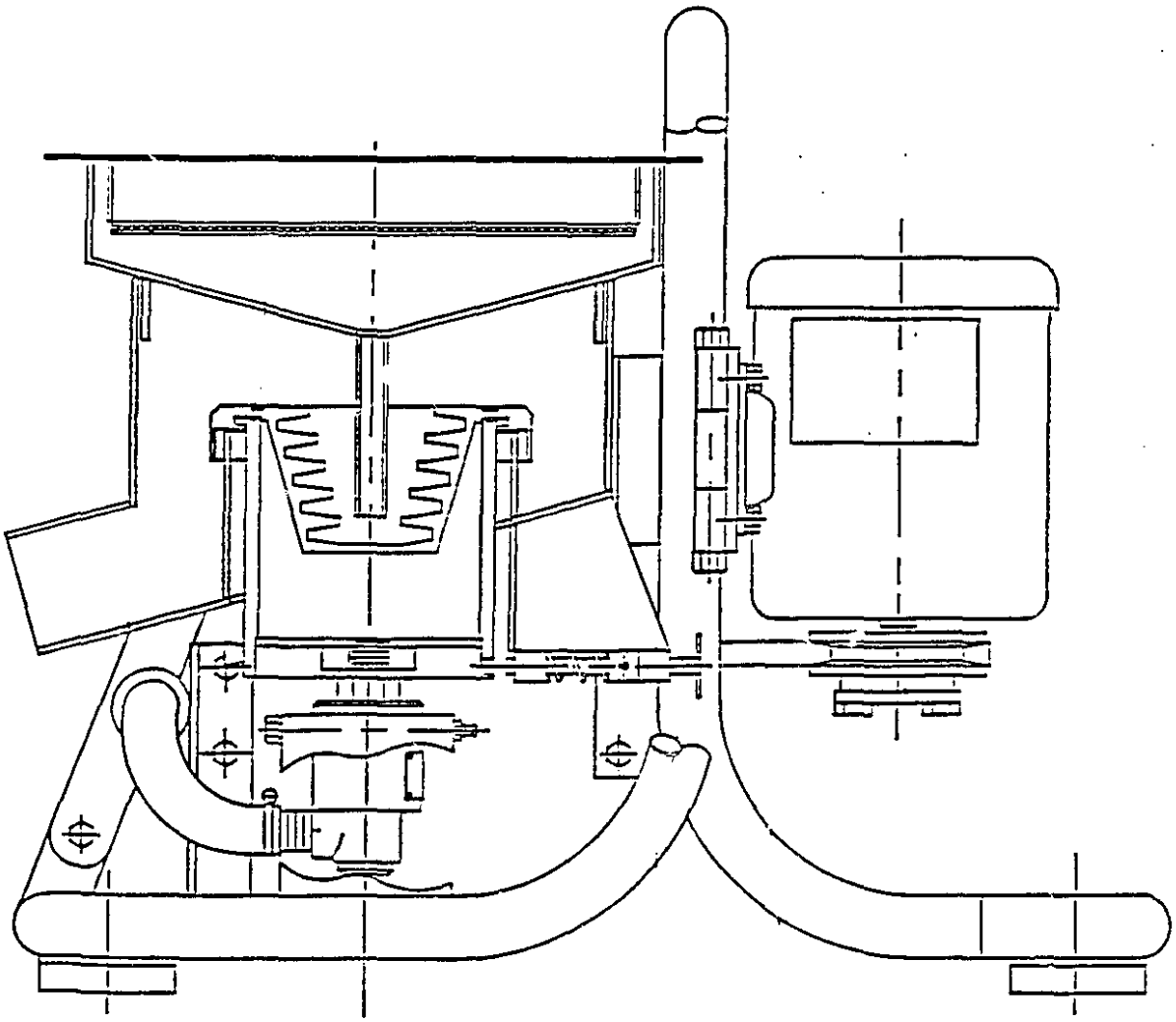

Figure 2.1: The 7.6 cm (3") Knelson concentrator.

displacement or interstitial trickling [Silva, 1986]. The addition of the water prevents the material from attaining the same speed as the cone. This produces a shear which favours the recovery of fine dense particles --i.e. the Bagnold effect. The shear is rotational and is very similar to that used by Bagnold himself to demonstrate the existence of dispersness induced by shear [Bagnold, 1954]. As processing continues, lighter particles in the mobile bed are replaced by incoming heavier ones until the heaviest particles in the feed are retained.

Removing of concentrate is accomplished by stopping the cone, opening a drain at the bottom and flushing out the concentrate. In the small units (e.g. 7.6 cm and 19 cm) it is usually done by releasing the inner bowl from the outer bowl and washing the concentrate out.

2.1.3 Bowl Design

Tangential injection of the back pressure water was chosen over straight injection due to the higher recovery of fine gold and the easy removal of the concentrate. Knelson (1990) claims that tangential injection of the back pressure water in the direction opposite to the bowl rotation increases turbulence within the rings, which results in an increase in the capture of high specific gravity particles. It is also likely that injection forms a more homogenous dispersion of back water

into the bed.

An earlier bowl design had a cylindrical shape with an increasing ring depth from top to the bottom (Fig. 2.2). This resulted in an excess volume of concentrate in the bottom rings. Consequently, it was difficult to fluidize the bed properly. The theoretical G forces in the inner face of the bottom and top rings were 47 and 59 G, respectively. This was equal to an increase of one G per 6 mm (0.25") increase in diameter, which resulted in a need for extra water to fluidize the bed. Another difficulty was the large difference in G in each ring. For example, the bottom ring changes in G from 47 to 68 G. This significantly lowered the performance of the concentrator. To solve these problems, a conical bowl was designed (Fig. 2.3).

During operation of the conical bowl with the square rings, a non-uniform concentration of material in rings was observed (Fig. 2.4). This stemmed from the fact that within each ring superficial flowrate (flowrate per unit area) increased with increasing diameter. In other words, the superficial flowrate is at a minimum at the walls, where the "hydrostatic" pressure of concentrate is highest. This caused dead or non-turbulent areas in each ring. This was overcome by designing a wedge profile for the bowl rings (Fig. 2.5), which increases wash water superficial velocity close to the wall (by decreasing the cylindrical cross-section).

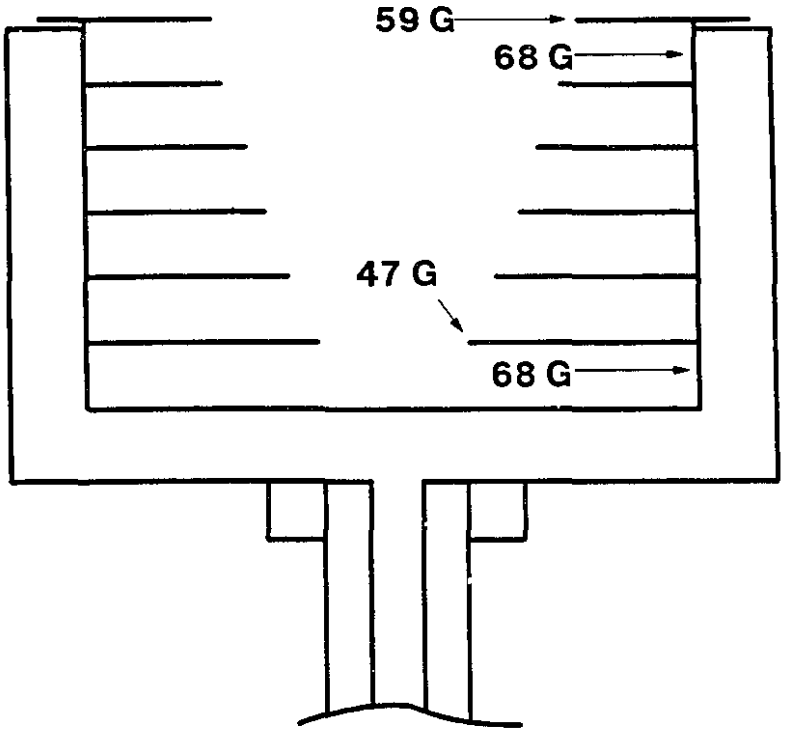

Figure 2.2: Cylindrical Knelson bowl design.
(from Knelson, 1990)

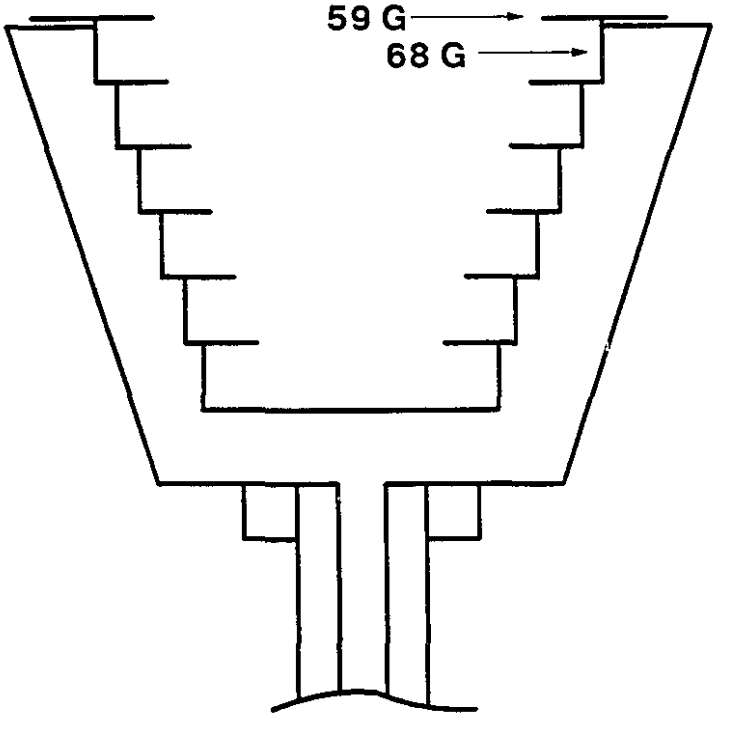

Figure 2.3: Conical Knelson bowl design.

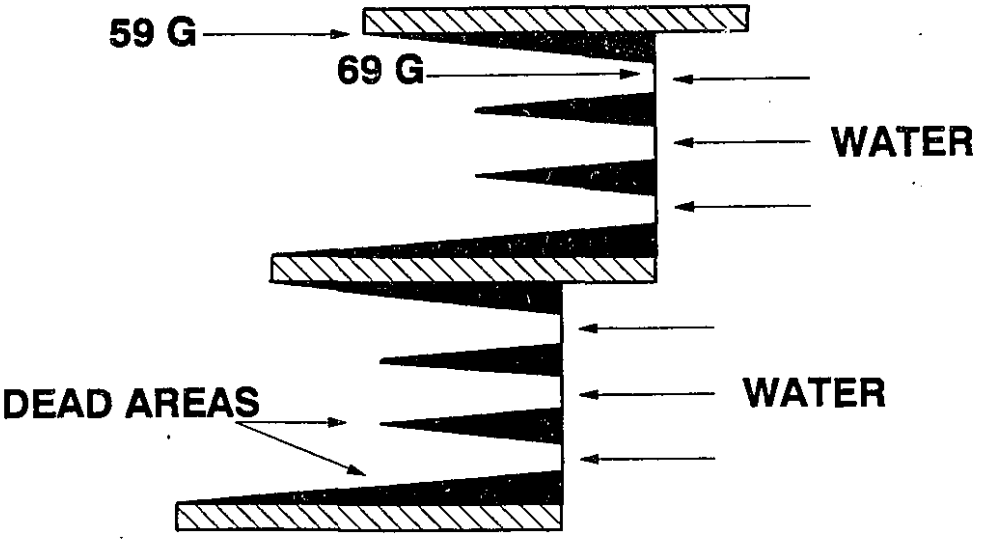

Figure 2.4: Dead areas in the non-wedge profile rings in the Knelson concentrator.

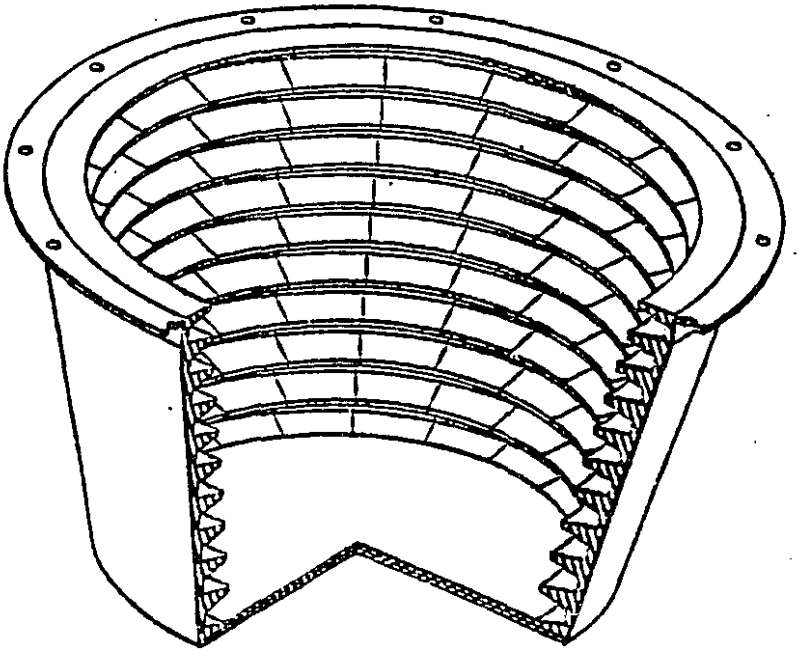

Figure 2.5: Knelson concentrator present bowl design.

2.2 Amalgamation

The use of amalgamation to entrap gold dates back to 13 B.C [Pryor, 1955]. It became important from the sixteenth century onward, and with sluicing and panning was virtually the only gold recovery process in use before the arrival of cyanidation. From 1860 to 1925 much of the world's gold was concentrated by surface contact methods [Pryor, 1965]. The collected amalgam was heated in a mercury retort to distil off the mercury. The residue, which was relatively clean bullion, was melted with a flux of silica, soda-ash and borax to remove the remaining impurities as a slag. The bullion, which contained gold, silver and possibly some copper, was then poured into bars, refined and sold. In the last century, it has been replaced by cyanidation (CIP, CIL, etc.), flotation and gravity in industrial gold recovery circuits. However, it is still practised by gold artisans.

2.2.1 Amalgamation Physics

In mineral processing, amalgamation is the process of separating gold and silver from their associated minerals by binding them into a liquid alloy with mercury. If a grain of clean metal, for example, gold, comes in contact with clean mercury, the particle becomes either entirely combined or superficially coated with

mercury according to its thickness. If two such particles come in contact with each other they are loosely cemented together. Such aggregates are called amalgams. Many metals such as zinc, tin, copper, cadmium, lead, bismuth and sodium can be amalgamated [Richards, 1940].

The wetting of gold into mercury is not alloying but a phenomenon of moderate deep sorption involving a limited degree of inter-penetration of the two elements (solid gold and liquid mercury). In all wetting phenomena, the surface tensions of the substances involved influence the nature of the reaction. Gold is readily wetted by mercury because of the higher surface tension of mercury. Density is another factor which is involved in the process. The density of mercury and gold are 13.5 and 19.6, respectively. With mercury as the separating bath, gold sinks. In fact, gravity may well be the most important factor in the process since extremely small particles of gold cannot be amalgamated.

One important condition for efficient amalgamation is that the surface of both gold and mercury must be clean. Another important condition is that the mercury must offer an adequate receiving surface to the particles of gold. If mercury is divided into minute droplets, known as floured mercury, it cannot open its surface to gold and the droplets cannot be readily reunited. A serious loss of mercury occurs when it is handled so roughly that it becomes floured.

Mercury can be contaminated or "sickened" by several substances likely to be present in a slurry. Fatty-acid oils and their salts (greases), which are caused

by oil leakages, are sources of contamination. Such oils have a low surface tension and if they make contact with the mercury they will coat its surface. This "sick" mercury no longer attempts to minimize its total surface area by gathering itself into spherical buttons but rolls sluggishly as a tear-shaped globule. The attractive force across the interface is now that of the contaminating oil and amalgamation does not result from contact of this "sick" mercury with clean gold. Another difficulty of the contamination is that an oil film attracts graphite, talc, calcium and metal sulphides which tend to form an impermeable film even if the mercury below has not been sickened. Mercury can be contaminated by sulphur and some sulphides, particularly those of antimony, arsenic and bismuth. This tendency is minimized if the pulp is alkaline [Pryor, 1955].

2.2.2 Amalgamation Practice

The amalgamation methods utilised in industry and which now have very limited laboratory applications are:

1- Plate amalgamation, in which pulp flows over a viscous film of mercury anchored to a metal plate (surface contact).

2- Presentation of pulp to a pool of mercury (immersion contact).

3- Dispersion of globules of mercury through the pulp

followed by the collection of the amalgam (grinding contact).

2.2.3 Amalgamation Laboratory Practice

Due to health hazards, amalgamation nowadays is performed differently. There are two common approaches:

1- Amalgamation of a sample and dissolution of the amalgam concentrate in nitric acid. The recoverable free gold content will be determined from fire assaying the amalgam concentrates. Usually the tailings of amalgamation is also assayed to estimate the overall gold content of the sample.

2- Amalgamation of the sample and assaying of the amalgamation tailings. The free gold content is the difference between the head grade and tailings grade.

In this study, the second approach, which is less hazardous, was used. However the results of the first approach give more information about the free gold and total gold content of the sample.

Like other processes, amalgamation can give unsatisfactory results. Poor amalgamation can be caused by [Pryor, 1955]:

1- Lack of suitable contact between gold and mercury.

2- Fine gold grains which do not come in contact with the mercury.

3- Rusty gold, including gold surrounded by a film of any foreign substance which prevents it from coming in contact with mercury.

4- Compounds of gold such as tellurides.

5- Sickened or floured mercury which is unable to attack gold properly or is so fine as to be lost in tailings and carry gold in solution.

2.3 Experimental

2.3.1 Objective

The objective will be to assess the efficiency of the 7.6 cm (3") Knelson concentrator in recovering free gold in comparison to amalgamation and the MLS.

2.3.2 Test Work Design

The grinding circuit of the Meston mill in Chibougamau, Quebec, was sampled for the test work. The samples were taken from the ball mill discharge (BMD), cyclone underflow (CUF) and cyclone overflow (COF) (Table 2.1).

Stream	BMD	CUF	COF
Weight (kg)	12.333	9.902	9.192

Table 2.1: Samples of the Meston grinding circuit.

Two samples were also taken from the primary cyclone overflow (PCOF) and the secondary cyclone overflow (SCOF) of the Hemlo grinding circuit for MLS and Knelson tests. The samples were screened at 1.7 mm (10 mesh) and the undersize was split in half. The sub-samples were fed to the 7.6 cm knelson concentrator.

The unit was operated with a feed rate of 500 g/min and back-water pressure of 31 kPa (4.5 psi). Gold size-by-size analyses were performed on the concentrates. During operation four samples of tailing were taken and assayed. In order to determine free gold losses to tails with the Knelson concentrator, the tailings of the CUF and COF were amalgamated (Table 2.2). Amalgamation was performed at the Centre de Recherche Minérales, in Québec City.

Stream	Knelson Feed (kg)	Knelson Tailings (kg)
CUF	1.303	2.449
COF	2.301	2.131

Table 2.2: Weight of the amalgamated samples of the Knelson concentrator feed and tailings.

The amalgamation tailings (mercury free) were screened and analyzed size-by-size. Due to health hazards, the amalgam concentrates were not further processed. The feed of the Knelson concentrator of the CUF and COF was also amalgamated to estimate the overall free gold content.

The sized samples of the PCOF and SCOF were processed with a MLS to compare its gold recovery with that of the 7.6 cm (3") Knelson concentrator. Tailings, middlings and concentrates of each size class were analyzed. All gold analyses were performed by fire assay.

2.3.3 Results and Discussion

Amalgamation: Table 2.3 and 2.4 show the size-by-size grade of amalgamation tailings and the grade of the tailings of the Knelson concentrator for the CUF and COF.

Size (μm)	Gold Content (g/t)	
	Amal. Tailings (Knelson Feed)	
	CUF	COF
+850	19.99	-
+600	11.82	-
+425	9.64	9.64
+300	13.37	7.47
+212	9.64	6.22
+150	12.44	6.69
+106	10.11	6.38
+75	9.02	5.91
+53	7.15	4.36
+38	4.72	4.04
-38	5.13	4.51
Total	8.16	5.16

Table 2.3: Size-by-size grade of amalgamation tailings of the Knelson feed.

No	Gold Content (g/t)	
	CUF	COF
1	7.77	-
2	8.24	4.82
3	9.17	6.22
4	8.86	4.82
Ave.	8.53	5.25
S.D.	0.63	0.81

Table 2.4: Gold content of tailings of the Knelson concentrator for the CUF and COF.

It can be seen that the gold assays of the amalgamation and the Knelson concentrator tailings are in good agreement. The overall gold content for the CUF is 8.16 g/t (amalgamation tailings) vs. 8.53 g/t (Knelson tails) and for the COF is 5.16 g/t vs. 5.25 g/t. The amalgamation tails have a slightly lower grade, which implies that more free gold was recovered with amalgamation (Table 2.5). The same trend is valid for the COF (Table 2.3). The differences are small, and indicate that both methods yield very similar results.

Feed Grade (g/t)		Recovery (%)			
		Amalgamation		Knelson	
CUF	COF	CUF	COF	CUF	COF
17.89	6.77	54.39	23.78	52.87	18.63

Table 2.5: Gold recovery by amalgamation and the Knelson.

It has been established that amalgamation and the Knelson concentrator recovery was very similar. But is the same gold being recovered? If processing the Knelson tails with amalgamation yields a significant gold recovery, then it can be concluded that both methods do not extract the same gold-bearing particles. Table 2.6 shows the size-by-size analysis of the amalgamation of the Knelson concentrator tailings for the CUF and COF.

Size (μm)	Gold Content (g/t)	
	Amalgam Tailings of Knelson Tailings	
	CUF	COF
+850	26.21	-
+600	9.95	-
+425	6.84	15.09
+300	7.15	6.84
+212	8.09	7.47
+150	7.31	7.78
+106	6.22	6.22
+75	5.91	6.53
+53	4.67	4.51
+38	3.89	3.89
-38	2.96	2.64
Total	6.36	4.35

Table 2.6: Size-by-size grade of the amalgamation rejects of the Knelson concentrator tailings for the CUF and COF.

The total grade of the amalgamation of the Knelson tailings is 6.36 g/t which is 2.17 g/t lower that of the Knelson tailings (8.53 g/t). This indicates that the Knelson concentrator has recovered some gold which was not recovered by the amalgamation, most likely locked gold. This can be attributed to the fact that in amalgamation only free and clean gold particles can be recovered.

At the Meston mill, free gold recovery or "gravity recoverability", of the BMD, CUF and COF with the Knelson concentrator are 36%, 53% and 19%, respectively (see Appendix A.1). The low recovery in the three streams stems from locking and the instability of the circuit.

Mozley Laboratory Separator: Table 2.7 and Figure 2.6 show the cumulative recovery of the PCOF and SCOF with the MLS and 7.6 cm (3") Knelson concentrator. The size-by-size recovery is shown in Appendix A.2.

Stream	Cumulative Recovery (%)			
	PCOF		SCOF	
	Knelson	MLS	Knelson	MLS
Concentrate	39.67	24.40	30.73	27.77
Middling 1	-	34.54	-	32.89
Middling 2	-	38.30	-	35.51

Table 2.7: Cumulative recovery of the PCOF and SCOF with the MLS and Knelson concentrator.

As will be shown in chapter 4, the PCOF and SCOF yielded the lowest gold recovery with the Knelson concentrator, and are the most refractory streams to

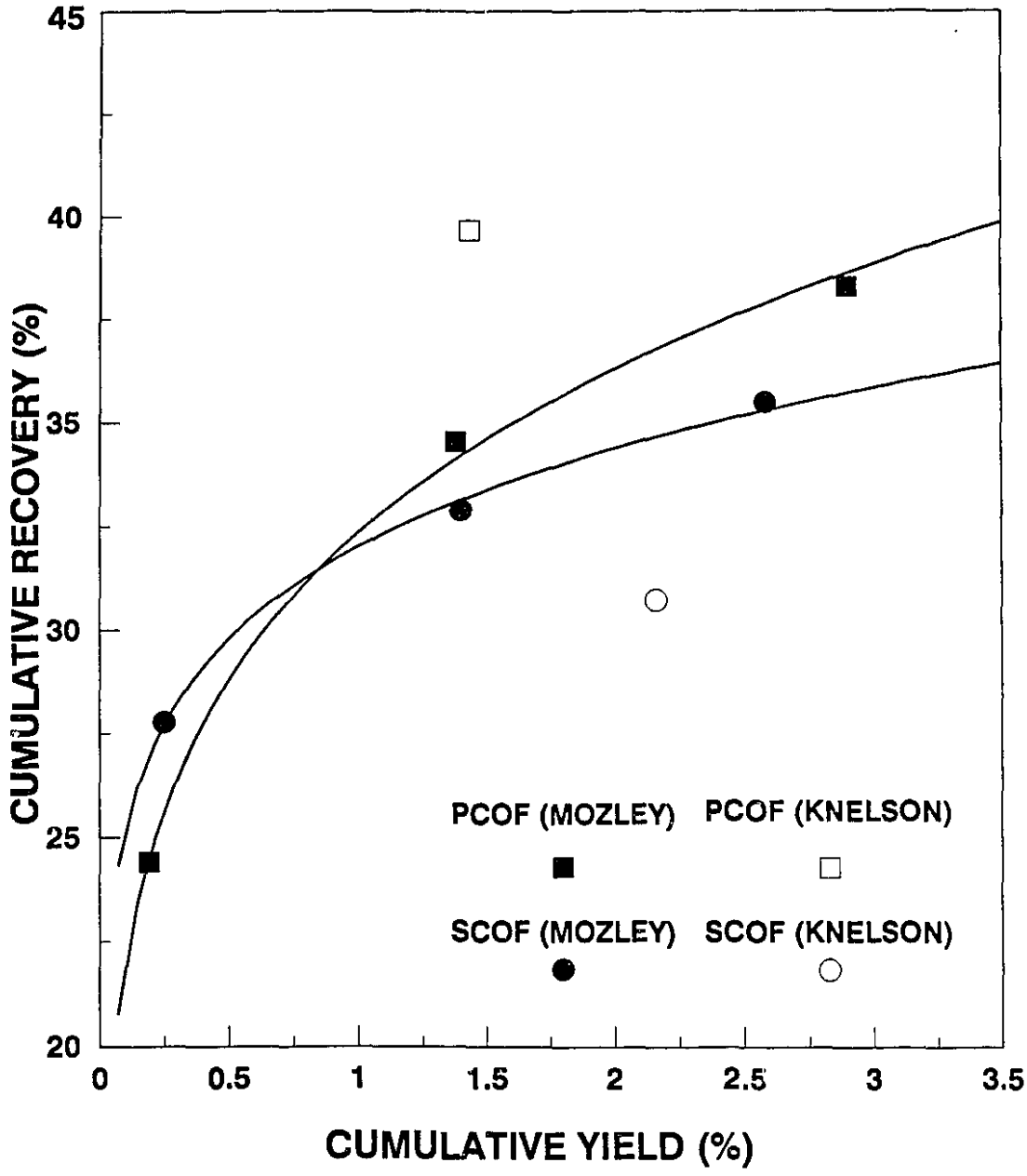

Figure 2.6: Overall gold recovery by the Mozley and the Knelson.

gravity recovery. This is due to incomplete liberation, gold particle shape, and gold's very fine size distribution (e.g. see Fig. 4.2). As the MLS is used in this case on single Tyler classes, gold particles are separated from particles of comparable size, for increased efficiency. As expected, the performance of the Knelson concentrator decreased with increasing fineness from the PCOF to the SCOF. As a result, the Mozley actually outperformed the Knelson on the SCOF, by about 5% recovery at equivalent yield.

2.3.4 Conclusions

1- Gold recovery with the 7.6 cm Knelson concentrator is comparable to amalgamation and the MLS.

2- Amalgamation recovers some gold (fine gold or very flaky) which cannot be recovered by the Knelson Concentrator. On the other hand, the Knelson concentrator can recover locked gold particles where amalgamation is not as effective.

3- The MLS (with single Tyler classes) is comparable to the Knelson concentrator for streams where the Knelson concentrator is expected to behave very poorly because gold is much finer than the ore. The Knelson concentrator would thus be expected to be superior with streams or products samples that would be tested for gravity recovery, where gold is coarse and of size similar to that of other minerals.

Chapter 3

The Grinding Behaviour and Morphology of Gold Particles

Introduction

The study of a grinding operation as a rate process has become a well-established practice [Kelsall et al., 1967, 1968, 1973a, 1973b; Hodouin et al., 1978]. It enables mineral processors to simulate the grinding process more accurately. It can dramatically facilitate control and optimization of the grinding circuits. Simulators can also predict the response of the circuit to various changes

before any actual changes are performed [Narayanan, 1987; Herbst et al., 1987, Samskog et al., 1990].

Due to its malleability, gold behaves differently than other minerals in grinding circuits. This has been frequently mentioned in the literature. For example, an investigation has been carried out on the effect of various grinding devices on the morphology of gold particles [Hallbauer et al., 1973]. Giusti (1986) has categorized fine-grained gold from gold placer deposits of Alberta based on their morphology. However, there is no available quantitative study on this phenomenon.

In this study, the grinding behaviour of gold was thoroughly investigated by using the concepts of breakage and selection functions. Furthermore, the gradual changes in the shape of gold flakes during the grinding were closely monitored.

3.1 Theoretical Considerations

3.1.1 Breakage Function

The breakage function, b_{ij}, is defined as the weight fraction of broken material upon single breakage from size class j which reports to size class i. The cumulative breakage function, B_{ij}, is the proportion of broken material which, upon single breakage from size class j, is finer than size class i [Austin et al.,

al., 1971b]. The relationship between breakage function and cumulative breakage function is defined by:

$$b_{ij} = B_{ij} - B_{i+1j} \qquad i>j$$

The breakage and selection functions represent averages over various particle shape and sizes in a size fraction. The breakage function is assumed to be environment-independent [Herbst et al., 1968; Kelly et al., 1990]; each size class has a unique breakage function, not affected by operating conditions. Laboratory data have been shown to agree with this assumption [Shoji et al., 1980].

3.1.2 Selection Function

It has been found that grinding kinetics follows first order with respect to the disappearance of material from a given size class due to breakage [Kelly et al., 1982]:

$$\frac{dM_i(t)}{dt} = -S_i(t)\, M_i(t) \tag{3.1}$$

where

$M_i(t)$: mass in size class i after a grinding time of t

$S_i(t)$: rate constant for size class i (t^{-1})

The rate constant has been described as the "selection function" by early investigators [Herbst et al., 1968]. We will retain this term, which is less awkward than the more generally accepted "rate parameter" [Gupta et al., 1985] or "specific rate of breakage" [Klimpel et al., 1984; Austin, 1976]. For the coarsest size class in a batch mill, Eq. 3.1 fully describes the rate of change in $M_i(t)$; it can be readily solved, yielding:

$$M_i(t) = M_i(0)\, e^{-S_i(t)t} \tag{3.2}$$

If the fraction of the mass remaining in size class i is plotted as a function of time on the semi-log scale, the relationship will be linear.

3.1.3 General Batch Grinding Equation

By applying the concepts of selection and breakage functions, a differential

mass balance in terms of $m_i(t)$, the mass fraction of particles in the ith size fraction at time t, yields :

$$\frac{dM_i(t)}{dt} = -S_i(t)M_i(t) + \sum_{j=1}^{i-1} b_{ij}S_j(t)M_j(t) \qquad (3.3)$$

The first term on the right hand side represents the disappearance of the material from size class i and the second term represents the appearance of material from the coarser size classes due to grinding. The discretization assumption becomes increasingly valid as the sieve ratio approaches unity. It has been shown that this assumption is valid for $x_i/x_{i+1} \leq \sqrt{2}$ [Reid, 1965]. Equation 3.3 can be written for each of n size fractions (i=1, 2, ..., n) and the resulting set of differential equations can be given as a single matrix equation :

$$\frac{d\bar{M}(t)}{dt} = -[\bar{I}-\bar{B}]\bar{S}(t)\bar{M}(t) \qquad (3.4)$$

where

$\bar{I}$: identity matrix

$\bar{S}$: selection function matrix (diagonal)

$\bar{B}$: breakage function matrix (lower triangular matrix)

$\bar{M}$: mass fraction matrix

Equation 3.4 is called the size discretized (size discrete, time continuous) batch grinding equation. It has been shown that under normal operating conditions selection functions are usually environment-independent ($S_i = S_i(t)$ for all t's) [Herbst et al., 1968; Weigao et al., 1989].

3.1.4 Normalizable and Non-normalizable Breakage Function

A breakage function is defined as normalizable when

$$b_{21} = b_{32} = b_{43} = \ldots = b_{n+1\,n}$$

$$b_{31} = b_{42} = b_{53} = \ldots = b_{n+2\,n}$$

This means that the fragment distribution is geometrically similar for all size classes. Similarly, when

$$b_{21} \neq b_{32} \neq b_{43} \neq \ldots \neq b_{n+1\,n}$$

$$b_{31} \neq b_{42} \neq b_{53} \neq \ldots \neq b_{n+2\,n}$$

the breakage function is called non-normalizable [Austin, et al., 1971a]. Non-normalizable breakage functions occur when material is brittle and/or heterogenous; however, there have been efforts to estimate non-normalizable breakage distribution parameters from batch grinding tests [Austin et al., 1971a]. In most simulations the breakage function is assumed to be normalizable. Although it appears that this assumption is not very realistic, it has been found that most simulators are not sensitive to this simplification [Laplante, 1985]. It has been shown that non-normalizable breakage functions can be replaced by equivalent normalizable breakage functions using the back calculation method [Weigao et al., 1989].

3.1.5 Breakage and Selection Functions Determination

There are several methods to estimate the breakage function [Austin et al., 1971b; Gardener et al., 1973; Gupta et al., 1980]. In this study, Herbst's and Fuerstenau's, in its original method and its modified form, was used to estimate the breakage function. The zero order production rate relationship can be described by Eq. 3.5 [Herbst et al., 1968]:

$$\frac{dY(x,t)}{dt} = F(x) \tag{3.5}$$

where

Y(x,t) : cumulative mass fraction finer than x at time t

F(x) : cumulative zero order production rate constant for size x

The use of this equation is restricted to the systems in which fine sizes are being produced at an initially constant rate [Herbst et al., 1968]. It has been found that the production rate constant, F(x), is related to particle size x [Arbiter et al., 1960]. The relationship is as follows:

$$F(x) = k_0 \left(\frac{x}{x_0}\right)^a \tag{3.6}$$

where

a : the distribution modulus of the portion of the product size distribution described by the Gaudin- Schuhmann distribution

x_0 : reference size

k_0 : constant

Equation 3.5 can be expressed discretely thus:

$$\frac{dY_i(t)}{dt} = F_i \tag{3.7}$$

The rate of change of the cumulative mass fraction finer than x_i with time can also be given by:

$$\sum_{j=1}^{n} \frac{dM_j(t)}{dt} = \sum_{j=1}^{i-1} B_{ij} S_j(t) M_j(t) \tag{3.8}$$

where B_{ij} is the cumulative breakage function. For the environment-independent selection function [$S_j = S_j(t)$], the equation will be :

$$\frac{dY_i(t)}{dt} = \sum_{j=1}^{i-1} B_{ij} S_j M_j(t) \tag{3.9}$$

Examination of Eq. 3.9 shows that the right hand side is a function of time for all sizes x_i [Herbst et al., 1968]. This implies that $B_{ij}S_j$ is only a function of i, not j. It has been suggested that the relationship between B_{ij} and S_j is as follows:

$$B_{ij} S_j = F_i \tag{3.10}$$

where j=1,i-1. Physically, this means that the specific rate of production of material finer than size i from larger size j is not dependent on j [Austin et al., 1971]. By substituting Eq. 3.10 to Eq. 3.9 we arrive with:

$$\frac{dY_i(t)}{dt} = F_i \sum_{j-1}^{i-1} M_j(t) \tag{3.11}$$

$\Sigma M_j(t)$ is the fraction of material coarser than i. For short grinding times and fine sizes it will be very close to 1. Consequently, Eq. 3.11 and Eq. 3.7 will be equal.

Arbiter and Bhrany (1960) observed that the zero order production rate constants, F_i, and particle size are related in this manner :

$$F_i = k_0 \left(\frac{x_i}{\sqrt{x_1 x_2}}\right)^{\epsilon} \tag{3.12}$$

$$i = 2,3,\ldots,n$$

For short grinding times, Eq. 3.10 can be written thus:

$$B_{il} = \frac{F_i}{S_1} \tag{3.13}$$

Epstein (1947) suggested that if the breakage function is normalizable, the following relation is valid:

$$B_{il} = \frac{k_0}{s_1}\left(\frac{x_i}{\sqrt{x_j x_{j+1}}}\right)^{\alpha} \tag{3.14}$$

In general form, equation 3.10 can be expressed as:

$$S_j = \frac{F_n}{B_{nj}} \tag{3.15}$$

Using Eq. 3.14, the selection functions relation will be equal to:

$$S_j = S_1\left(\frac{\sqrt{x_j x_{j+1}}}{\sqrt{x_1 x_2}}\right)^{\alpha} \tag{3.16}$$

It has been shown [Herbst et al., 1968] that Eq. 3.16 adequately agrees with experimental results.

Herbst's and Fuerstenau's method does not adequately describe the longer grinding times (about 5 minutes in their system) [Herbst et al., 1968]. In order to improve the validity of the method, they suggested a modified method. They stated that the cumulative mass coarser than size x_i and the cumulative material

finer than size x_i can be related through the following equation :

$$\sum_{j=1}^{i-1} M_j(t) = 1 - Y_i(t) \tag{3.17}$$

By substituting Eq. 3.17 into Eq. 3.8 it becomes :

$$\ln[1-Y_i(t)] = -B_{i1}S_1 t \tag{3.18}$$

By plotting $[1-Y_i(t)]$ on a semi-log scale vs. time, or by linear regression, the breakage function can be obtained. This method will be used here.

3.2 Experimental

3.2.1 Sample Preparation

A sample of 2200 g was taken from the oversize of the 7.6 cm (3") Knelson Concentrator at the gold room from the Camchib mill. The sample was washed with hydrochloric and nitric acids sequentially to remove the layers of sulphide mineral from the surface of the gold flakes, whilst not attacking gold itself. To

recover the gold flakes, the sample was split into 100 g subsamples and each subsample was run twice through the Mozley Laboratory Separator (MLS). The recovered flakes were examined for their malleability and appearance to make sure they were gold. By secondary acid washing remaining sulphide minerals were further removed. As tramp metal can also yield flakes upon grinding, some 'suspicious' flakes were examined with the EDS (Energy Dispersive Spectrum) analyzer, and found to be gold (see Appendix B.2).

The recovered gold flakes were screened into three size classes: 1700/850 μm, 850/600 μm and -600 μm. The breakage function test was done on the 850-1200 μm because of the high number of flakes. The total mass in 850-1200 μm size class was 4.88 g, consisting of 1240 flakes.

To compare the breakage and selection functions of gold and silica, approximately 250 g of 850-1200 μm silica was prepared by screening white silica No.10 from Indusmin Ltd (Quebec).

3.2.2 Apparatus

Grinding was performed dry in a 23 cm diameter by 20 cm long porcelain mill. The grinding medium was a 6.1 kg charge consisting of 2.4 - 2.6 cm steel balls which occupied 17% of the mill volume. A mill speed of 65 r.p.m. (74%

of the critical speed) was applied. The standard sieves of the Tyler series were used for size analysis. Screening was performed on a Rotap machine. Some gold flakes were photographed on the SEM (Scanning Electron Microscope, JEOL 840) and they were analyzed using the Tracor Northern EDS (Energy Dispersive Spectrum) analyzer.

3.2.3 Procedure

The samples were screened before grinding to determine the initial size distribution. Grinding was done incrementally for total times of 15, 30, 60, 90, 150 and 210 seconds, respectively. After each grinding increment, the samples were screened for 20 minutes and then returned to the mill for the next grinding increment.

3.3 Results and Discussion

3.3.1 Breakage and Selection Functions

Tables 3.1 and 3.2 show the size distributions of gold and silica for various grinding times. Figure 3.1 shows the same data, as mass fraction finer than size i vs. time, to illustrate that fines production follows zero order kinetics. Gold grinds more slowly than silica, despite the smaller weight (5 g vs. 50 g).

Time (s)	0	15	30	60	90	150	210
Size (μm)	Weight (%)						
+850	99.39	97.15	93.50	90.16	87.93	83.13	75.26
+600	0.61	2.04	4.47	7.38	8.38	11.93	17.53
+425	0.00	0.41	0.81	0.82	1.23	1.85	3.09
+300	0.00	0.20	0.41	0.41	0.82	1.03	1.65
-300	0.00	0.20	0.81	1.23	1.64	2.06	2.47

Table 3.1 : Gold flakes size distribution.

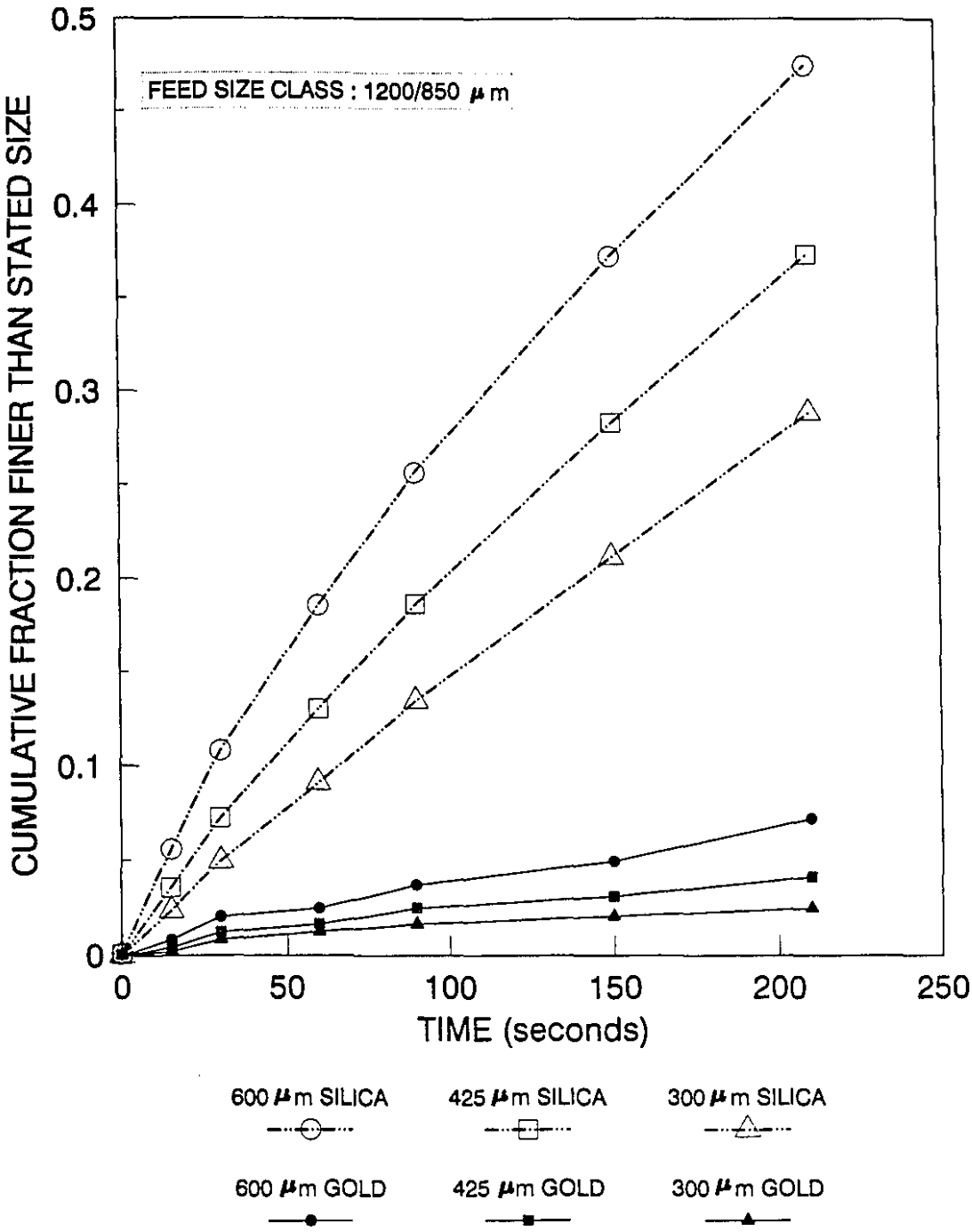

Figure 3.1: Zero order production rate plot for silica and gold.

Time (s)	0	15	30	60	90	150	210
Size (μm)	Weight (%)						
+850	99.66	87.52	78.74	67.38	58.21	44.91	34.07
+600	1.28	6.90	10.46	14.04	16.17	17.85	18.49
+425	0.02	2.02	3.56	5.56	6.98	8.93	10.11
+300	0.02	1.22	2.3	3.93	5.18	7.13	8.51
-300	0.02	2.34	4.94	9.09	13.46	21.18	28.82

Table 3.2 : Silica size distribution.

To calculate the breakage functions, the slope of each of these curves --the fines production rate constant, F_i-- was estimated and is shown in Table 3.3.

Size (μm)	F_i (mass fraction/s)	
	Gold	Silica
+600	0.0004140	0.003064
+425	0.0002815	0.002161
+300	0.0002148	0.001516

Table 3.3: Fines production rate constants of gold and silica.

To estimate the breakage and selection functions, only the linear portion of these curves (the first four points) was used. The lack of linearity is particularly

obvious for the +600 μm, both for silica and (to a lesser extent) gold. This is because the weight fraction coarser than 600 μm is much smaller than unity (a necessary condition for zero order fines production, according to Eq. 3.11) for the longer grinding times.

Another cause of deviation from zero order is the heterogeneity of the material and the presence of microfractures, which give rise to fast and slow breaking particles. This is sometimes attributed to changes in the particle strength and shape distributions that can be traced to the machine used for production of the particles [Gupta et al.,1985]. This factor does not appear dominant in this case.

The values of F_i for the coarsest size classes are inaccurate since it is difficult to establish an initial slope for these sizes [Herbst et al., 1968]. Equation 3.12 can be rearranged as follows:

$$F_i = \frac{k_0}{(\sqrt{x_1 x_2})^a}(x_i)^a \tag{3.19}$$

or

$$\log[F_i] = a \log[x_i] + \log[\frac{K_0}{(\sqrt{x_1 x_2})^a}] \tag{3.20}$$

The distribution modulus, a, is the slope of the plot of F_i vs. x_i. Using the power regression, the distribution modulus is 1.015 for silica and 0.946 for gold (Fig. 3.2). The fine production rate constant of the +850 μm size class of gold was not included in the estimation of a.

To calculate the selection function of the first size class as suggested by Eq. 3.2 mass fraction of the remaining material on the different screens is plotted vs. time (Fig. 3.3). The selection functions are 0.00628 s^{-1} and 0.00166 s^{-1} for silica and gold, respectively. The linearity of the plots verifies the fact that the grinding of gold and silica follows first order kinetics. Using Eq. 3.16, S_2, S_3, and S_4 can be calculated. For the calculation of the selection functions of the lower size classes (S_5, S_6, ..., S_{10}), a linear extrapolation of a log-log plot of S_j vs. $\sqrt{x_j x_{j+1}}$ was used (Fig. 3.4, see Appendix B.1). As anticipated from Eq. 3.16, the relationship between S_j and $\sqrt{x_j x_{j+1}}$ on a log-log scale is linear.

Austin and Luckie (Austin et al. 1971) fitted the cumulative breakage functions to:

$$B_{ij} = Q_1 R^{\gamma} + (1 - Q_1) R^{\beta} \tag{3.21}$$

where

Q_1, γ, β : parameters of the model

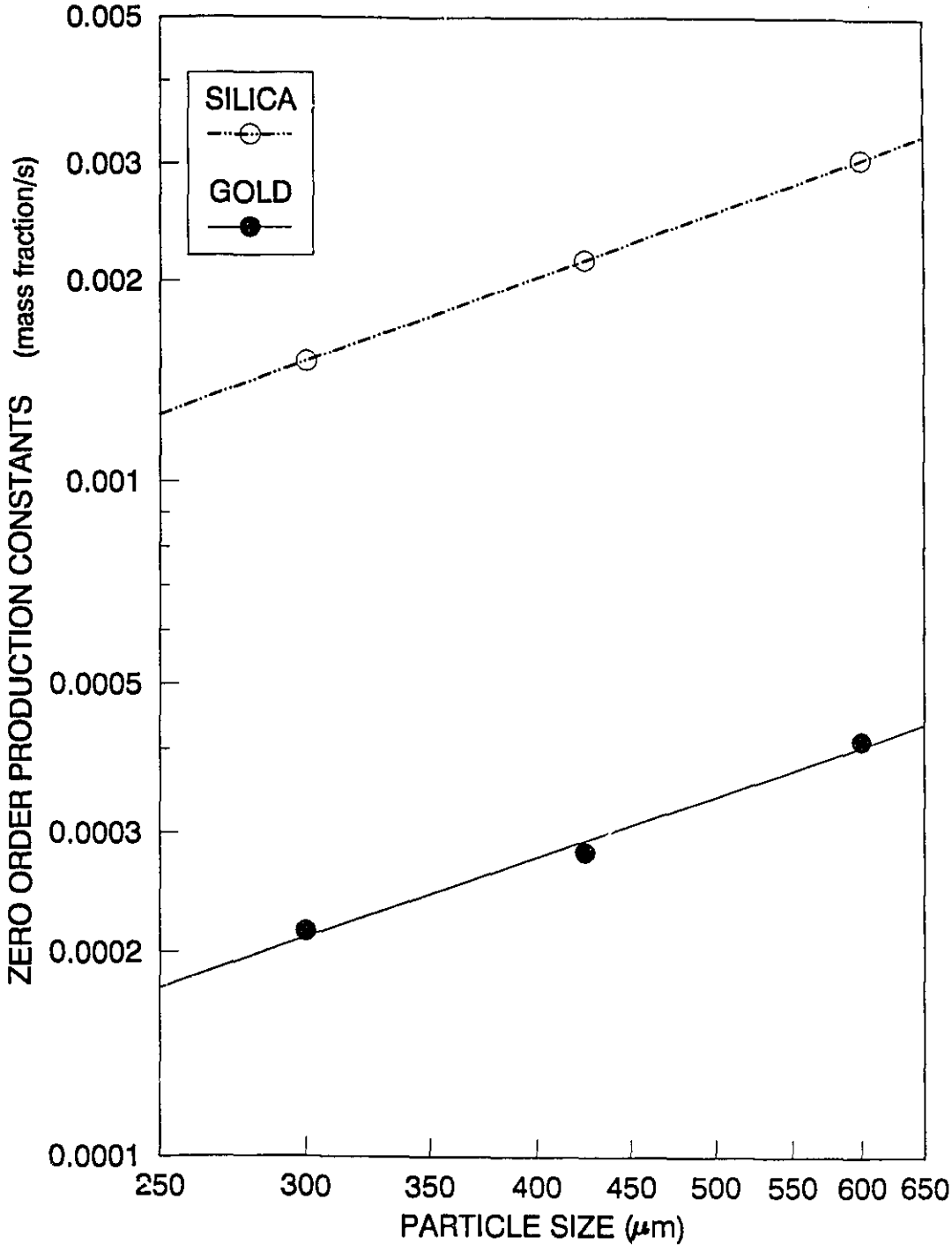

Figure 3.2: Zero order rate constant vs. size for silica and gold.

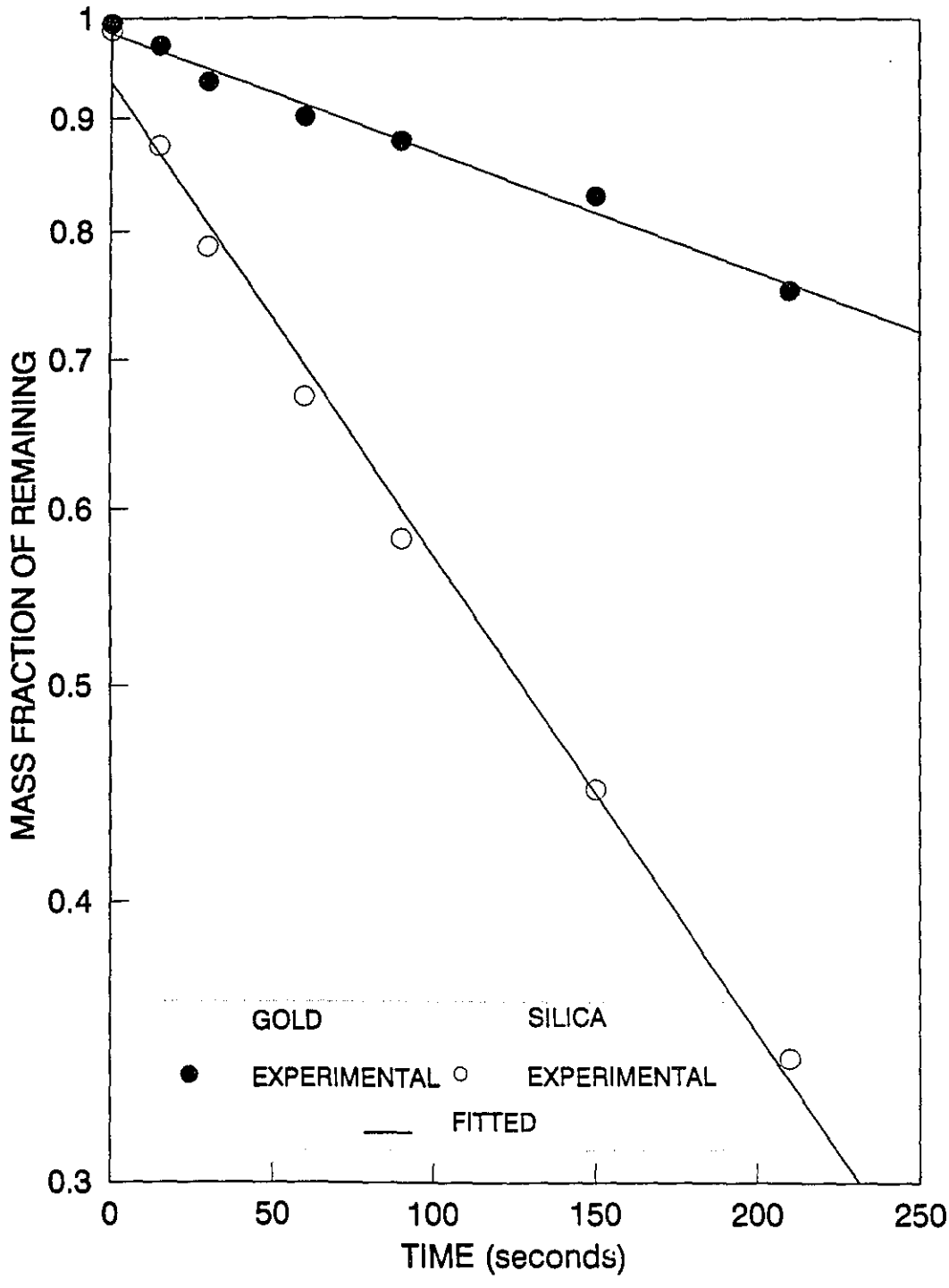

Figure 3.3: Determination of feed size selection function.

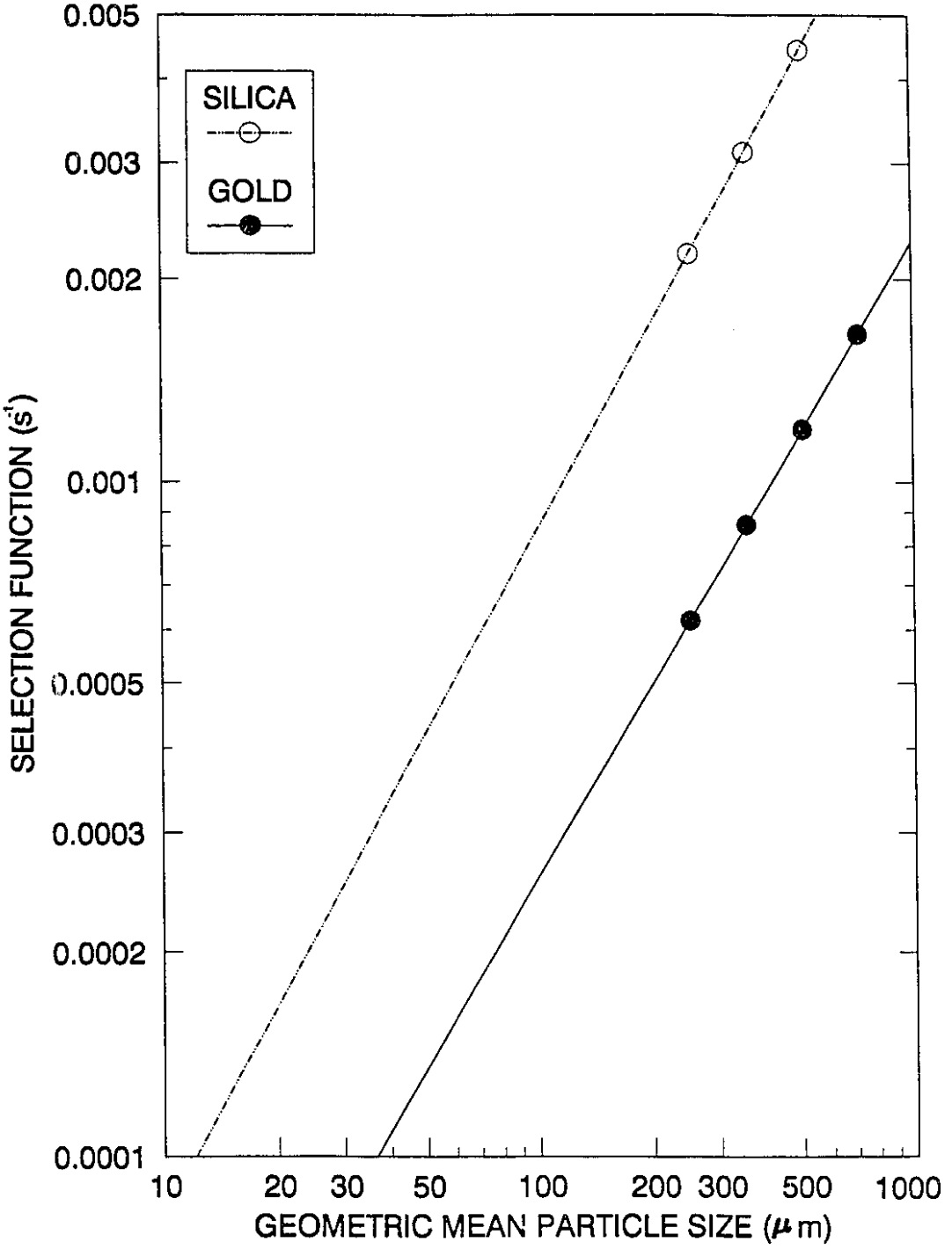

Figure 3.4: Selection function vs. size.

R: the ratio of the lower particle size limits for size class i and 1.

If ß is large, the second term of the right side of Eq. 3.21 can be neglected and it becomes:

$$B_{il} = Q_1 R^{\gamma} \tag{3.22}$$

This breakage function is then said to be 'standardizable' [Laplante, 1985]. Breakage functions of the first three size classes were calculated using Eq. 3.13. For the determination of the breakage functions of the lower size classes (B_{51}, B_{61}, ...,B_{n1}), based on Eq. 3.22, cumulative breakage function vs. particle size were plotted on a log-log scale (Fig. 3.5) by linear extrapolation, the desired breakage functions were obtained. Table 3.4 shows the results.

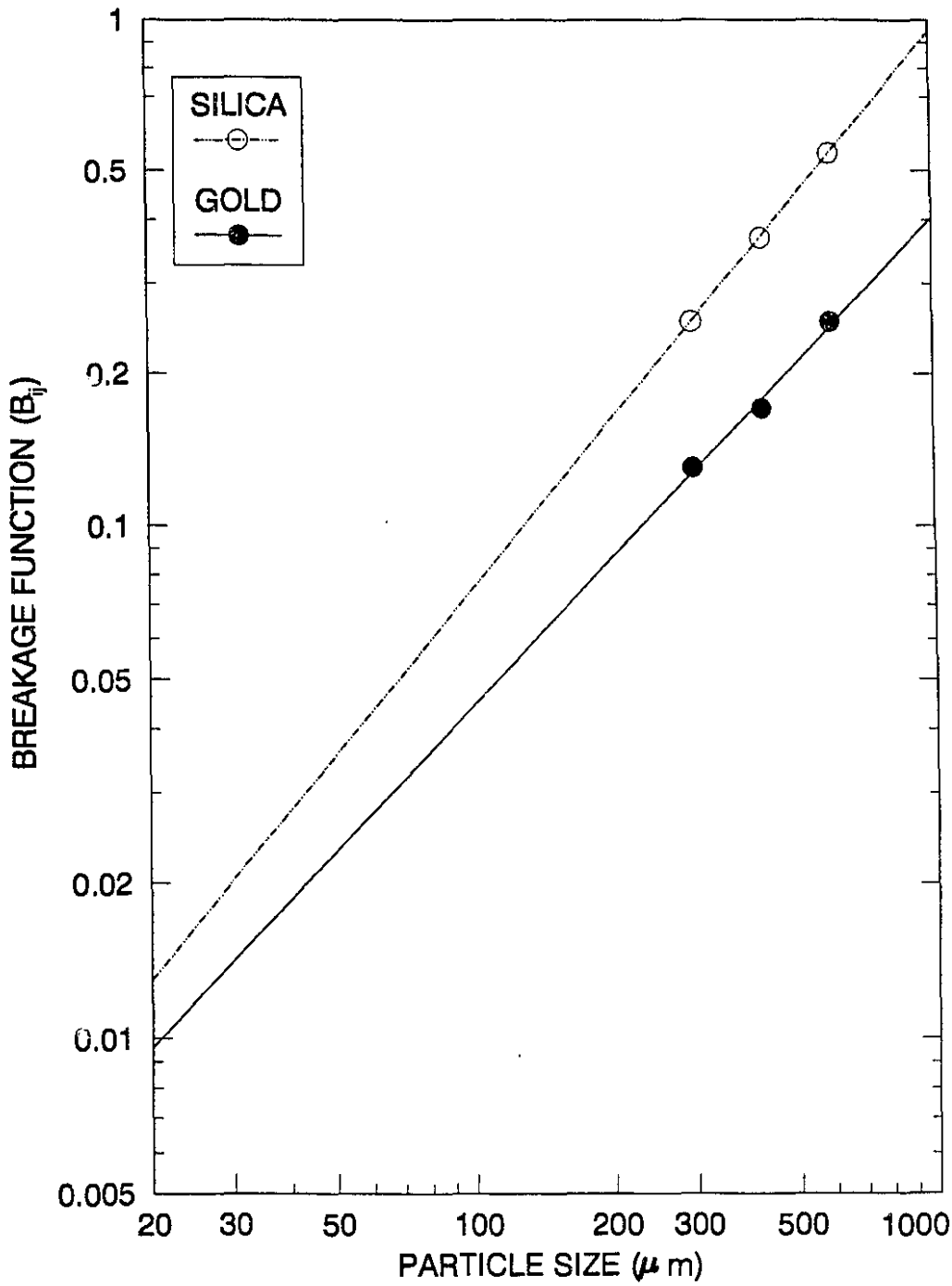

Figure 3.5: Cumulative breakage function vs. size.

Size class (μm)	Method I(B_{ij})		Method II (B_{ij})	
	Gold	Silica	Gold	Silica
+850	1	1	1	1
+600	0.2500	0.4877	0.2530	0.5420
+425	0.1700	0.3440	0.1709	0.3695
+300	0.1297	0.2413	0.1304	0.2534
+212	0.0930	0.1706	0.0935	0.1782
+150	0.0673	0.1267	0.0664	0.1283
+106	0.0477	0.0850	0.0456	0.0891
+75	0.0345	0.0600	0.0337	0.0556
+53	0.0252	0.0414	0.0260	0.0384
+38	0.0160	0.0272	0.0175	0.0270

Table 3.4: Breakage function of gold and silica using method I and method II.

It has been shown that Herbst's and Fuerstenau's method is inaccurate for the coarse size classes and underestimates the breakage functions [Herbst et al., 1968]. Equation 3.20 dictates that the slope of a plot of $[1-Y_i(t)]$ vs. time on a semi-log scale is equal to $B_{i1}.S_1$ (Fig. 3.6). The breakage functions can easily be calculated from S_1. Comparing the two methods (Table 3.4) shows for the upper size classes a significant difference between the breakage functions of silica; for gold, the difference is negligible. However, for the lower size classes, breakage functions converge for both methods. In practice, method II is commonly used in simulators [Herbst et al., 1968].

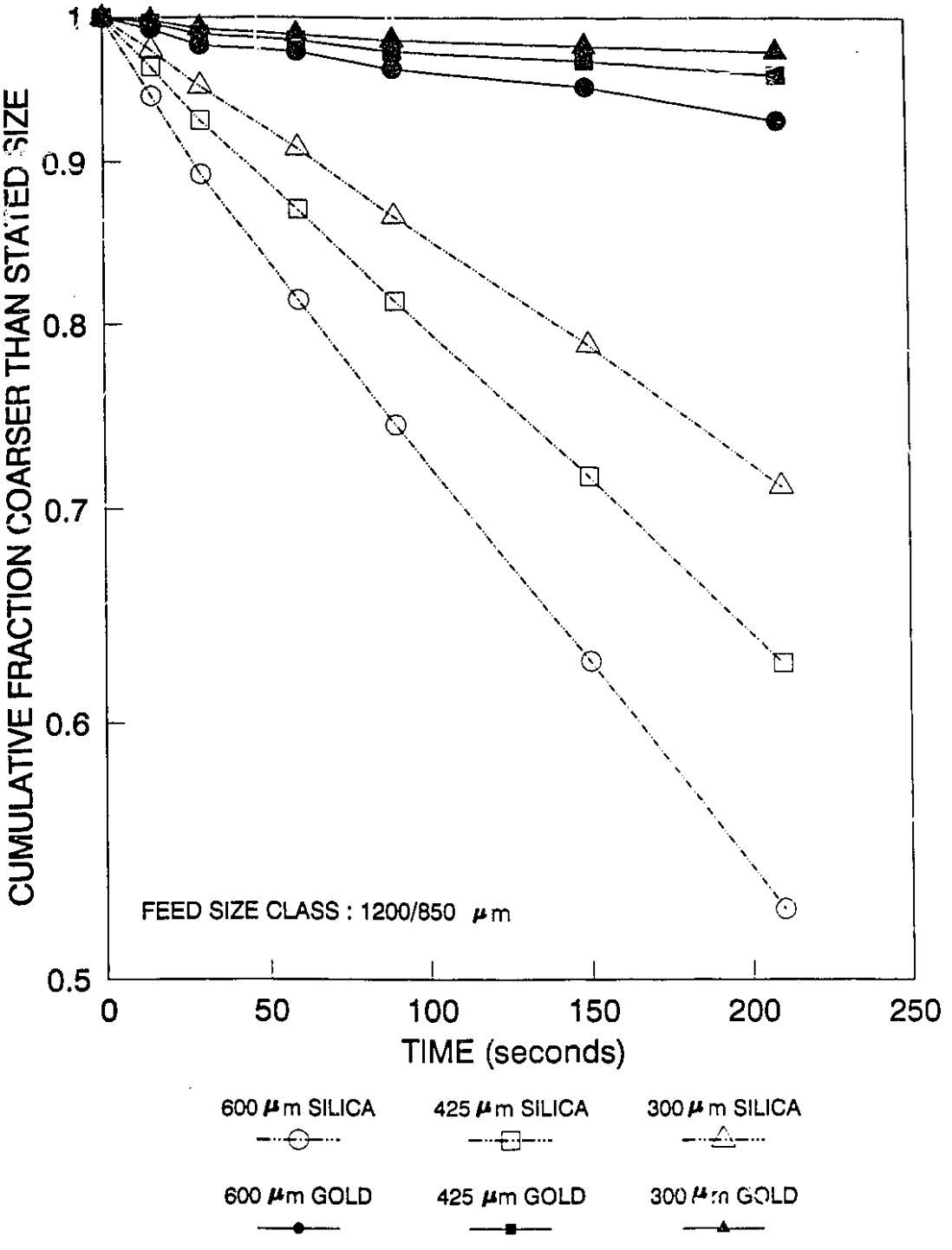

Figure 3.6: Determination of the breakage function by method II.

3.3.2 The Effect of Mass on the Selection and Breakage Functions

The breakage and selection functions of the 25 g silica sample were estimated using Herbst's and Fuerstenau's method. As expected the breakage functions for the two masses were within normal experimental error (Fig. 3.7).

By decreasing silica mass from 50 to 25 g, the selection function increased by 17% from 0.0063 to 0.0074 s^{-1}. The relationship between the mineral mass and the selection function has been formulated by a number of investigators [Gupta et al., 1974; Shoji et al., 1980; Forssberg, 1985; Weigao et al. 1989]. They have shown that by increasing the load mass selection function decreases. However, most experimental work was performed at much higher fractional volume filling than what was used here and cannot be applied to this work. Nevertheless, an upper limit for the selection function of silica at a weight of 5 g can be estimated if it is assumed that the relationship between the two variables is log-linear. This yields a selection function of 0.011 s^{-1} for 5 g of silica, slightly more than six times that of gold. It is concluded that at constant mass, the selection function of silica is between 5 to 6 times that of gold.

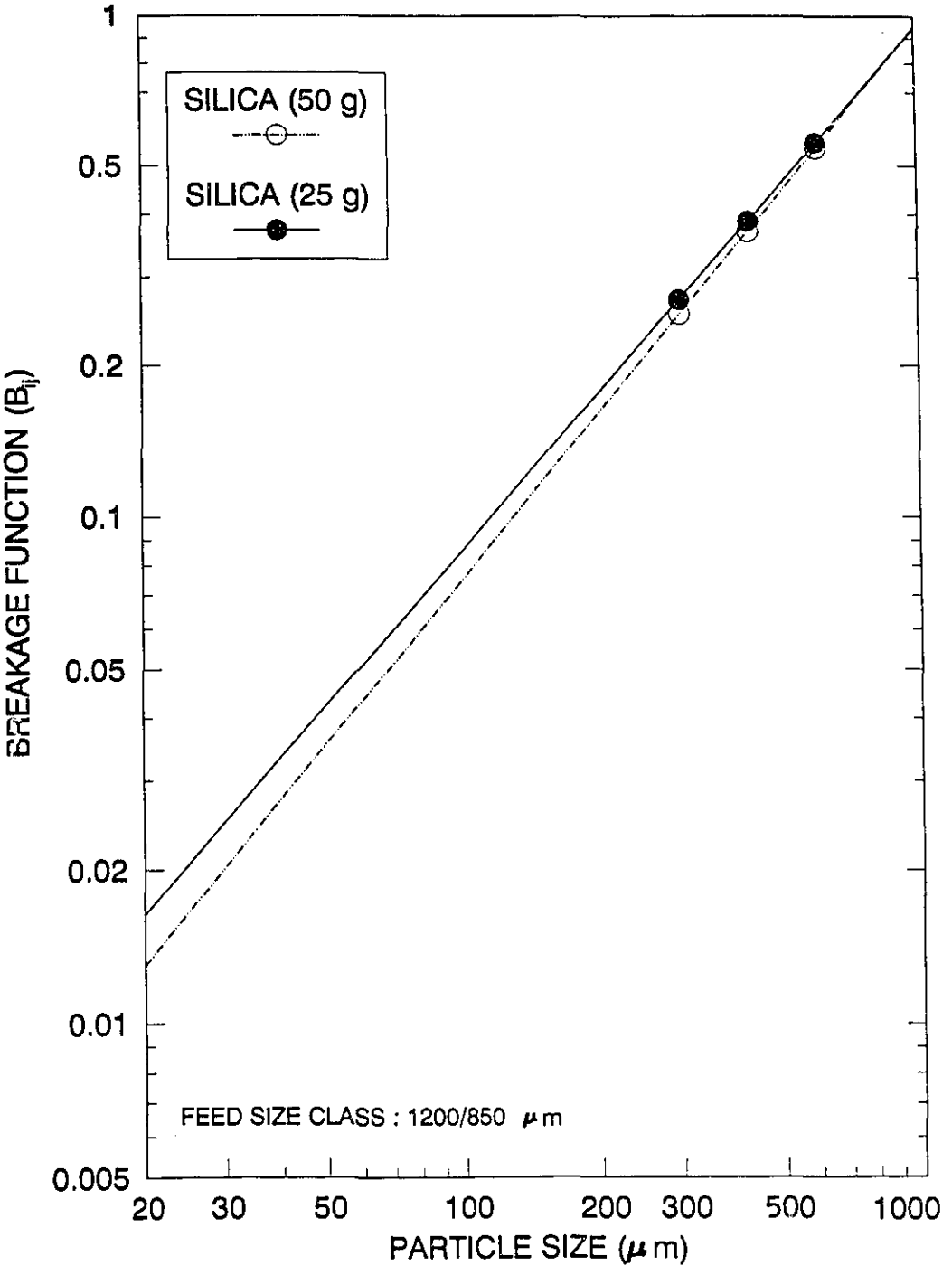

Figure 3.7: Breakage function vs. size for silica.

3.3.3 Weight Variations of Individual Gold Particles

The initial amount of gold for grinding consisted of 1240 flakes. In order to study weight variations with time and size, 52 flakes were randomly chosen and weighed before grinding. After each grinding increment, a number of flakes from the four top size classes were randomly chosen and weighed (see Appendix B.2). The mean and the standard deviation of each size class are shown in Table 3.5. It can be seen that the weight of flakes in each size class is independent of grinding time, even for the coarsest size class.

The mean weight of all size classes was averaged over time. Details are in Table 3.6. The ratio of these averages can give some clues as to the breakage mechanisms and evolution of particle shape with decreasing size. If it is assumed that the flakes are disk-shaped with a constant ratio of the major axis to the minor axis, the weight ratio can be calculated. Assuming that the flakes have the same density, the weight ratio will be equal to:

$$W_R = \frac{W_i}{W_{i+1}} \tag{3.23}$$

or

$$W_R = \frac{a^2}{b^2} = \frac{(\sqrt{2}\,b)^2}{b^2} = 2 \tag{3.24}$$

Grinding (s)	Mean (g)	Standard Deviation (g)	Degrees of Freedom
Size Class +850 μm			
0	0.0048	0.0024	51
15	0.0045	0.0024	51
30	0.0048	0.0023	51
60	0.0049	0.0025	29
90	0.0049	0.0038	20
150	0.0049	0.0020	18
210	0.0053	0.0029	67
Size Class +600 μm			
30	0.0030	0.0013	10
60	0.0032	0.0009	11
90	0.0033	0.0015	13
150	0.0031	0.0009	17
210	0.0029	0.0011	58
Size Class +425 μm			
30	0.0010	0.0005	6
90	0.0011	0.0004	11
150	0.0016	0.0007	10
210	0.0015	0.0005	63
Size Class +300 μm			
30	0.00046	0.00019	7
60	0.00047	0.00018	6
90	0.00040	0.00011	5
150	0.00063	0.00084	6
210	0.00060	0.00062	9

Table 3.5: Mean and standard deviation of weight of gold flakes.

where

W_i : Weight of flake (size class i), g

W_{i+1} : Weight of flake (size class i+1), g

a,b : Sieve size, μm

The actual ratio will be equal to 2 if thickness is constant, and 2.8 if thickness is proportional to the major axis (constant shape). If the weight ratio is less than 2, flake thickness is actually increasing with decreasing particle size. A similar comparison can be made with non-adjacent size classes, in which case the ratios would be higher. Thus, for classes once removed, the ratio becomes 8 for constant particle shape and 4 for constant thickness. For classes twice removed, the ratios are 8 and 5.7, respectively. The compilation of the possible ratios can be presented as a lower triangular matrix, similar to the breakage function. Table 3.6 compares this matrix for the constant thickness and constant geometry cases to experimental value. Experimental values lower than the constant thickness ratios indicate an increase in thickness, whereas values between the constant geometry and constant thickness cases would indicate that thickness decreases with decreasing particle diameter, but not as rapidly (particles become less flaky). Table 3.6 shows that particle thickness increases from the 850-1200 μm to the 600-850 μm, whereas from the 425-600 μm to the 300-425 μm, the ratio is equal (within experimental errors) to that which would be predicted from constant

particle shape. From the 850-1200 μm to the 300-425 μm, the ratio is significantly lower than what is predicted by constant geometry, which again suggests less "flakiness". What does it say about breakage mechanisms? Particles produced into the 600-850 μm have an average increase in thickness due to folding (as will be pictorially shown in the next section). In the finer classes, thickness does decrease, but particles become more compact.

Size Class (μm)		Weight Ratio			
		+850	+600	+425	+300
+850	M	1			
	T	1			
	N	1			
+600	M	1.6	1		
	T	2	1		
	N	2.8	1		
+425	M	3.5	2.1	1	
	T	4	2	1	
	N	8	2.8	1	
+300	M	9.4	5.7	2.7	1
	T	8	4	2	1
	N	23	8	2.8	1

M: measured T: constant thickness N: t/a constant

Table 3.6: Comparison of the weight ratios.

3.3.4 Shape Variation in Gold Flakes

The shape of most flakes as extracted from the Knelson concentrator can be categorized into the three groups:

1- Flakes which have regular, round-flattened shapes (Fig. 3.8). These are 'young' flakes because they are more likely to fold than grind. In other words, they are in the early stage of the deformation cycle.

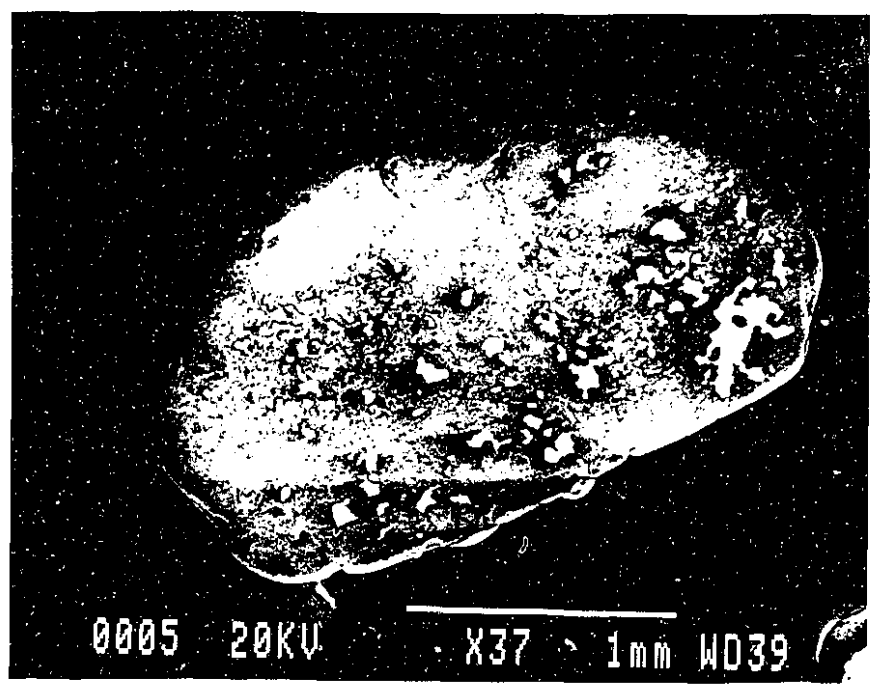

Figure 3.8: A flattened-shaped gold flake, 'young' flake (SEM photograph).

2- Flakes with irregular shapes which are not totally distorted (Fig. 3.9). These flakes can be called 'middle-aged' because the probability of folding or grinding is about the same. In fact, these are transitional flakes whose age is between the ages of the 'old' and 'young' flakes.

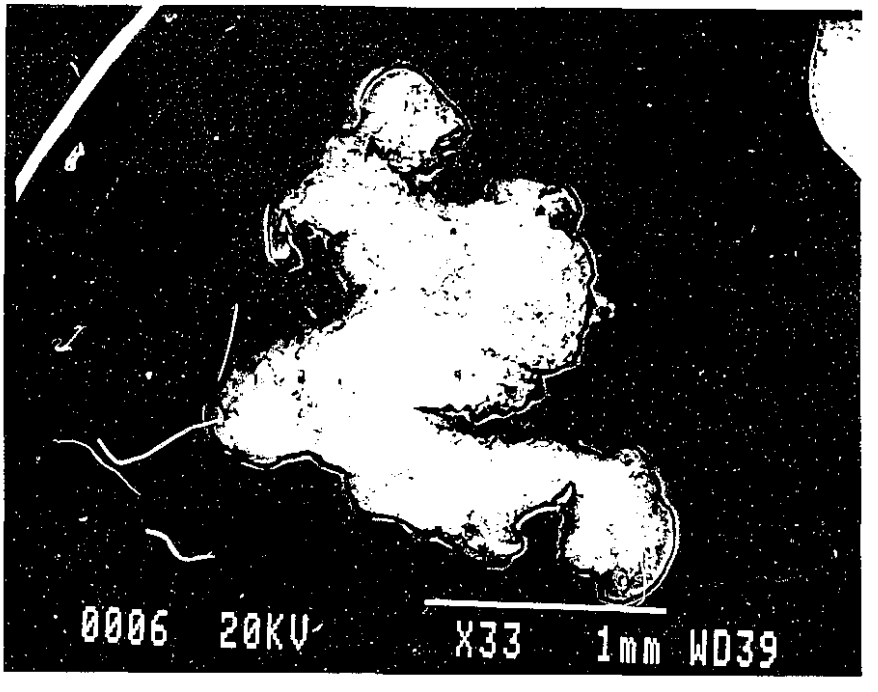

Figure 3.9: A 'middle-aged' gold flake (SEM photograph).

3- Totally distorted flakes (Fig. 3.10). These flakes are 'old' and the probability of grinding is very high.

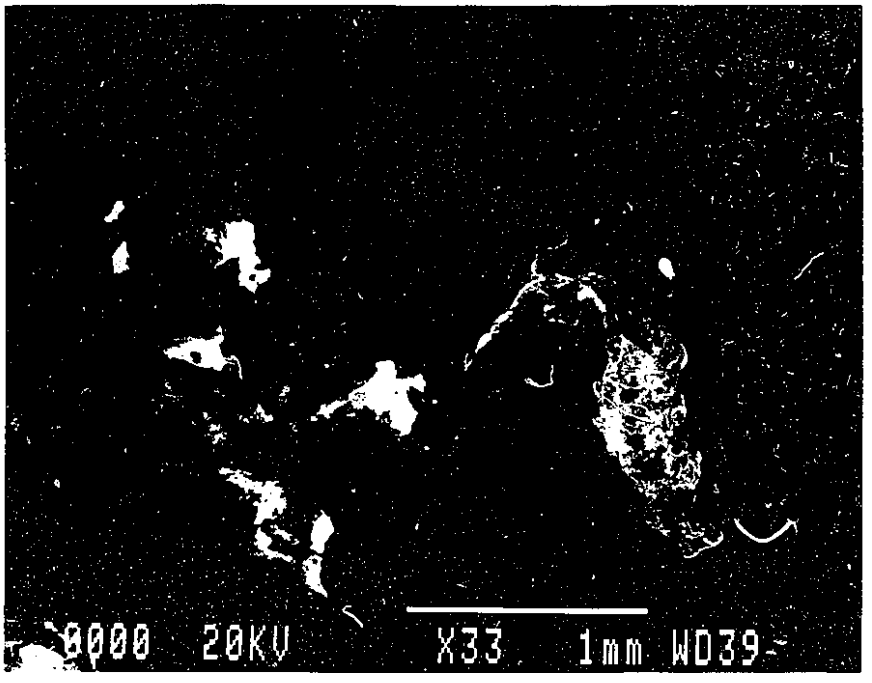

Figure 3.10: A totally distorted or irregular gold flake, 'old' flake (SEM photograph).

During grinding, after each grinding increment, the shape of flakes was closely monitored and categorized. It was observed that the three groups behaved differently. Portions of the 'old' flakes were ground, and the remaining portions started to flatten and/or fold. The 'middle-aged' flakes either folded or deformed into 'old' flakes. Some of the 'young' flakes deformed into 'middle-aged' flakes, but the majority of the flakes folded. Most of the flakes or portions of flakes that folded folded into 'young' flakes.

As mentioned in the weight variation section, the change in mean particle weight from the 850-1200 μm to the 600-850 μm class was not as high as would be expected. If thickness or the ratio of thickness to diameter were constant, the weight ratio would be 2 or greater than 2 (Table 3.6). It was observed that 90% of the particles in the size class +600 μm were folded (Fig. 3.11, 3.12, 3.13, 3.14). The shape of the folded flakes fall into two groups: rounded (spherical) and cylindrical; however, the majority of the flakes are rounded (Fig. 3.15, 3.16).

3.3.5 Embedding of Silica in Gold Flakes

The breakage function estimation tests were sequentially performed on silica (50 g), gold (5 g) and silica (25 g), respectively. It was observed that silica particles were embedded on the surface of gold flakes (Fig. 3.17). These silica

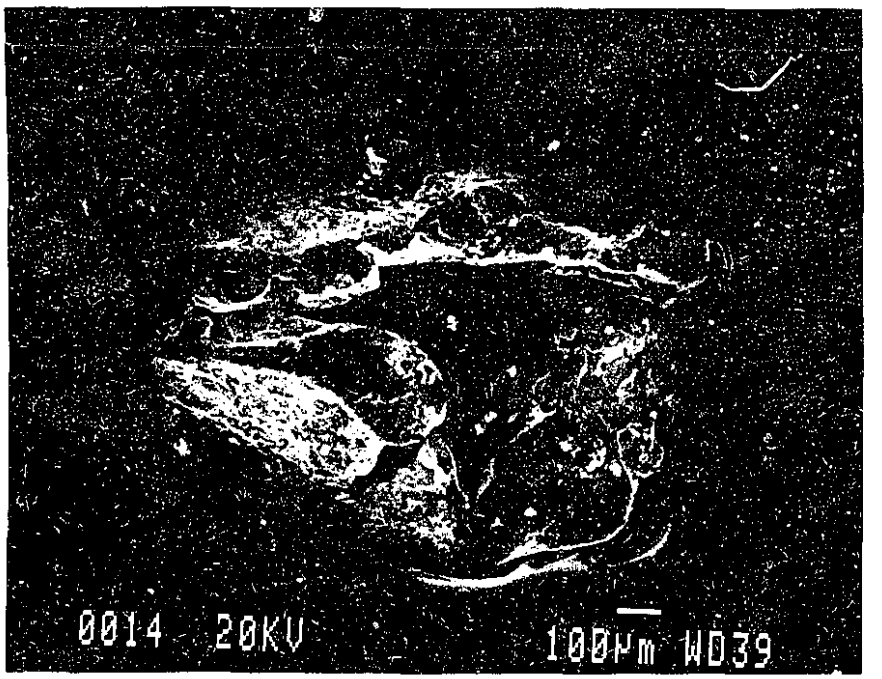

Figure 3.11: A folded gold flake (an early stage of the formation of a round flake. SEM photograph).

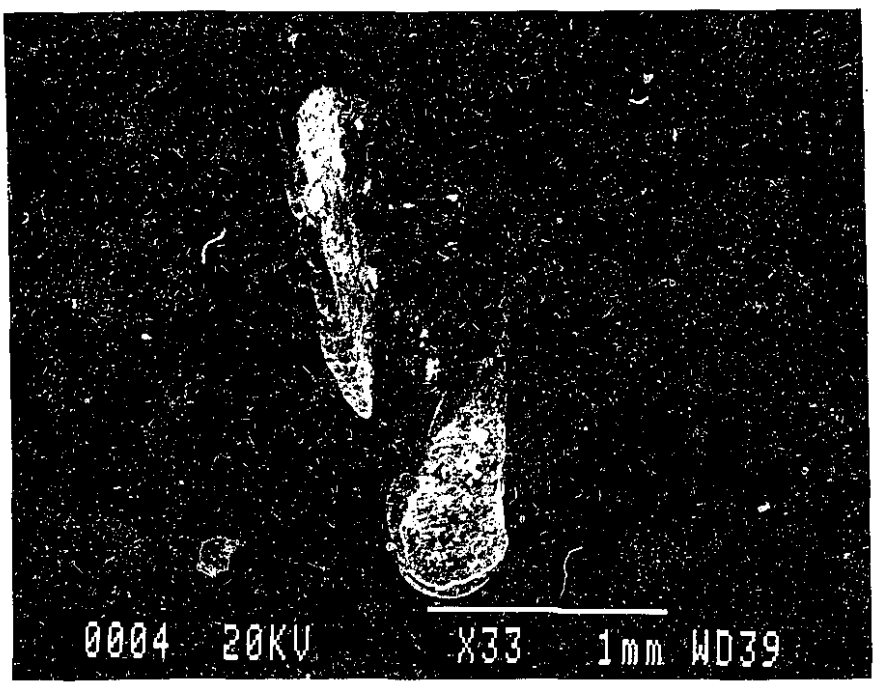

Figure 3.12: A folded gold flake (an early stage of the formation of a cylindrical flake. SEM photograph).

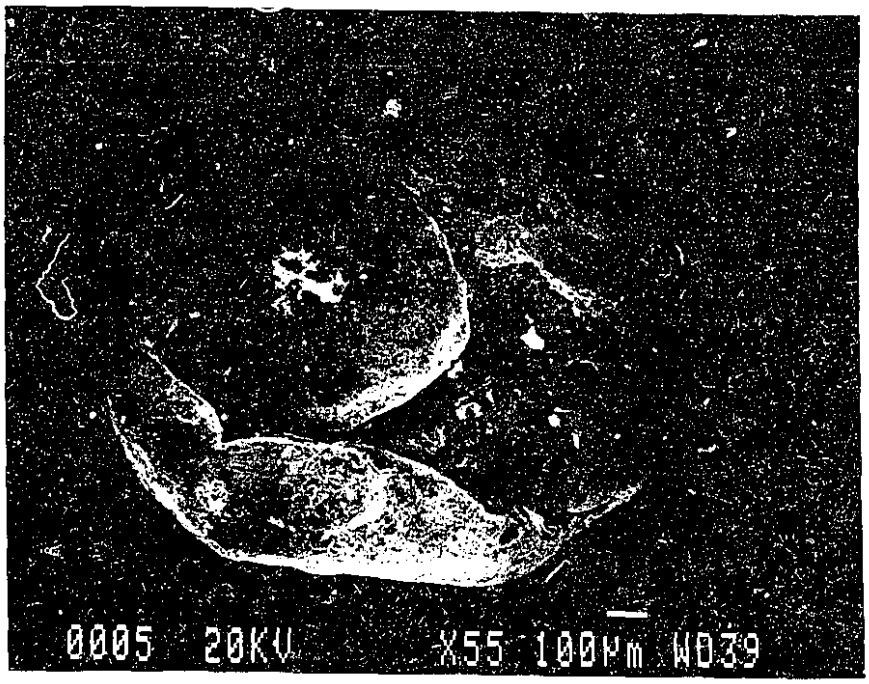

Figure 3.13: A folded gold flake (the formation of a round flake. SEM photograph)

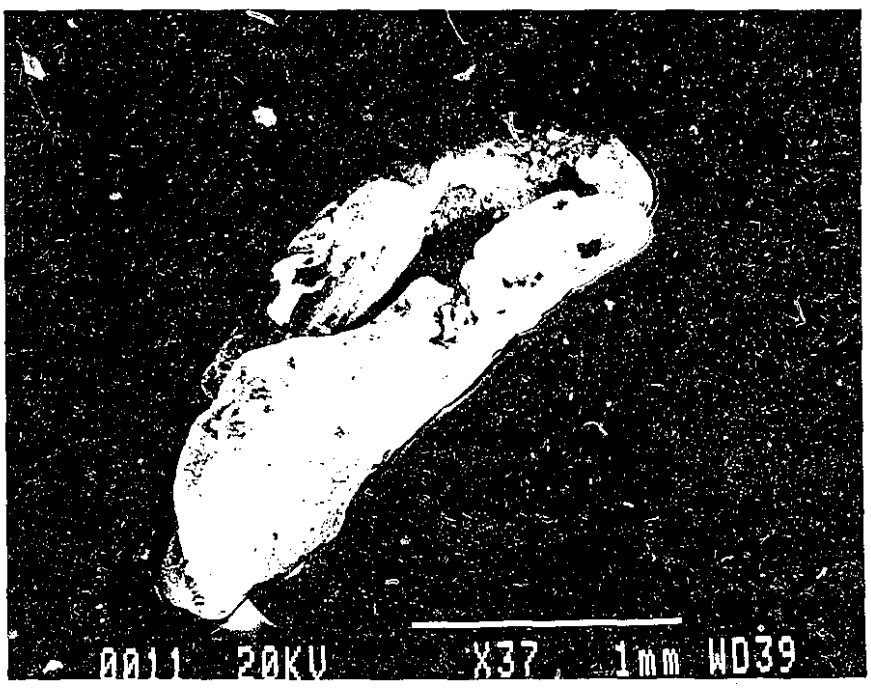

Figure 3.14: A folded gold flake (the formation of a cylindrical flake. SEM photograph).

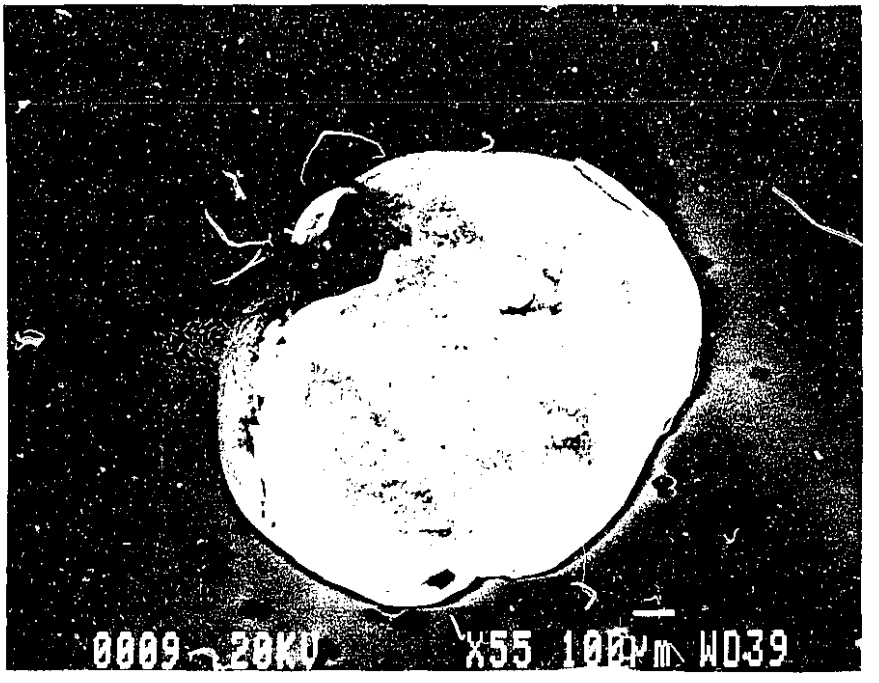

Figure 3.15: A round flake (a last stage of the shape formation. SEM photograph).

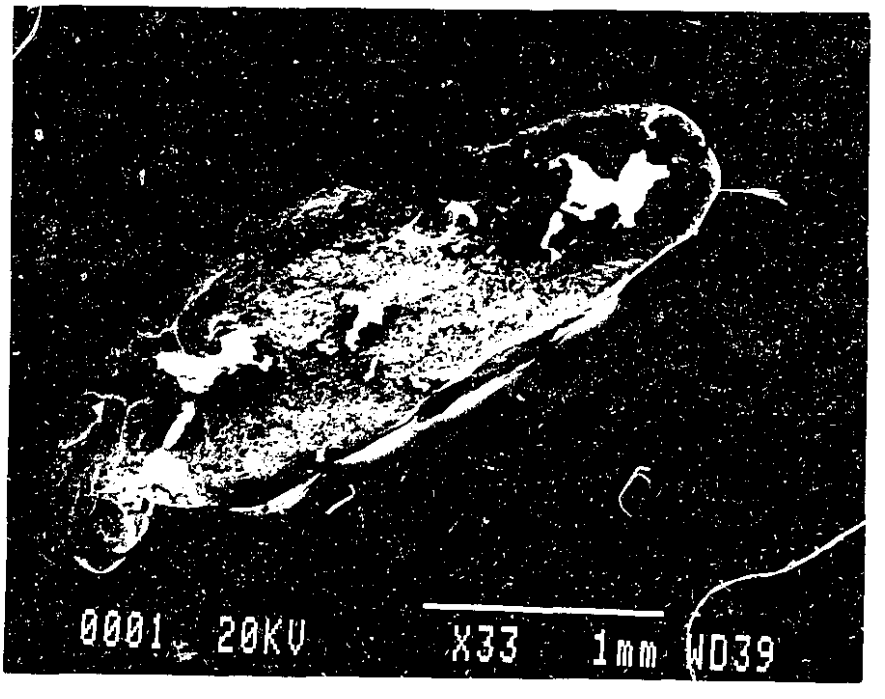

Figure 3.16: A cylindrical gold flake (last stage of the shape formation. SEM photograph).

particles came from the 50 g silica tests in the mill. Similarly, gold was smeared on the surface of silica particles from the 25 g grind, as verified by examining a sample of ground silica with the SEM. It appears that the grinding of silica had a cleaning action (scouring) inside the mill. It is anticipated that these phenomena occur at the plant scale for all minerals harder than gold.

Another evidence of silica embedding into gold is the nearly identical weight of the final and initial gold weights. It implies that there was no gold losses during the screening and grinding (with six time increments), which to some extent is unrealistic. Gold losses were compensated by silica which was loosened during gold grinding, and embedded onto gold particles.

Embedding of silica into gold flakes and smearing of gold blebs onto the surface of silica could affect the efficiency of mineral separation. The former, in flotation circuits, may decrease grade by going to concentrate or decrease recovery by making the gold flakes surfaces hydrophilic (although this is highly unlikely, as a very significant fraction of the gold surface would have to be covered by hydrophilic gangue). The nature and the extent of embedding determines the type of effect. The latter, smearing, could cause a loss of gold to tailings in flotation and gravity circuits. The magnitude of this loss is difficult to establish, but recovery improvements originating from gravity circuits have been reported in the range of 1 to 3% [e.g., Laplante, 1987]. In gravity circuits the embedded silica lowers concentrate grade slightly, but this is not significant (metallurgically or

economically). Thus, the main impact of the interaction of gold with other minerals is a net decrease in gold recovery in gravity or flotation circuits. Most cyanidation circuits would not be affected, as gold smeared onto the surface of other minerals would readily be cyanided.

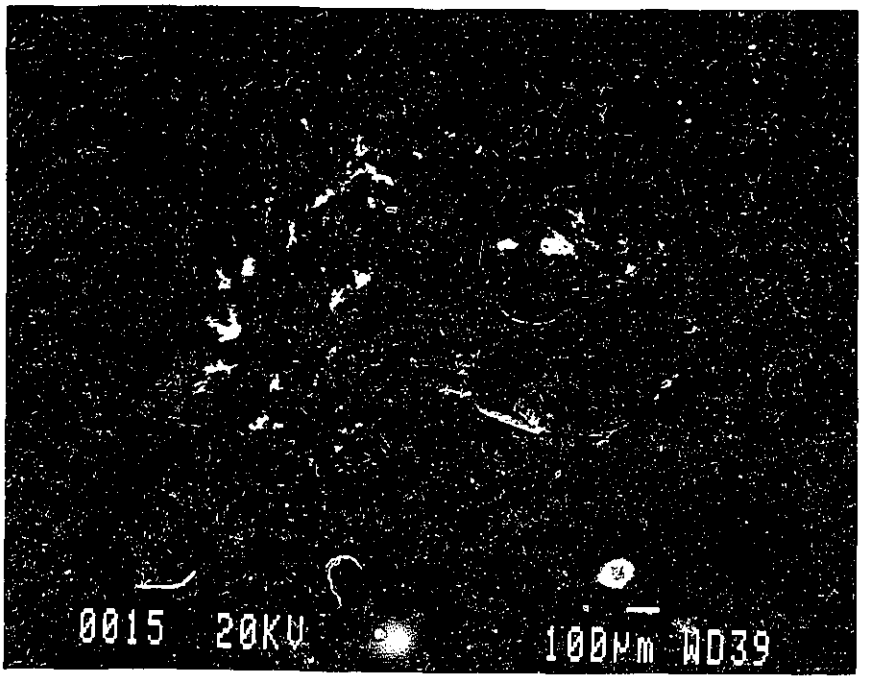

Figure 3.17: A folded gold flake; embedded silica particles show up white (SEM photograph).

3.4 Conclusions

1- It was found that grinding of single size classes of gold and silica follows first order kinetics.

2- The selection function of silica (50 g) is more than four times that of gold (5 g) under similar operating conditions, despite a lower gold weight being used.

3- The breakage function of gold and silica using Herbst's and Fuerstenau's modified method was calculated. The estimated breakage functions can be used to study the behaviour of gold flakes in grinding circuits.

4- The breakage function of gold is significantly different from that of silica (or most minerals). Fines production is limited, and 75% of the broken mass reports to the size class immediately finer than the original one.

5- In the grinding of gold, folding was found to be an important factor for size reduction. About 95% of gold flakes which changed size class after grinding were either spherical or cylindrical, and showed strong evidence of folding.

6- It was observed that gold goes through a deformation cycle, starting with the folding and flattening of regular flakes. Irregular flakes are then formed. These flakes fall into two categories: spheres and cylinders. Meanwhile, the thinner flakes are broken. The last stage of the cycle involves the flattening of the regular-shaped flakes. In industrial gravity circuits, this cycle would continue until

all of the flakes are ground to the desired size.

7- Embedding of remaining silica in the mill on the surface of the flakes and smearing of gold into silica were observed. Smearing of gold onto harder minerals can be a source of gold losses in flotation and gravity circuits, but will be inconsequential in most cyanidation circuits.

Chapter 4

The Evaluation of Industrial Grinding Circuit Performance

4.1 The Hemlo Mill

The Golden Giant (Hemlo) mill is located about 25 km east of Marathon on the north shore of Lake Superior, Ontario [Larsen, et al., 1987]. Ore reserves total 20.8 million mt grade 8.7 g/t (0.25 tr oz/st) [Anon., 1987]. Milling started in 1985 at a rate of 1200 t/d. Since then the milling rate has increased and was 3000 t/d at the time of this study (August 3, 1989).

The mineralized zones are dominated by quartz, feldspars, sericite, pyrite,

barite, molybdenite and vanadium bearing mica. Occasional visible gold occurs within quartz pods or along fractures.

The ore is reduced to minus 12 mm in a crushing plant consisting of a 2.44 m x 4.88 m double deck vibrating scalping screen (19 mm), an open circuit 2.13 m standard crusher, a closed circuit 2.44 m x 6.10 m double deck vibrating secondary screen (13 mm), and a 2.13 m short-head crusher. The grinding circuit consists of three 3.66 m x 4.27 m ball mills and two cyclopaks (381 mm and 254 mm diameter) [Larsen, 1987]; a fourth mill has since been installed for custom milling and is operated independently of the main grinding circuit, shown in Figure 4.1. The ground product, which is 80% passing 75 μm, reports to a 41 m thickener. The thickened slurry is pumped to the preaeration and cyanidation plant. Dissolved gold is recovered in a nine tank CIP circuit. The loaded carbon is pressured-stripped in 10 tonne batches. Gold is recovered from the loaded strip solution by electrowinning. The average analysis of the gold bullion poured in January 1986 was 96.2% Au, 3.5% Ag and 0.3% impurities [Larsen, 1987]. CIP (Carbon In Pulp) tailings are pumped to the molybdenum flotation circuit. In January 1986, the average molybdenum head and concentrate grades were 0.115% and 46% Mo, respectively. The Mo circuit has since been shut down, and was not operating at the time of the survey.

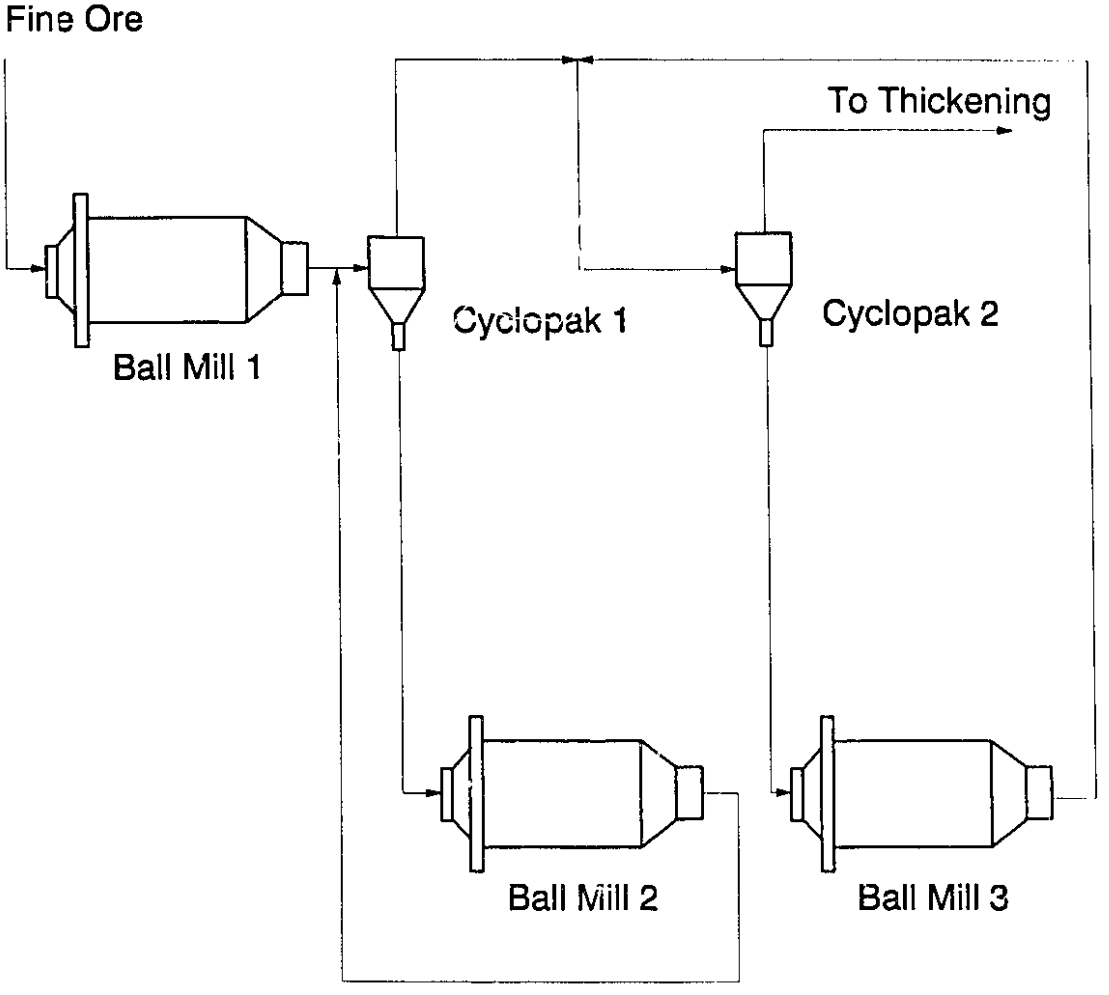

Figure 4.1: Flowsheet of the Hemlo Grinding Circuit.

4.2 Test Work Design

The grinding circuit was sampled on August 3, 1989 at a feed rate of 134.9 t/h. The description, average weight and number of samples are shown in Table 4.1. The samples were taken during a two-hour period at 15 minute time intervals. The samples were screened at 1.7 mm (10 mesh) and the undersize fed to the 7.6 cm (3") Knelson concentrator with a feed rate of 500 g/min and a back-water pressure of 31 kPa (4.5 psi). The tailings and concentrates were weighed, dried and screened. A size-by-size analysis of the concentrates and tailings was performed at the Hemlo Mines laboratory.

Description	Weight (g)	Number of samples
Primary Mill Discharge (PMD)	1030	2
Primary Cyclone Underflow (PCUF)	8419	2
Secondary Mill Discharge (SMD)	7048	2
Primary Cyclone Overflow (PCOF)	6043	1
Secondary Cyclone Underflow (SCUF)	6237	2
Tertiary Mill Discharge (TMD)	1043	1
Secondary Cyclone Overflow (SCOF)	3598	1

Table 4.1: Grinding circuit samples description.

4.3 Grinding Circuit Size Distributions

Table 4.2 shows the concentrate and tailings weight of the 7.6 cm (3") Knelson concentrator for each stream. The size distribution of the various streams

Stream	Conc.(g)	Tl. (g)	Stream	Conc. (g)	Tl. (g)
PMD 1,2	101.73	12886	PMD 3	94.86	7513
PCUF 1	131.66	8929	PCUF 2	117.65	7659
SMD 1,3	120.88	8434	SMD 2	127.55	5412
PCOF	86.56	5956			
SCUF 1	91.14	5708	SCUF 2	101.39	6572
TMD	99.87	10328			
SCOF	77.58	3520			

Table 4.2: Concentrates and tailings weight of the 7.6 cm Knelson concentrator.

was calculated from the tailings and concentrate size distributions (see Appendix C.1). When there were two samples per stream, such as PMD and PCUF, the average of the two size distributions was taken.

The size distribution were adjusted with the NORBAL2 software package [Spring, 1985]. Table 4.3 shows the adjusted size distributions for the streams of the primary loop. The size distributions of the streams of the secondary loop and the unadjusted size distributions of the primary loop are shown in Appendix C.2.

Size (μm)	Adjusted Data (%)			
	PMD	SMD	PCOF	PCUF
+1200	0.91	0.06	0.00	0.38
+850	1.54	0.23	0.00	0.78
+600	2.71	0.48	0.00	1.44
+425	4.00	1.26	0.00	2.69
+300	7.04	4.35	0.00	6.86
+212	10.46	11.27	1.17	14.59
+150	12.16	16.13	4.98	18.69
+106	14.66	20.49	14.17	20.66
+75	11.82	14.58	14.00	13.81
+53	9.22	12.79	12.38	11.66
+38	7.29	7.34	14.21	4.87
-38	18.19	11.02	39.09	3.57

Table 4.3: Adjusted size distributions of the streams of the primary loop.

The primary circulating load was estimated at 280%, with only minor adjustments to the size distributions.

4.4 'Free' Gold and Gold Size-by-Size Distributions

For each sample processed with the Knelson, the grade and recovery of each size class as well as the total grade and recovery was computed; detailed results are in Appendix C.3. To demonstrate the calculation of these parameters, the computational approach is shown below.

The grade, G, recovery, R, and units, U, of each size class can be calculated by the following equations :

$$G = \frac{E + K\frac{C}{D}}{F + H\frac{C}{D}} * 1000 \qquad (4.1)$$

$$R = \frac{E}{E + K\frac{C}{D}} * 100 \qquad (4.2)$$

where

E: Concentrate gold content of the size class (mg)

$$U - G\frac{F + H\frac{C}{D}}{A} * 100 \qquad (4.3)$$

K: Tailing gold content of the size class (mg)

C: Total tailing weight (g)

H: Tailing weight of the size class (g)

D: Sampled tailing weight (g)

F: Concentrate weight of the size class (g)

A: Total weight mass processed (g)

As an example the grade, recovery and units of the 150/212 μm size class of the SMD 1,3 and SMD 2 are shown in Table 4.4. It can be seen that the results are

Stream	Size Class +150 μm		
	G (g/t)	R (%)	U $(\%)^2$
SMD 1,3	260.1	93.6	4368.7
SMD 2	261.3	94.4	4284.6

Table 4.4: Grade, recovery and units of the size class 150-212 μm of the SMD 1,3 and SMD 2.

in good agreement for the two samples. Table 4.5 shows the overall results for the circuit.

Stream	G (g/t)	R (%)	Stream	G (g/t)	R (%)
PMD	16.6	35.6	TMD	60.7	60.0
SMD	402.9	91.5	SCUF	81.7	63.5
PCUF	397.6	89.1	SCOF	44.5	30.7
PCOF	15.9	39.7			

Table 4.5: The overall grade and recovery of the streams of the circuit calculated from size-by-size assays.

At steady state the grades of PMD, PCOF and SCOF should be the same; however, the SCOF has a markedly higher grade, 44.5 g/t. This grade is definitely suspicious, since the daily feed grade was estimated at 15 g/t. Furthermore the SCUF and TMD assays are significantly different, 60.7 vs. 81.7 g/t (this can compares poorly with the agreement of the PCUF and SMD, 397.6 vs. 402.9 g/t). As a result of the poor agreement of the second loop, it was decided to focus the study on the first loop -- i.e. PMD, SMD, PCUF and PCOF. Table 4.6 shows the size-by-size grade and overall grade of gold for the 4 streams of the primary loop. The same results for the secondary cyclone are shown in Appendix C.4.

Size (μm)	Grade (g/t)			
	PMD	SMD	PCOF	PCUF
+1200	15.66	1819.81	0.00	401.17
+850	51.12	1992.04	0.00	317.48
+600	10.60	800.60	0.00	368.78
+425	21.87	733.24	0.00	337.83
+300	19.88	429.03	0.00	269.23
+212	14.79	271.02	114.96	186.78
+150	12.75	260.67	3.67	250.54
+106	12.11	299.94	3.73	251.46
+75	10.53	423.64	4.37	499.25
+53	12.62	477.91	7.09	567.46
+38	34.39	795.72	12.66	816.65
-38	18.56	433.20	26.33	1131.55
Σ	16.57	402.85	15.87	397.54

Table 4.6: Size-by-size grade and overall grade of the streams of the primary loop.

The NORBAL2 software package was used to balance the size distribution of gold in the various streams. NORBAL2 balances gold size by size, but leaves out the constraints on the calculated overall grades (i.e. the overall gold content of the PMD and the PCOF, and that of the PCUF and the SMD are equal). Although there are software packages that are capable of doing this type of balancing, none were available at McGill. The same Lagrangian formulation used

by these packages was used to mass balance the gold of the primary loop. This part of the circuit corresponds to one node and four streams which are the PMD, SMD, PCOF and PCUF. The constraints are as follows:

12 constraints for the mass conservation of the 12 size classes (including pan). This can be expressed by :

$$\sum_{i=1}^{12} W(1,i)C(1,i) + L\,W(2,i)C(2,i) - W(3,i)C(3,i) - L\,W(4,i)C(4,i)] = 0 \qquad (4.4)$$

where

W(j,i): percent retained on the screen i (i=1 to 12) in stream j (j=1 to 4)

C(j,i): gold content of the size class i of stream j

L: circulating load

The 13th constraint is that the overall gold assay of the PMD and the PCOF is equal:

$$\sum_{i=1}^{12} [W(1,i)\,C(1,i) - W(3,i)\,C(3,i)] = 0 \qquad (4.5)$$

Similarly, the fourteenth equals the overall gold content of the SMD and the PCUF:

$$\sum_{i=1}^{12} [W(2,i)\,C(2,i) - W(4,i)\,C(4,i)] = 0 \qquad (4.6)$$

Using the Lagrangian formulation, the adjustment (correction) matrix [Smith et al., 1973], $\underline{dc}$, is equal to :

$$\underline{dc} = -V\,B^t\,(B\,V\,B^t)^{-1}\,B\underline{c} \qquad (4.7)$$

where

$\underline{dc}$: 48 x 1 column matrix of the grade adjustments

V : 48 x 48 diagonal matrix of the variances

B : 14 x 48 matrix expressing the mass balance constraints (from NORBAL2)

$\underline{c}$: 48 x 1 column matrix of unadjusted grades

The balanced grades will be equal to :

$$\underline{C} = \underline{dc} + \underline{c} \qquad (4.8)$$

where

$\underline{C}$: 48 x 1 column matrix of the adjusted grades, shown in Table 4.7.

Size (μm)	Adjusted grade (g/t)			
	PMD	SMD	PCOF	PCUF
+1200	209.05	2978.80	0.00	650.94
+850	44.54	1638.91	0.00	510.27
+600	17.29	13.97	0.00	16.30
+425	17.90	728.36	0.00	350.49
+300	18.02	428.57	0.00	278.27
+212	11.93	265.92	114.96	205.15
+150	9.85	263.59	3.68	229.40
+106	8.14	276.38	3.77	275.24
+75	7.72	456.91	4.40	483.17
+53	10.49	499.28	7.12	547.98
+38	41.92	612.70	12.95	932.22
-38	13.08	397.00	27.04	1143.28
Σ	16.00	381.76	15.97	381.71

Table 4.7: Adjusted grades for the streams of the primary loop.

Having obtained the adjusted ore size distribution, size-by-size grade and overall grade, the gold size distribution was estimated. This relationship can be expressed by:

Gold (%) = {Weight (%)*Grade (g/t)}/{ Overall grade (g/t)}

The gold size distribution of the streams of the primary loop is shown in Table 4.8. Since approximately 80% of the gold in the underflow is coarser than 53 μm, a gravity system to recover gold could be used. The size distribution of gold and ore is shown in Figure 4.2. Both Table 4.8 and Figure 4.2 show the impact of the high gold content of the 212/300 μm in the PCOF, which contains 8.42 % of the gold of the PCOF. This anomaly most likely stems from a sampling error akin to the nugget effect. Liu (1989) reports a similar phenomenon in a cyclone overflow sample.

Size (μm)	PMD (%)	SMD (%)	PCOF (%)	PCUF (%)
+1200	11.89	0.47	0.00	0.65
+850	4.29	0.99	0.00	1.04
+600	2.93	0.02	0.00	0.06
+425	4.48	2.40	0.00	2.47
+300	7.93	4.88	0.00	5.00
+212	7.80	7.85	8.42	7.84
+150	7.49	11.14	1.15	11.23
+106	7.46	14.83	3.34	14.90
+75	5.70	17.45	3.86	17.48
+53	6.05	16.73	5.52	16.74
+38	19.11	11.78	11.52	11.89
-38	14.87	11.46	66.18	10.69

Table 4.8: Gold size distribution of the streams of the primary loop.

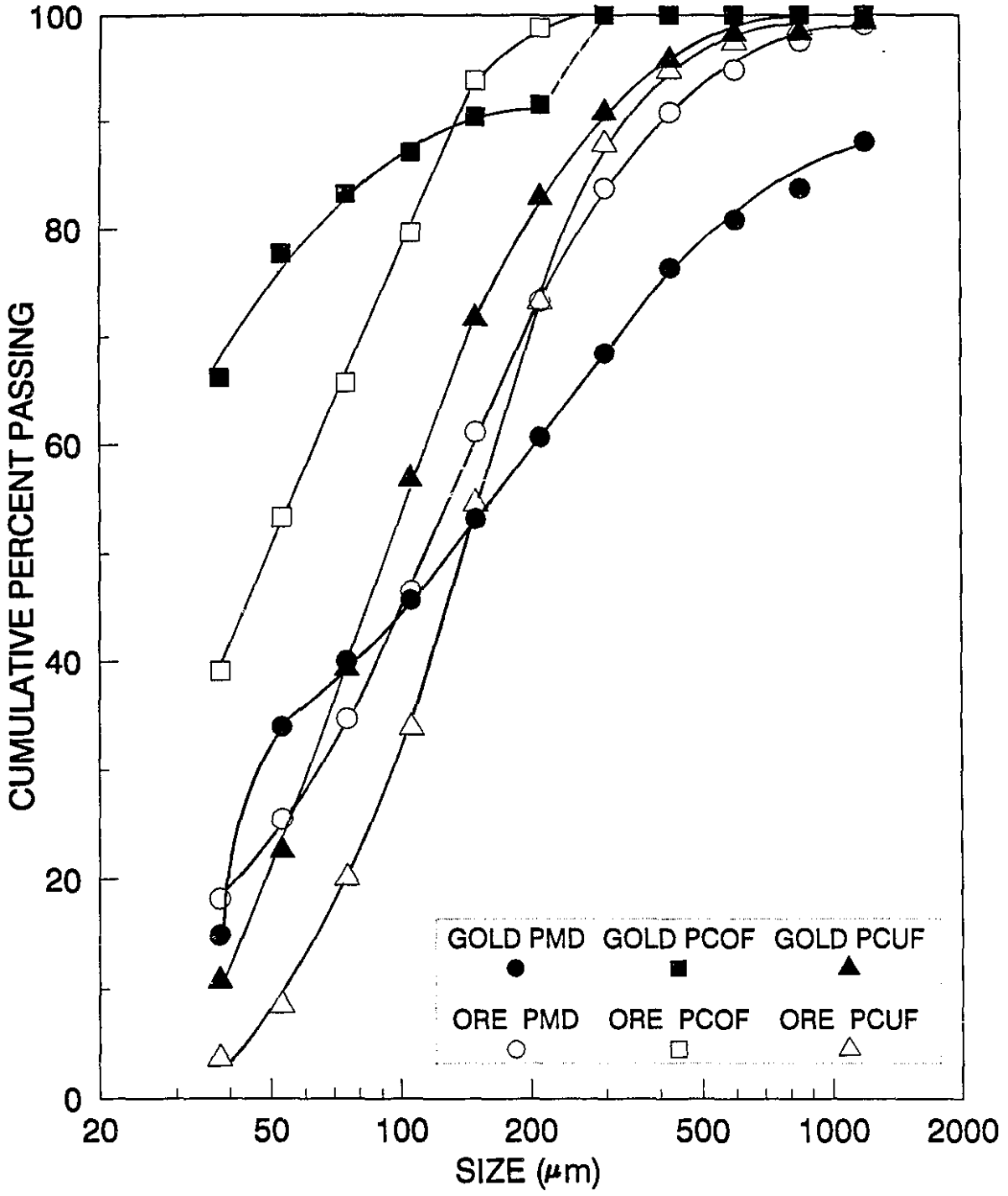

Figure 4.2: Size distribution of the gold and ore.

4.5 Evaluation of Cyclone Classification

4.5.1 Actual classification Function

The circulating load of the primary cyclone as determined in section 4.1.2 using the NORBAL2 software package is 280%. In this case the feed fraction to the underflow and overflow will be 74% and 26%, respectively. Table 4.9 gives the classification functions for the ore and 'free' gold. The classification curves are shown in Figure 4.3.

Size (μm)	PCUF			
	Ore (%)	Gold (%)	'Free' Gold (%)	'corrected' Ore (%)
+1200	100.00	100.00	100.00	100.00
+850	100.00	100.00	100.00	100.00
+600	100.00	100.00	100.00	100.00
+425	100.00	100.00	100.00	100.00
+300	100.00	100.00	100.00	100.00
+212	97.72	98.42	97.82	96.51
+150	91.32	99.85	99.97	89.10
+106	80.34	99.67	99.93	75.32
+75	73.44	99.67	99.91	66.65
+53	72.53	99.51	99.73	65.51
+38	49.00	98.57	99.13	35.96
-38	20.38	91.54	96.60	0.04

Table 4.9: Cyclone classification efficiency curves.

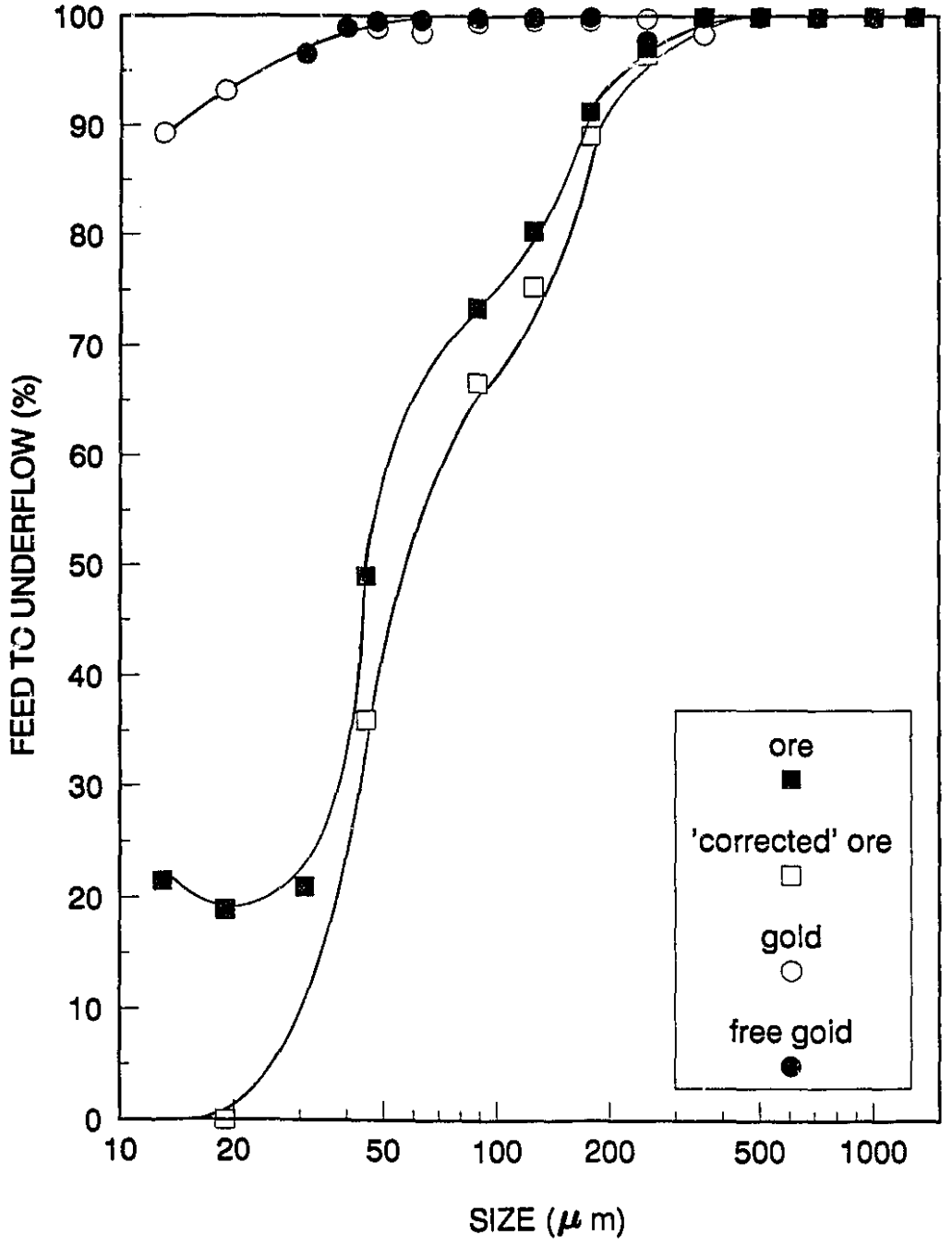

Figure 4.3: Cyclone classification efficiency curves.

It can been seen that the classification efficiency curves of the ore and the 'corrected' ore have a hump in the size range 40 to 100 μm. This type of 'unusual' cyclone performance (efficiency) curve to originate from classification of minerals of different density and different size distribution [Laplante et al. , 1984]. The overall classification curve consists of two curves, one for heavies (sulphides) and one for lights (non-sulphides). The overall curve tends to follow the lights curve above 100 μm and the heavies curve below 40 μm. The transition from light to heavy creates the hump in the curve.

The d_{50} (the particle size which has an equal probability of reporting to the underflow and overflow products) for the ore is around 38 μm, whereas for gold and 'free' gold the d_{50} is far below 38 μm and in fact cannot be determined without sub-sieve data.

4.5.2 'Corrected' Classification Function

It is assumed that in all classifiers, fines are entrained in the coarse product liquid in direct proportion to the fraction of feed water reporting to the coarse product [Wills, 1988]. This phenomenon in cyclones causes fines to report to the underflow. Therefore, the actual cut size (d_{50}) is lower than the ideal ('corrected') cut size. In the Hemlo primary cyclone, 20% of the size class -38 μm reports to

the underflow. In order to estimate the 'corrected' classification curve, the effect of short circuiting should be subtracted. This is carried out as follows:

$$y_c = \frac{y - R}{1 - R} \tag{4.9}$$

where

y_c: the 'corrected' mass fraction of a particular size class reporting to the underflow

y : the actual mass fraction of a particular size class reporting to the underflow

R : the fraction of the feed water which is recovered in the underflow

At the time of sampling, the percent solids of the cyclone overflow and underflow were 77.5% and 24%, respectively. R can be determined from a water balance of the cyclone as follows:

water in U/F = ((100-77.5)/77.5) * 2.73 = 0.86

water in O/F = (100-24)/24 = 3.17

therefore :

$$R = 0.86/(3.17 + 0.86) = 20.35\%$$

The fraction of the feed water in the underflow is in good agreement with the mass fraction of the size class -38 μm which reports to the underflow. This is an indication of sound data. The 'corrected' classification curve and mass fractions are shown in Figure 4.3 and Table 4.8, respectively.

The 'corrected' cut size (d_{50c}) can be determined by the 'corrected' curve. The commonly used equation which represents a 'corrected' classification curve is [Plitt, 1976]:

$$y_c = 1 - \exp[-0.693(\frac{d}{d_{50c}})^m] \qquad (4.10)$$

where

d_{50c}: the particle size in which the probability of reporting to the overflow and underflow products is equal

m : a representation of the classification sharpness

Equation 4.11 can be rearranged to form a linearized equation as follows:

$$\ln\left[\ln\frac{1}{1-y_c}\right] = m\ln(d) + \ln(0.693) - m\ln(d_{50_c}) \qquad (4.11)$$

By plotting ln [1/(1-y_c)] versus d on a log-log scale, m and d_{50c} can be determined. Figure 4.4 shows that m is 1.03 and d_{50c} is 57 μm. By substituting d_{50c} and m into Eq.4.11, the 'corrected' classification function will be :

$$y_c = 1 - \exp[-0.693(\frac{d}{57})^{1.03}] \tag{4.12}$$

In terms of the actual classification it will be :

$$\frac{y-R}{1-R} = 1 - \exp[-0.693(\frac{d}{57})^{1.03}] \tag{4.13}$$

or

$$y = 0.80\, y_c + 0.20 \tag{4.14}$$

By using the above equations, the size distribution of the underflow and overflow can be predicted for any given feed with the three known parameters, d_{50}, m and R.

By assuming a d_{50} for the ore and using Plitt's cyclone model, the d_{50} of gold can be predicted. A simplified form of Plitt's formula is as follows :

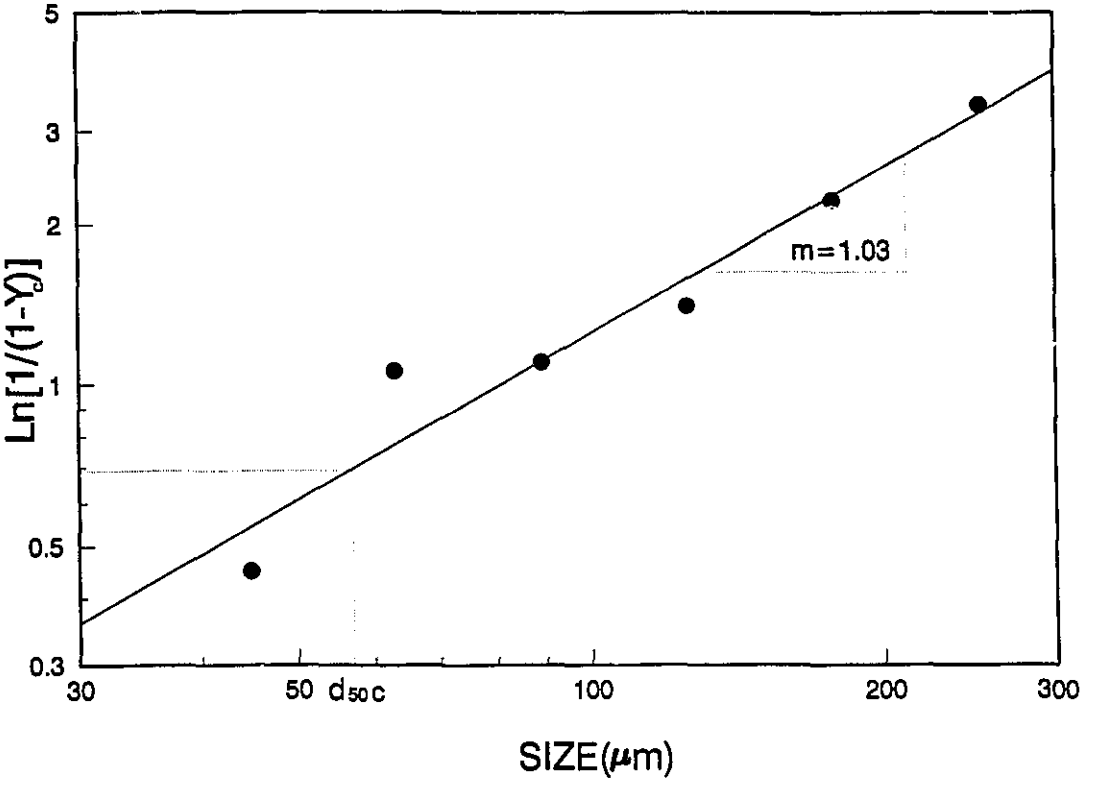

Figure 4.4: Determination of m and d_{50c}.

$$d_{50} = \frac{K}{(\beta_s - 1)^{0.5}} \qquad (4.15)$$

where

K: Constant

$ß_s$: Density (g/cm^3)

If it is assumed that the d_{50c} of ore with density of 3.2 is 57 μm, the d_{50c} gold with density of 19 will be 20 μm. This implies that the cut size for gold is much lower than the ore.

4.6 Sub-Sieve Analysis

In order to determine the efficiency of the 7.6 cm (3 ") Knelson concentrator in recovering fines (-38 μm), micro screening of the various streams was performed. The -38 μm of the Knelson tailing and concentrate of the various streams was screened into the three size classes of +25 μm, 25/15 μm and -15 μm. Screening was performed in a ultrasonic cleaning bath filled with water. For each screening, a mass of approximately 3 grams for tailings (total mass screened: approximately 10 g) and 1 gram for concentrates (single screening) was screened

for 15 minutes. All of the samples were assayed at the Hemlo mine laboratory.

The Lagrangian formulation (see section 4.1.3) was used to balance the size distribution of the sub-sieve classes (see Appendix C.5). For overall ore, 21.0, 18.9 and 21.5% of the mass reports to the underflow for the 38/25, 25/15, and -15 μm, respectively. This causes a dip or fish-hook in the fine end of the cyclone efficiency curve (Fig. 4.3). The fish-hook has been explained and modeled by considering an entrainment component to recovery to the underflow which is a function of particles size [Finch, 1984]. It is assumed that below a certain size, particles move less readily relative to the water and, with decreasing size, progressively separate in the same proportion as water.

The grade of the -38 μm of each stream was then determined by combining of the tailing and concentrate assays. The gold content of the sub-sieve size classes and the overall grade of the size class -38 μm can be estimated using the following equations:

$$A_u = E\frac{L}{F} + K\frac{M}{H}\frac{C}{D} \tag{4.17}$$

$$G = \frac{T_{Au}}{L + M\frac{C}{D}} \tag{4.18}$$

where

A_u: Gold content of the sub-sieve size class (mg)

E: Concentrate gold content of the sub-sieve size class (mg)

L: Concentrate weight of the size class -38 μm (g)

F: Concentrate weight of the sub-sieve size class (g)

K: Tailing gold content of the sub-sieve size class (mg)

M: Tailing weight of the size class -38 μm (g)

H: Tailing weight of the sub-sieve size class (g)

C: Total tailing weight (g)

D: Sampled tailing weight (g)

G: Overall grade of the size class -38 μm (mg)

T_{Au}: Total gold content of the size class +25 μm, 15/25 μm and -15 μm (mg)

An example of the calculation of the gold content and the overall grade of the sub-sieve fractions of the PMD 1,2 is shown below. Table 4.10 shows the weight and gold content of the concentrate and tailings of the sub-sieve size classes of the PMD 1,2.

Size (μm)	Weight			
	Concentrate		Tailing	
	(g)	Au (mg)	(g)	Au (mg)
+25	0.19	0.3168	0.98	0.0365
+15	0.44	0.1305	3.95	0.0281
-15	0.30	1.2036	4.68	0.1067
Total	0.93	1.6509	9.61	0.1713

Table 4.10: Weight and gold content of the concentrate and tailings of the sub-sieve size classes of the PMD 1,2.

Concentrate weight (-38 μm) = 6.6 g

Tailing weight (-38 μm) = 62.6 g

Au (+25 μm) = 0.316*6.6/0.93+0.036*62.6/9.61*(12988-101)/315 = 11.99 mg

Au (+15 μm) = 0.1305*6.6/0.93+0.028*62.6/9.61*(12988-101)/315 = 8.56 mg

Au (-15 μm) = 1.2036*6.6/0.93+0.106*62.6/9.61*(12988-101)/315 = 37.02 mg

Grade (-38 μm) = (11.99+8.56+37.025)/(6.6+62.6*(12988-101)/315 = 22.4 g/t

Detailed results are shown in Appendix C.4. A Lagrangian formulation was used to balance the gold content of the sub-sieve classes (see Appendix C.6). The percent of gold in the feed which reports to the underflow in 38/25 μm, 25/15 μm and -15 μm size classes is 98.78 %, 93.20 % and 89.35 %, respectively (Fig. 4.3).

The -38 μm gold content of the various streams estimated from sub-sieve analysis and from direct assaying is shown in Table 4.11. It can be seen that the

agreement is poor. This problem is caused mostly by an insufficient mass of concentrates in the sub-sieve fractions in the assaying. Micro screening and assaying errors also contribute to the overall assay error. The recovery of the sub-sieve ranges did not show a specific trend (Appendix C.7). Therefore, drawing any legitimate conclusions about the efficiency of the Knelson concentrator in the sub-sieve ranges proved very difficult. It was concluded that to study the sub-sieves ranges a mass of approximately 5 g is required for each size classes of the concentrate.

Stream	Grade (g/t)	
	Sub-Sieve (indirect)	Measured (direct)
PMD 1,2	22.39	17.27
PMD 3	22.67	19.86
PCUF 1	512.96	1039.11
PCUF 2	938.21	1223.98
SMD 1,3	412.58	485.80
SMD 2	383.50	380.59
PCOF	24.52	26.33
SCUF 1	416.10	365.97
SCUF 2	380.31	247.25
TMD	110.90	103.91
SCOF	61.62	29.52

Table 4.11: Grade of the size class -38 μm of the various streams measured directly and estimated from sub-sieve analysis.

4.7 Evaluation of Grinding Kinetics

In chapter 3 it was shown that there is a rather large difference in the selection functions of gold and silica at laboratory scale. To study this phenomenon with plant data, the selection functions of the ore and gold were determined and compared using the balanced size distribution of Tables 4.3 and 4.8 and the estimated breakage functions in chapter 3. It is assumed that the breakage function of the ore is equal to that measured for silica in chapter 3. BALLDATA and BALLMILL, two BASIC programs developed at McGill, were used for the calculation. Results are shown in Table 4.12 (see Appendix A.5). It can be seen (Table 4.12) that the ratio of the selection functions decreases with decreasing particle size. Although in the finer size classes results are noisy, the trend is similar. The ore grinds over twenty times faster than gold in the 700-1000 μm size range. As concluded in chapter 3, folding, which is the dominant factor in decreasing of grinding kinetics, is less likely to occur for the finer size classes.

It has been shown that the selection function is proportional to the mill diameter through the following expression [Gupta, et al., 1985]:

$$S_i \propto D^{\tau} \tag{4.19}$$

where

S_i: selection function of size class i (s^{-1})

D: mill diameter (m)

τ: material-dependent constant

In other words, the rate of the change of the selection function with mill diameter is material dependent.

Size (μm)	Selection Function (s^{-1})		
	Gold	Ore	Ratio
+1010	0.066	1.935	29
+714	0.094	2.076	22
+505	0.062	1.441	23
+357	0.050	0.801	16
+252	0.041	0.483	12
+178	0.038	0.381	10
+126	0.027	0.236	9
+89	0.023	0.256	11
+63	0.023	0.229	10
+45	0.043	0.143	3

Table 4.12: Estimated selection functions of the ore and gold and their ratio.

For example, the constant τ was found to differ significant for quartz and limestone, 0.61 vs. 0.26 [Gupta, 1985]. In this study, the diameter of the laboratory and plant mill were 20 cm and 4 m, respectively. Based on the above

relationship (4.19), the ratio of the selection functions in the two mills will be equal to:

$$R = \frac{S_{plant}}{S_{lab}} = \left(\frac{D_{plant}}{D_{lab}}\right)^{\tau} \tag{4.20}$$

For the sake of discussion if it is assumed that the constant τ for the ore is the same as quartz (0.61) then the constant τ can be estimated for gold. The ratio of the selection functions of the ore (S_o) to the gold (S_g) for the size class 714/505 μm in the lab (l) and the plant (p) are 4 and 22, respectively. The ratio of the two ratios can be expressed as follows:

$$\frac{R_o}{R_g} = \frac{S(o,p)}{S(g,p)} \cdot \frac{S(g,l)}{S(o,l)} = \frac{22}{4} \tag{4.21}$$

By substituting Eq.4.20 and τ of the ore into Eq.4.21, it will be:

$$\left(\frac{D_{plant}}{D_{lab}}\right)^{0.61} \left(\frac{D_{lab}}{D_{plant}}\right)^{\tau} = \frac{22}{4} \tag{4.22}$$

Equation 4.22 yields an estimate of τ equal to 0.04 for gold. This shows that the selection function of gold in the coarser size classes is not significantly affected by mill diameter. τ increases with decreasing particle size to reach a value of 0.6 (that of silica) at 50 μm (Fig. 4.5). This supports the fact that folding occurs for the coarser size classes in the plant and laboratory alike i.e. the grinding mechanisms are similar. However, for the finer size classes, where folding is very limited, grinding kinetics is different in the plant and the laboratory (Figure 4.6).

Figure 4.7 shows the selection functions of the ore and gold. They follow the relationship of $S_i = A\ x_i^{\alpha}$ (A and α are constant and x_i is the particle size) (Figure 4.7). The value of α for the ore and gold is 0.96 and 0.57, respectively. This is in good agreement with published data (e.g. α in a small laboratory mill has been found to vary between 0.5 and 0.8, depending on the mill filling [Shoji, et al., 1980]).

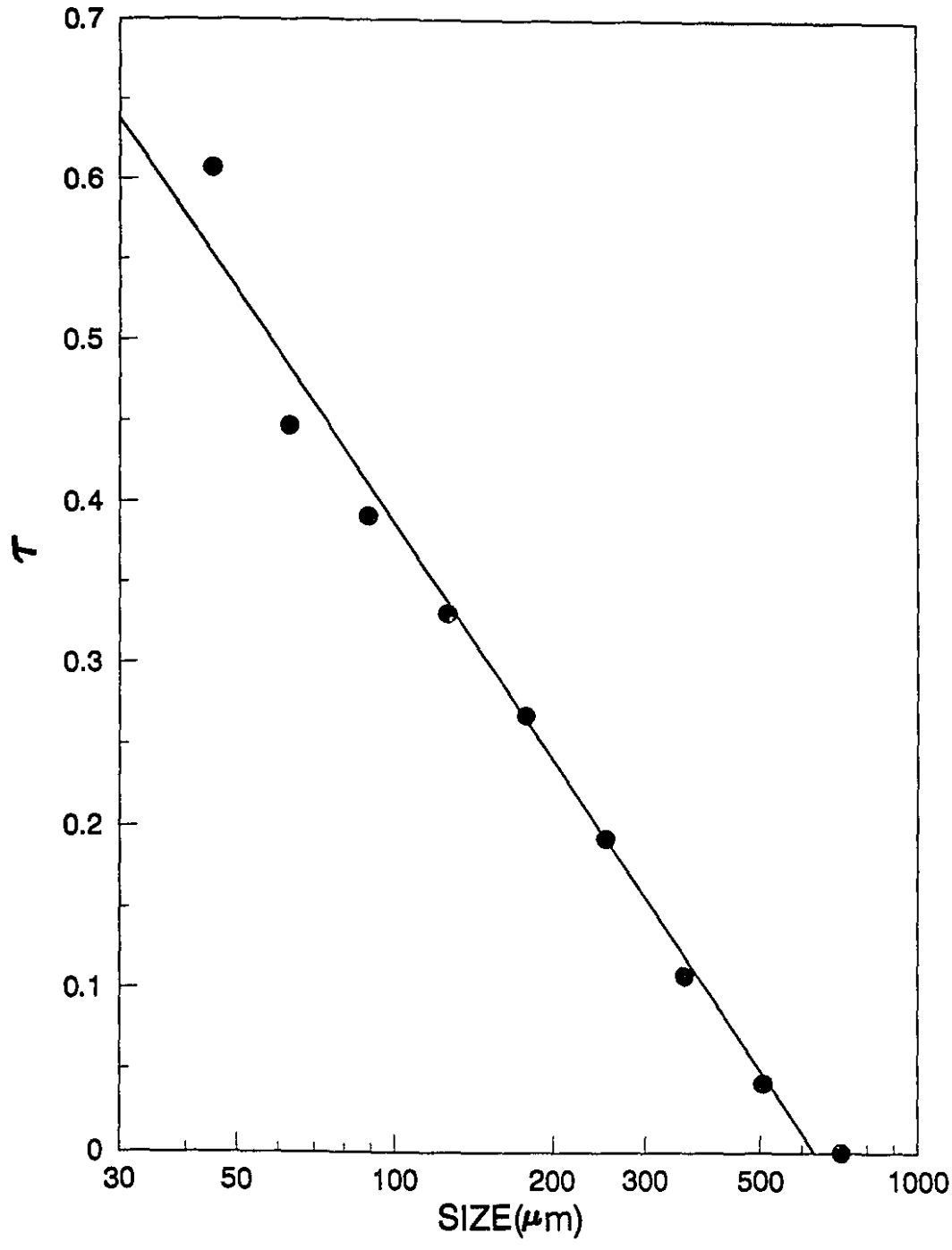

Figure 4.5: τ vs. size for gold.

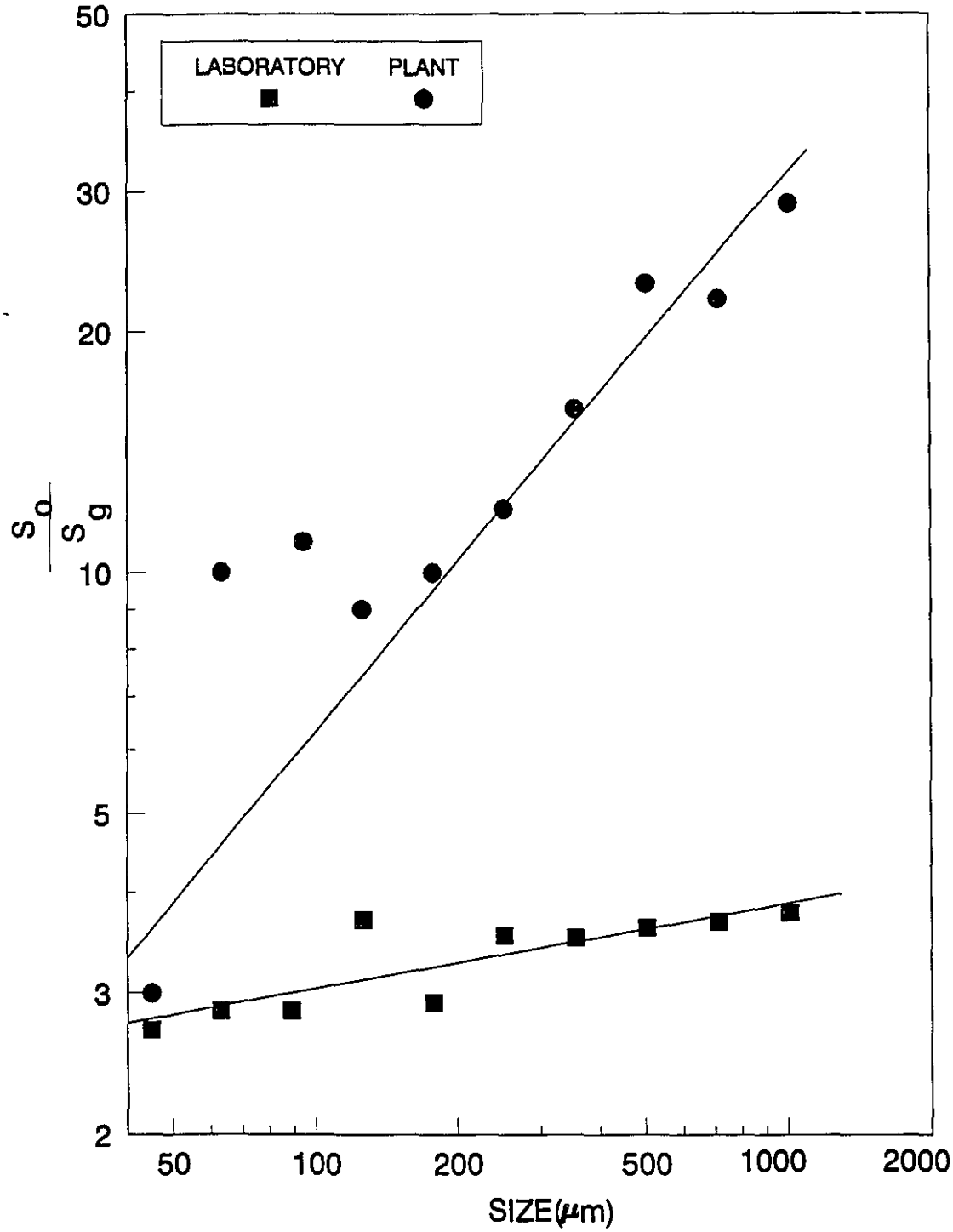

Figure 4.6: Ratio of selection functions of the ore and gold in the laboratory and the plant.

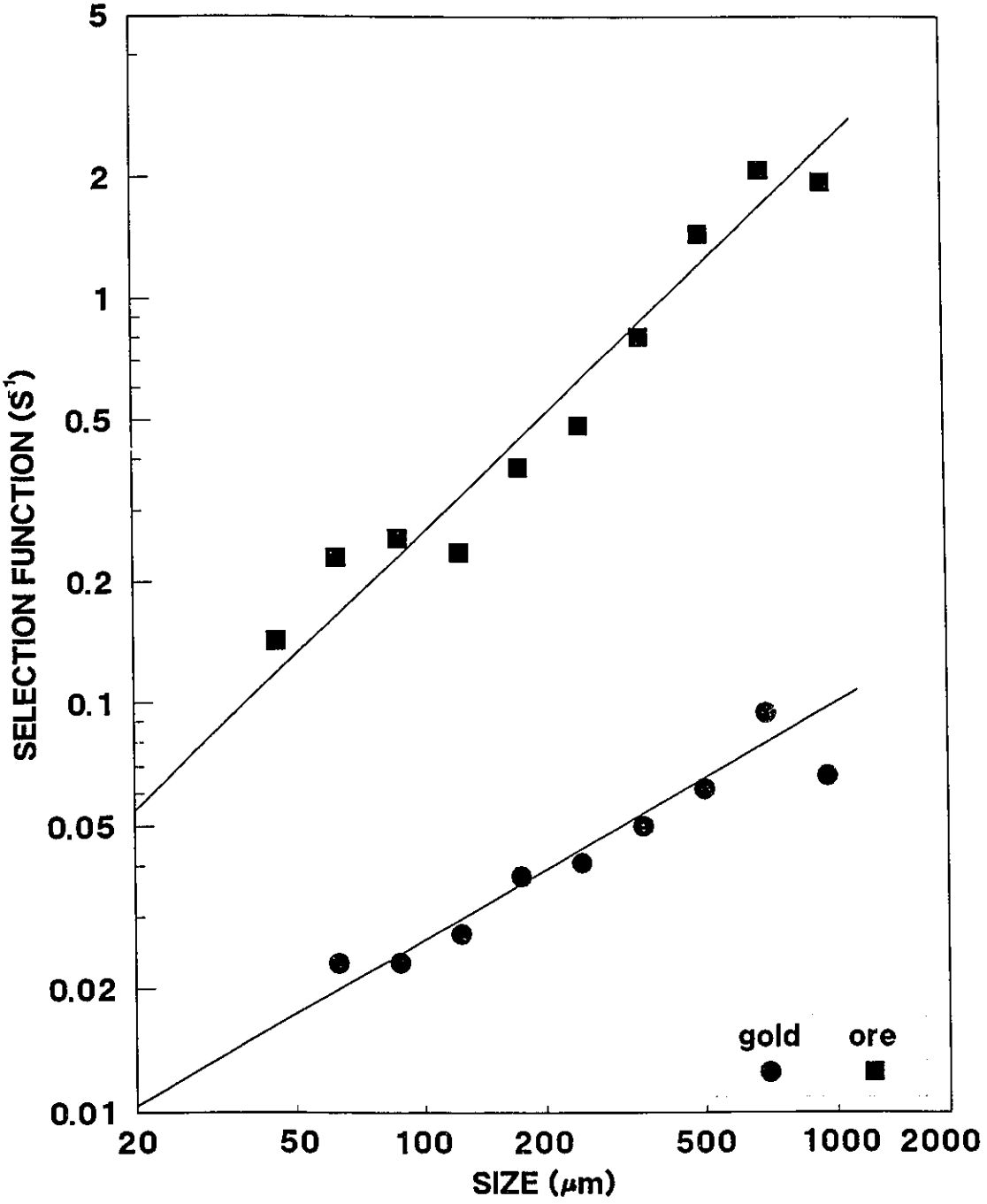

Figure 4.7: Selection function vs. size for the ore and gold.

4.8 Conclusions

1- There is a circulating load of 280% for ore in the primary cyclone. The high circulating load of gold (6700%) stems from its classification behaviour and grinding kinetics.

2- The selection function of silica is four times that of gold in a 23 cm laboratory mill. In the Hemlo secondary mill, selection function of the ore is six to twenty times that of gold. This difference can be mostly attributed to the effect of the mill diameter on the relative change of selection function.

3- More than 99% of the 'free' gold reports to the underflow product. This makes it a good candidate for recovery by gravity, possibly with a Knelson concentrator.

4- The cut size (d_{50c}) of the primary cyclone for the ore and gold are approximately 57 μm and 20 μm, respectively.

5- The d_{50} and the efficiency of the Knelson concentrator in the sub-sieve range could not be estimated due to inaccuracies in the sub-sieve data. The small weight of the screened samples is the likely source of error.

6- The differences in the selection functions of gold and the ore are largest in the coarse range, where gold folding is expected to predominate.

Chapter 5

Conclusions

5.1 General Conclusions

The 7.6 cm (3") Knelson concentrator is a reliable and safe method to estimate free gold content. This novel approach can facilitate the evaluation of the grinding and gravity circuit performance.

The behaviour of gold in grinding circuits is unusual; high circulating loads are the consequence of primarily grinding kinetics, and secondarily classification behaviour. Gold grinds six to twenty times slower than most other minerals, and

into coarser fragments. The slower kinetics are not the consequence of hardness, but of malleability, which results in some flakes folding and assuming cylindrical and spherical shapes upon impacting. Gold's cut size is three times smaller than that of minerals with a density of 3 g/cm^3. Gold's malleability promotes interaction with other minerals and the grinding media, in the form of embedding of harder minerals into gold and smearing of gold unto other minerals. In some circuits, especially flotation, this can result in a loss of recovery, as smeared gold may be lost if the carrier particle is hydrophilic. This may lead to the decision of recovering gold with gravity or unit flotation within the grinding circuit. The recycled streams, cyclone underflows and secondary mill discharges, are then the better candidates for recovery. High gold circulating loads (e.g. 6700% in Hemlo mill) make it unnecessary to process the full streams. Rather, part of the streams can be bled and presented to the gold recovery unit. Two approaches can then be taken; the first would aim for coarse gold recovery, presumably through a high capacity recovery unit such as sluices, Reichert cones, or jigs; fine gold recovery is then forfeited. The second would aim at recovering fine gold, and bleeding could be performed with a screen; coarse gold would therefore not be recovered directly, but following grinding into finer particles. The first approach appears to be the industry standard; the second, a rather novel approach, offers interesting potential.

5.2 Future Work

Four main topics are of interest for further research:

1- Quantifying the recovery, classification, liberation and grinding of sub-sieve gold particles. Particular attention could be given to the recovery of sub-sieve gold particles with the 7.6 cm (3") Knelson concentrator.

2- Determining the effect of feed size distribution and shape as well as bowl geometry, feed rate and the back-water pressure on the performance of the Knelson.

3- Quantifying the effect of gold gravity recovery ahead of flotation on the overall recovery.

4- Comparing further the efficiency of the Knelson and amalgamation by processing the rejects of amalgamation with the Knelson. This can clarify the ability of the two methods in recovering free gold.

5- Using the methodology in various industrial grinding and gravity circuits.

Bibliography

[1] Adamson, R.J., 1972, "Gold Metallurgry in South Africa," ed., Johannesburg, Chamber of Mines of South Africa.

[2] Anon., 1987, "Hemlo: A North American Gold Success Story," Engineering and Mining Journal, June, pp. 10-13.

[3] Arbiter, N. and Bhrany, U.N., 1960, "Correlation of Product Size, Capacity and Power in Tumbling Mills," AIME Trans., Vol. 217, pp. 245-252.

[4] Austin, L.G. and Luckie, P.T., 1971/72a, "The Estimation of Non-Normalizable Breakage Distribution Parameters from Batch grinding Test," Powder Technol., Vol. 5, pp. 267-271.

[5] Austin, L.G. and Luckie, P.T., 1971/72b, "Methods for Determination of Breakage Parameters," Powder Technol., Vol. 5, pp. 215-222.

[6] Austin, L.G. and Bhatia, V.K., 1971, "Experimental Methods for Grinding Studies in Laboratory Mills," Powder Technol., Vol. 5, pp. 261-266.

[7] Austin, L.G., Shoji, K. and Luckie P.T., 1976, "The Effect of Ball Size on Mill Performance," Powder Technol., Vol. 14, pp. 71-79.

[8] Bagnold, R.A., 1954, "Experiments in Gravity-Free Dispersion of Large Solid Spheres in a Newtonian Fluid Under Shear," Proc. Royal Sco. London, 225A, pp. 49-63.

[9] Bath, M.D., Duncan, A.J. and Rudolph, E.R., 1973, "Some Factors Influencing Gold Recovery by Gravity Concentration," Journal of the South African Institute of Mining and Metallurgy, June, pp. 363-385.

[10] Bradford, B., 1987, "Gravity Concentration for Gold Recovery," Engineering & Mining Journal, June, pp. 64-65.

[11] Brittan, M.I. and Van Vuuren, E.J.J., 1973,"Computer Analysis, Modelling and Optimisation of Gold Recovery Plants of the Angol American Group," African Institute of Mining and Metallurgy, Vol. 73, No. 7, pp. 211-222.

[12] Dorr, J.V.N., and Bosqui, F.L., 1950, "Cyanidation and Concentration of Gold and Silver Ores," 2nd edition, New York, McGraw Hill.

[13] Douglas, J.K.E. and Moir, A.T., 1961, "A Review of South African Gold Recovery Practice," Trans. 7th Commonwealth Min. and Met. Congress, Johannesburg. Vol. III, pp. 171-1003.

[14] Epstein, B., 1947, "The Mathematical Description of Certain Breakage Mechanisms Leading to the Logarithmatico-Normal Distribution," J. Frank. Inst., Vol. 224, pp. 471-477.

[15] Ferree, T.J., 1984, "The Mark-7 Reichert Spiral Concentrator, A New Concept for Fine Gold Recovery," The First International Symposium on Precious Metals Recovery, Reno, Nevada, June 10-14.

[16] Finch, J.A., 1982, "Modelling a Fish-hook in Hydrocyclone Selectivity Curves," Powder Technology, Vol. 36, pp. 127-129.

[17] Forssberg, E., 1985, "3-D Behaviour of the Key Parameters Affecting Grinding in a Batch Ball Mill," Scand. J. Metallurgy, Vol. 15, pp. 53-58.

[18] Forssberg, E. and Nordquist, T., 1987, "Pilot Plant Trials of New Gravity Concentration Equipment," Minerals Metallurgical Processing, Vol. 4, No. 2, May, pp. 97-89.

[19] Gardener, R.P. and Sukanjinajtee, K., 1973, "A Combined Tracer and Back-Calculation Method for Determining Particulate Breakage Functions in Ball Milling. Part III. Simulation of an Open-Circuit Continuous Milling System," Powder Technology, Vol.7, pp. 169-179.

[20] Giusti, L., 1986, "The morphology, Mineralogy, and Behaviour of 'Fine-Grained' Gold from Placer Deposits of Alberta: Sampling and Implications for Mineral Exploration," Can. J. Earth Sci. Vol. 23, pp. 1662-1672.

[21] Graham, P.R., 1989, "Following the Gold Through Manhattan's Gravity Circuit by Size Distribution and a Flotation Method of Processing Gravity Concentrates," SME Annual Meeting, Las Vegas, Nevada, February 27-March 2.

[22] Guest, R.N. and Dunne, R.C., 1985, "An Evaluation of Gravity Separator by Use of a Synthetic Ore," Journal of the South African Institute of Mining and Metallurgy, June, Vol. 85, No. 6, pp. 121-124.

[23] Gupta, V.K., Hodouin, D., Bérubé M.A. and Everell, M.D., 1980, "The Estimation of Rate and Breakage Distribution Parameters from Batch Grinding Data for a Complex Pyrite Ore Using a Back-Calculation Method," Powder Technol., Vol.28, pp. 97-106.

[24] Gupta V.K., Zouit H. and Hodouin, D., 1985, "The Effect of Ball and Mill Diameter on Grinding Rate Parameters in Dry Grinding Operation," Powder Technol., Vol. 42, pp. 199-208.

[25] Gupta, V.K. and Kapur, P.C., 1974, "Empirical Correlations for the Effects of Particulate Mass and Ball Size on the Selection Parameters in the Discretized Batch Grinding Equation," Powder Technol., Vol. 10, pp. 217-223.

[26] Hallbauer, D.K. and Joughin, N.C., 1973, "The Size Distribution and Morphology of Gold Particles in Witwatersrand Reefs and Their Crushed Products," Journal of the South African Institute of Mining and Metallurgy, June, pp. 395-402.

[27] Herbst, J.A., Lo, Y.C. and Bohrer, J.E., 1987, "Increasing the Capacity of a Phosphate Grinding with the Aid of Computer Simulation," Minerals & Metallurgical Processing, Vol. 4, No. 3, August, pp. 155-160.

[28] Herbst, J.A. and Fuerstenau, D.W., 1968, "The Zero Order Production of Fine Sizes in Comminution and Its Implications in Simulation," Trans. AIME, Vol. 241, pp. 538-548.

[29] Hinds, H.L., Trautman, L.L. and Ommen, R.D., 1989, "Homestake's Improved Gravity Gold Recovery Circuit," SEM Annual Meeting, Las Vegas, Nevada, February 27 - March 2.

[30] Hodouin, D., Bérubé, M.A. and Everell, M.D., 1978, "Modelling In Industrial Grinding Circuits and Applications in Design," CIM Bull., Sept., pp. 138-145.

[31] Kelly, E.G. and Spottiswood, D.J., 1990, "The Breakage Function; What Is It Really?," Minerals Engineering, Vol. 3, No. 5, pp. 405-415.

[32] Kelly, E.G. and Spottiswood, D.J., 1982, "Introduction to Mineral Processing," John Wiley & Sons, pp. 144-151.

[33] Kelsall, D.F., Stewart, P.S.B. and Weller K.R., 1973a, "Continuous Grinding in a Small Wet Ball Mill, Part IV. A Study of the Influence of Grinding Media Load and Density," Powder Technol., Vol.7, pp. 293-301.

[34] Kelsall, D.F., Stewart, P.S.B. and Weller K.R., 1977b, "Continuous Grinding in a Small Wet Ball Mill, Part V. A Study of the Influence of Media Shape," Powder Technol., Vol.8, pp. 77-90.

[35] Kelsall, D.F., Reid, K.J. and Restarick, C.J., 1967, "Continuous Grinding in a Small Wet Ball Mill, Part III. A Study of the Influence of Ball Diameter," Powder Technol., Vol. 1, pp. 291-299.

[36] Kelsall, D.F., Reid, K.J. and Restarick, C.J., 1968/69, "Continuous Grinding in a Small Wet Ball Mill, Part II. A Study of the Influence of Hold-Up Weight," Powder Technol., Vol. 2, pp. 162-168.

[37] Klimpel, R.R. and Austin, L.G., 1984, "Simulation of a Mill Grinding Copper Ore by Scale-up of Laboratory Data," Proc. Mintek 50, Johannesburg, South Africa.

[38] Knelson, B.V., 1988, "Centrifugal Concentration and Separation of Precious Metals," 2nd International Conference on Gold Mining, Vancouver, Nov., pp. 303-317.

[39] Knelson, B.V., 1990, "Development and Economic Application of Knelson Concentrator in Low Grade Alluvial Gold Deposits," The AuslMIM 1990 Annual Conference, Rotorua, New Zealand, 18-21 March, pp. 123-128.

[40] Knelson, B.V., 1985, "Centrifugal Concentration and Separation of Precious Metals," 17 Annual Meeting of the CMP, Ottawa, pp. 346-357.

[41] Lammers, J.M., 1984, "The Process Design of the Ok Tedi Project,"The First International Symposium on Precious Metals Recovery, Reno, Nevada, June 10-14, Paper IV.

[42] Laplante, A.R., 1987, "Mineralogy and Metallurgical Performance of Various Gold-Copper Ores of the Chibougamau Area, Québec," Proc. Intern. Symp. on Gold Metallurgy, Eds. R. S. Salter, D.M. Wysouzil, G.W. Mcdonald, Winnipeg, Aug., pp. 141-155.

[43] Laplante, A.R., 1984, "Plant Sampling and Balancing for Gold Ores," 1st Intern. Symp. Precious on Metals Recovery, Reno, June, Paper V, p. 25.

[44] Laplante, A.R., 1985, Course Notes, "Modelling and Control of Mineral Processing Systems," Mining and Metallurgical Engng. Dept., McGill University, Sept., pp. 11-15.

[45] Laplante, A.R., Liu, L. and Cauchon, A., 1990, "Gold Recovery at the Mill of Les Mines Camchib, Inc., Chibougamau, Québec," Proc. - 22nd Annual Meeting of the Canadian Mineral Processors, Ottawa, 16-18 Jan., pp. 397-412.

[46] Laplante, A.R. and Finch, J.A., 1984, "The Origin of Unusual Cyclone Performance Curves," International Journal of Mineral Processing, Vol. 13, 1984, pp. 1-11.

[47] Larsen, C.R. and Tessier, R., 1987, "Golden Giant Mine Mill Description and Operating Highlights," Proceedings of 18th Annual Meeting of the CMP, Ottawa, Jan., pp. 108-135.

[48] Larsen, C.R., private communication.

[49] Liu, L., 1989, "An Investigation of Gold Recovery in the Grinding and Gravity Circuit at Les Mines Camchib Inc.," M. Eng. Thesis, Dept. of Mining and Metallurgical Engng., McGill University, Nov., pp. 92-93.

[50] Loveday, B.K. and Forbes, J.E., 1982, "Some Considerations in the Use of Gravity Concentration for the Recovery of Gold," Journal of the South African Institute of Mining and Metallurgy, May, pp. 121-124.

[51] McAlister, S.A., 1989, "Fine Gold Recovery Using the Falcon Concentrator," Northwest Mining Association 95th Annual Convention, Short Course and Trade Show, December 6.

[52] Mclean, J., 1975, "The Reichert Cone Gravity Concentration Pilot Plant, " Journal of the south African Institute of Mining and Metallurgy, October, pp. 95-97.

[53] Narayanan, S.S., 1987, "Modelling the Performance of Industrial Ball Mills Using Single Particle Breakage Data," International Journal of Mineral Processing, Vol. 20, No. 3-4, pp. 211-228.

[54] Plitt, L.R., 1976, "A Mathematical Model; of the Hydrocyclone Classifier, CIM Bull., Vol. 69, No. 776, Dec., pp. 114-123.

[55] Poling, G.W. and Hamilton, J.F., 1985, "Pilot Plant Study of Fine Gold Recovery of Selected Sluicebox Configurations," Department of Mining and Mineral Processing Engineering, University of British Columbia.

[56] Poling, G.W. and Wenqian, W., 1983, "Methods for Recovering Fine Placer Gold," CIM Bulletin, Vol. 76, No. 860, December, pp. 47-56.

[57] Pryor, E.J., 1955, "An Introduction to Mineral Dressing," Mining Publication, LTD., pp. 357-370.

[58] Pryor, E.J., 1965, "Mineral Processing," Elsevier Publishing Co., LTD., pp. 741-747.

[59] Reid, K.J., 1965, "A Solution to the Batch Grinding Equation," Chem. Eng. Sci., Vol. 20, pp. 953-963.

[60] Richards, R.H. and Locke, C.E., 1940, "Text Book of Ore Dressing," McGraw Hill, pp. 53-66.

[61] Robinson, C.N. and Dolphin, K., 1984, "Gold Placer in North America Using Reichert Spirals," Fourth Annual RMS-ROSS Seminar on Placer Gold Mining, Vancouver, British Columbia, February 6-9.

[62] Samskog, P., Bjorkman, J., Herbst, J.A. and Lo, Y.C., 1990, "Optimization of the Grinding Circuit at the Kiruna Plant of the LKAB Using Modelling and Simulation Techniques," Control '90 Mineral and Metallurgical Processing, AIME, pp. 279-287.

[63] Shoji, K., Lohrasb, S. and Austin, L.G., 1980, "The Variation of Breakage Parameters with Ball and Powder Loading in Dry Ball Milling ," Powder Technol., Vol. 25, pp. 109-114.

[64] Silva, M., 1986, "Placer Gold Recovery Methods," Special Publication 87, California Department of Conservation - Division of Mines and Geology, pp. 22-23.

[65] Smith, H.W. and Ichiyen, N., 1973, "Computer Adjustment of Metallurgical Balances, CIM Bull., Vol. 66, No. 737, Sept., pp. 97-100.

[66] Spiller, D.E. and Rau, E.L., 1982, Project NP-820134, Colorado School of Mines Research Institute, Nov., pp. 1-5.

[67] Splaine, M., Browner, S.J. and Dohm, C.E., 1982, "The Effect of Head Grade on Recovery Efficiency in a Gold-Reduction Plant," Journal of the South African Institute of Mining and Metallurgy, Vol. 82, January, pp. 6-11.

[68] Spring, R., 1985, "NORBAL2," Research Report N-8325; RR 85-1, Centre de Recherche Noranda, Poine Claire, Québec.

[69] Walsh, D.E. and Rao P.D., 1988, "Study of the Compound Water Cyclone's Concentrating Efficiency of Free Gold from Placer Material," CIM Bulletin, Vol. 81, No. 919, November, pp. 53-61.

[70] Weigao M. and Forssberg, E., 1989, "The Effect of Powder Filling on Selection and Breakage Functions in Batch Grinding," Powder Technol., Vol. 59, pp. 275-283.

[71] Wills, B.A., 1988, "Mineral Processing Technology," 4th Ed., Pergamon Press, Oxford, p. 359.

APPENDIX A

Appendix A.1: Size by size recovery by the Knelson Concentrator.

Appendix A.2: Cumulative gold recovery of the PCOF and SCOF with the MLS and 7.6 cm Knelson concentrator.

Appendix A.1: Size by size recovery by the Knelson Concentrator.

Size (μm)	Gold Reovery (%)		
	Knelson Concentrator		
	BMD	CUF	COF
+850	0.38	15.18	-
+600	3.61	3.69	-
+425	71.55	16.85	1.42
+300	56.17	37.59	4.88
+212	79.94	60.98	15.12
+150	83.19	63.83	24.69
+106	69.12	72.74	29.32
+75	51.57	62.51	29.44
+53	3.92	48.85	31.48
+38	29.49	60.82	18.87
-38	5.89	20.66	9.30
Total	36.09	52.87	18.63

Appendix A.2: Cumulative gold recovery of the PCOF and SCOF with the MLS and 7.6 cm Knelson concentrator.

Size (μm)		Cumulative Recovery (%)			
		PCOF		SCOF	
		Knelson	MLS	Knelson	MLS
-420/+150	C	20.10	5.73	37.81	11.04
	M1	-	11.23	-	19.54
	M2	-	14.39	-	50.24
+105	C	16.35	6.06	36.48	14.54
	M1	-	9.62	-	29.25
	M2	-	13.60	-	29.25
+75	C	26.70	4.29	39.81	20.54
	M1	-	5.54	-	24.89
	M2	-	7.81	-	27.91
+53	C	50.49	14.38	22.17	51.01
	M1	-	16.80	-	55.77
	M2	-	38.08	-	57.91
+38	C	51.76	34.43	16.63	39.70
	M1	-	38.15	-	42.62
	M2	-	43.68	-	43.70
-38	C	30.13	27.97	32.63	23.59
	M1	-	42.25	-	28.95
	M2	-	43.27	-	35.51

C: Concentrate M1: Middling 1 M2: Middling 2

APPENDIX B

B.1 Selection functions of gold and silica

B.2 Weight of randomly chosen flakes

B.1 Selection functions of gold and silica

Size class (μm)	Selection Function (s^{-1})		
	Silica	Gold	Ratio
+1010	0.00628	0.00166	3.78
+714	0.00442	0.00120	3.68
+504	0.00311	0.00086	3.62
+357	0.00218	0.00062	3.52
+252	0.00163	0.00046	3.54
+178	0.00108	0.00037	2.99
+126	0.00076	0.00024	3.17
+89	0.00054	0.00017	2.85
+63	0.00037	0.00013	2.85
+45	0.00027	0.00010	2.70

B.2: Weight of randomly chosen flakes

WEIGHT VARIATION OF GOLD FLAKES

1) GRINDING TIME = 0 s

ORIGINAL SIZE CLASS, 1200/850 um (+20 MESH)

NO	WEIGHT (g)	NO	WEIGHT (g)
1	0.0050	27	0.0083
2	0.0045	28	0.0042
3	0.0069	29	0.0027
4	0.0089	30	0.0021
5	0.0019	31	0.0057
6	0.0046	32	0.0064
7	0.0030	33	0.0038
8	0.0027	34	0.0040
9	0.0030	35	0.0027
10	0.0026	36	0.0034
11	0.0064	37	0.0059
12	0.0077	38	0.0067
13	0.0070	39	0.0024
14	0.0033	40	0.0036
15	0.0055	41	0.0045
16	0.0030	42	0.0052
17	0.0043	43	0.0021
18	0.0048	44	0.0025
19	0.0069	45	0.0141
20	0.0043	46	0.0051
21	0.0091	47	0.0025
22	0.0055	48	0.0089
23	0.0030	49	0.0058
24	0.0020	50	0.0046
25	0.0044	51	0.0019
26	0.0034	52	0.0043

WEIGHT VARIATION OF GOLD FLAKES

2) GRINDING TIME = 15 s

ORIGINAL SIZE CLASS, 1200/850 um (+20 MESH)

NO	WEIGHT (g)	NO	WEIGHT (g)
1	0.0042	27	0.0059
2	0.0049	28	0.0023
3	0.0036	29	0.0039
4	0.0046	30	0.0030
5	0.0114	31	0.0036
6	0.0030	32	0.0034
7	0.0130	33	0.0018
8	0.0054	34	0.0063
9	0.0029	35	0.0030
10	0.0036	36	0.0055
11	0.0068	37	0.0042
12	0.0067	38	0.0042
13	0.0034	39	0.0049
14	0.0026	40	0.0035
15	0.0025	41	0.0048
16	0.0037	42	0.0009
17	0.0042	43	0.0024
18	0.0045	44	0.0018
19	0.0051	45	0.0112
20	0.0041	46	0.0019
21	0.0046	47	0.0040
22	0.0035	48	0.0028
23	0.0070	49	0.0029
24	0.0046	50	0.0067
25	0.0039	51	0.0021
26	0.0032	52	0.0093

WEIGHT VARIATION OF GOLD FLAKES

3) GRINDING TIME = 30 s

SIZE	+850 um	+600 um	+425 um	+300 um
NO	W (g)	W (g)	W (g)	W (g)
1	0.0061	0.0030	0.0012	0.0003
2	0.0040	0.0053	0.0004	0.0002
3	0.0057	0.0029	0.0009	0.0004
4	0.0029	0.0041	0.0018	0.0008
5	0.0048	0.0041	0.0016	0.0005
6	0.0033	0.0006	0.0006	0.0006
7	0.0047	0.0029	0.0007	0.0003
8	0.0143	0.0033		0.0006
9	0.0034	0.0019		
10	0.0050	0.0031		
11	0.0062	0.0014		
12	0.0054			
13	0.0029			
14	0.0018			
15	0.0060			
16	0.0029			
17	0.0063			
18	0.0022			
19	0.0040			
20	0.0051			
21	0.0035			
22	0.0042			
23	0.0043			
24	0.0041			
25	0.0051			
26	0.0062			

WEIGHT VARIATION OF GOLD FLAKES

4) GRINDING TIME = 60 s

SIZE	+850 um	+600 um	+300 um
NO	W (g)	W (g)	W (g)
1	0.0037	0.0023	0.0006
2	0.0069	0.0030	0.0001
3	0.0055	0.0032	0.0005
4	0.0075	0.0046	0.0002
5	0.0081	0.0067	0.0003
6	0.0054	0.0056	0.0005
7	0.0025	0.0009	0.0002
8	0.0047	0.0027	
9	0.0069	0.0029	
10	0.0022	0.0010	
11	0.0110	0.0020	
12	0.0028	0.0034	
13	0.0005		
14	0.0023		
15	0.0030		
16	0.0052		
17	0.0033		
18	0.0041		
19	0.0091		
20	0.0050		
21	0.0042		
22	0.0027		
23	0.0042		
24	0.0036		
25	0.0050		
26	0.0072		
27	0.0102		
28	0.0038		
29	0.0029		
30	0.0032		

WEIGHT VARIATION OF GOLD FLAKES

5) GRINDING TIME = 90 s

SIZE	+850 um	+600 um	+425 um	+300 um
NO	W (g)	W (g)	W (g)	W (g)
1	0.0067	0.0065	0.0012	0.0002
2	0.0030	0.0039	0.0006	0.0005
3	0.0048	0.0029	0.0017	0.0004
4	0.0091	0.0007	0.0006	0.0005
5	0.0035	0.0028	0.0015	0.0004
6	0.0080	0.0052	0.0012	
7	0.0016	0.0022	0.0013	
8	0.0026	0.0036	0.0005	
9	0.0034	0.0017	0.0010	
10	0.0045	0.0036	0.0017	
11	0.0047	0.0032	0.0009	
12	0.0164	0.0043		
13	0.0078	0.0022		
14	0.0023	0.0030		
15	0.0030			
16	0.0050			
17	0.0110			
18	0.0110			
19	0.0037			
20	0.0072			
21	0.0047			

WEIGHT VARIATION OF GOLD FLAKES

6) GRINDING TIME = 150 s

SIZE	+850 um	+600 um	+425 um	+300 um
NO	W (g)	W (g)	W (g)	W (g)
1	0.0089	0.0046	0.0006	0.0004
2	0.0092	0.0027	0.0009	0.0019
3	0.0050	0.0023	0.0009	0.0003
4	0.0048	0.0020	0.0019	0.0005
5	0.0036	0.0039	0.0015	0.0003
6	0.0049	0.0033	0.0027	0.0004
7	0.0039	0.0030	0.0022	
8	0.0039	0.0029	0.0023	
9	0.0043	0.0031	0.0019	
10	0.0040	0.0037	0.0017	
11	0.0058	0.0046	0.0011	
12	0.0015	0.0022		
13	0.0021	0.0043		
14	0.0080	0.0023		
15	0.0046	0.0032		
16	0.0044	0.0031		
17	0.0057	0.0018		
18	0.0049			
19	0.0039			

WEIGHT VARIATION OF GOLD FLAKES

7-1) GRINDING TIME = 210 s

SIZE	+850 um	+600 um	+425 um	+300 um
NO	W (g)	W (g)	W (g)	W (g)
1	0.0036	0.0030	0.0012	0.0005
2	0.0035	0.0026	0.0016	0.0006
3	0.0084	0.0018	0.0018	0.0011
4	0.0042	0.0021	0.0015	0.0004
5	0.0062	0.0025	0.0022	0.0006
6	0.0034	0.0016	0.0021	0.0008
7	0.0113	0.0037	0.0012	0.0007
8	0.0122	0.0036	0.0011	0.0004
9	0.0028	0.0061	0.0016	0.0006
10	0.0067	0.0030	0.0009	0.0003
11	0.0063	0.0032	0.0021	
12	0.0046	0.0035	0.0007	
13	0.0054		0.0013	
14	0.0021			
15	0.0019			
16	0.0051			

WEIGHT VARIATION OF GOLD FLAKES

7-2) GRINDING TIME = 210 s

ORIGINAL SIZE CLASS, 1200/850 um (+20 MESH)

NO	WEIGHT (g)	NO	WEIGHT (g)
1	0.0038	27	0.0055
2	0.0059	28	0.0044
3	0.0069	29	0.0035
4	0.0085	30	0.0050
5	0.0096	31	0.0041
6	0.0035	32	0.0084
7	0.0037	33	0.0032
8	0.0047	34	0.0036
9	0.0035	35	0.0025
10	0.0022	36	0.0025
11	0.0059	37	0.0034
12	0.0052	38	0.0063
13	0.0026	39	0.0039
14	0.0040	40	0.0036
15	0.0014	41	0.0039
16	0.0032	42	0.0040
17	0.0093	43	0.0135
18	0.0040	44	0.0070
19	0.0062	45	0.0023
20	0.0163	46	0.0049
21	0.0049	47	0.0047
22	0.0041	48	0.0072
23	0.0064	49	0.0029
24	0.0031	50	0.0096
25	0.0058	51	0.0069
26	0.0053	52	0.0036

WEIGHT VARIATION OF GOLD FLAKES

7-3) GRINDING TIME = 210 s

SIZE CLASS, 850/600 um (+28 MESH)

NO	WEIGHT (g)	NO	WEIGHT (g)
1	0.0025	24	0.0020
2	0.0017	25	0.0012
3	0.0024	26	0.0028
4	0.0011	27	0.0031
5	0.0035	28	0.0038
6	0.0039	29	0.0029
7	0.0039	30	0.0025
8	0.0020	31	0.0041
9	0.0028	32	0.0036
10	0.0047	33	0.0026
11	0.0026	34	0.0028
12	0.0030	35	0.0026
13	0.0012	36	0.0021
14	0.0023	37	0.0008
15	0.0031	38	0.0036
16	0.0059	39	0.0030
17	0.0017	40	0.0024
18	0.0021	41	0.0029
19	0.0025	42	0.0026
20	0.0036	43	0.0033
21	0.0037	44	0.0037
22	0.0022	45	0.0066
23	0.0024	46	0.0033

Appendix C

Appendix C.1: Size distribution of the various streams.

Appendix C.2: Recovery and grade of the various streams.

Appendix C.3: Size-by-size grade and overall grade of the streams of the secondary loop.

Appendix C.4: Grade of the various streams estimated from sub-sieve analysis.

Appendix C.5: The balanced size distribution of the ore in sub-sieve ranges.

Appendix C.6: The balanced size distribution of the gold in sub-sieve ranges.

Appendix C.7: Estimated recovery of sub-sieve ranges of the various streams.

Appendix C.8: Results of calculation of the selection function of the gold and ore.

Appendix C.1 : Size distribution of the various streams

Size class (μm)	PMD	PCUF	PCOF	SMD	SCUF	TMD	SCOF
	%						
+1200	0.90	0.39	0.00	0.06	0.00	0.00	0.00
+850	1.54	0.79	0.00	0.23	0.00	0.00	0.00
+600	2.71	1.46	0.00	0.48	0.00	0.00	0.00
+425	3.99	2.71	0.00	1.22	0.00	0.00	0.00
+300	6.98	6.89	0.00	4.16	0.27	0.00	0.00
+212	10.31	14.63	1.33	10.84	1.91	1.37	0.50
+150	12.35	18.72	4.81	16.60	1.96	5.51	1.74
+106	14.69	20.67	14.16	20.51	27.15	16.98	5.17
+75	11.94	13.80	13.90	14.85	23.25	19.98	12.97
+53	9.51	11.65	12.11	13.55	9.84	18.37	14.05
+38	6.93	4.53	14.58	6.30	15.56	15.16	14.11
-38	18.15	3.76	39.11	11.20	20.06	22.63	51.46

Appendix C.2 : Recovery and grade of the various streams

KNELSON CONCENTRTATOR STUDY
HEMLO MINE'S SAMPLES

I: PMD 1,2

MASS PROCESSED = 12988 g

Size (um)	W (g) TL.	Au (mg)	W (g) CONC.	Au (mg)	Au (g/t) TOTAL	R %	MASS (g)	MASS %	UNITS
+1200	2.506	0.0319	1.875	0.0351	12.84	2.61	104.57	0.80	10.30
+850	4.390	0.0711	2.064	6.1799	49.97	67.96	181.97	1.40	69.80
+600	8.088	0.0772	3.446	0.0453	9.58	1.41	334.90	2.57	24.63
+425	12.486	0.1285	5.458	1.5472	13.17	22.71	517.15	3.97	52.29
+300	21.225	0.3216	8.887	6.3793	22.26	32.62	878.71	6.74	150.12
+212	30.600	0.3058	13.376	6.6960	15.17	34.82	1267.40	9.73	147.58
+150	36.700	0.2722	15.800	8.6247	13.01	43.60	1519.81	11.66	151.81
+106	42.520	0.2855	16.300	8.4002	11.43	41.79	1758.82	13.50	154.26
+75	39.280	0.2574	13.700	8.9732	12.02	45.97	1623.44	12.46	149.83
+53	31.400	0.2734	7.525	5.9885	13.28	34.83	1294.33	9.93	131.96
+44	12.188	0.2062	4.384	4.5043	25.71	34.77	503.86	3.87	99.43
+38	11.461	0.8121	2.318	2.8175	76.48	7.81	472.00	3.62	277.06
-38	62.600	1.0359	6.600	1.9602	17.27	4.41	2572.02	19.74	340.88
TOTAL	315.444	4.07876	101.733	62.1514	17.60	27.10	13028.98	100.00	1759.95

I-2: PMD 3

MASS PROCESSED = 7608 g

Size (um)	W (g) TL.	Au (mg)	W (g) CONC.	Au (mg)	Au (g/t) TOTAL	R %	MASS (g)	MASS %	UNITS
+1200	4.645	0.0860	1.148	0.0194	18.49	1.39	75.67	0.99	18.39
+850	7.852	0.0995	1.936	5.0900	52.27	76.13	127.91	1.68	87.89
+600	13.300	0.1544	3.302	0.0381	11.61	1.51	216.68	2.85	33.06
+425	18.600	0.1809	5.552	6.3900	30.57	68.77	303.96	4.00	122.14
+300	33.500	0.2657	9.550	5.3076	17.50	55.46	547.01	7.19	125.79
+212	50.700	0.4546	12.789	4.6057	14.40	38.71	826.20	10.86	156.40
+150	60.600	0.4315	16.700	5.4271	12.40	43.94	988.95	13.00	162.33
+106	74.200	0.6549	14.524	4.9108	12.80	31.85	1204.97	15.84	202.65
+75	53.300	0.2100	10.277	4.4573	9.04	56.95	865.41	11.37	102.87
+53	42.400	0.2143	8.004	4.7919	11.96	58.22	688.26	9.05	108.18
+44	19.300	0.0960	3.099	2.2286	12.05	59.13	312.74	4.11	49.54
+38	10.395	0.0896	2.875	2.3417	22.28	61.96	169.65	2.23	49.67
-38	79.500	1.1798	5.100	6.5054	19.86	25.58	1280.57	16.83	334.30
TOTAL	468.292	4.11718	94.856	52.1136	15.53	44.10	7607.99	100.00	1553.21

II-1: PCUF 1

MASS PROCESSED =9061 g

Size (um)	W (g) TL.	Au (mg)	W (g) CONC.	Au (mg)	Au (g/t) TOTAL	R %	MASS (g)	MASS %	UNITS
+1200	1.477	0.0126	0.995	13.261	401.17	97.94	33.75	0.37	149.41
+850	2.925	0.0399	1.899	20.472	319.87	95.86	66.77	0.74	235.66
+600	5.357	0.1245	3.061	47.552	412.85	94.51	121.87	1.34	555.17
+425	10.227	0.2703	5.312	84.671	390.59	93.39	232.12	2.56	1000.44
+300	26.747	0.9578	11.212	145.184	275.36	87.24	604.40	6.67	1836.40
+212	59.300	1.3311	17.400	208.539	178.65	87.60	1332.54	14.70	2626.83
+150	70.000	1.1184	26.500	402.460	270.60	94.19	1578.94	17.42	4714.57
+106	85.033	1.7314	19.200	388.961	224.33	91.01	1905.04	21.02	4715.62
+75	55.870	1.1230	23.300	668.680	549.43	96.41	1262.37	13.93	7653.25
+53	47.300	1.8450	14.500	546.770	552.59	93.04	1063.51	11.74	6484.74
+44	16.458	1.2349	4.200	269.677	804.61	90.78	369.20	4.07	3277.90
+38	6.806	1.1978	1.984	192.482	1432.37	87.87	152.93	1.69	2417.03
-38	15.200	3.2605	2.100	280.158	1039.11	79.48	339.20	3.74	3889.26
TOTAL	402.7	14.2472	131.663	3268.8662	395.56	91.19	9062.62	100.00	39556.28

II-2: PCUF 2

MASS PROCESSED = 7777 g

Size (um)	W (g) TL.	Au (mg)	W (g) CONC.	Au (mg)	Au (g/t) TOTAL	R %	MASS (g)	MASS %	UNITS
+1200	2.134	6.1073	1.225	0.1049	2754.76	0.12	31.74	0.41	1124.20
+850	4.300	0.2604	1.985	16.2769	315.09	81.38	63.48	0.82	257.15
+600	8.100	0.3218	3.650	34.1937	324.70	88.14	119.48	1.54	498.79
+425	15.400	0.4690	5.624	57.6740	285.07	89.58	225.84	2.90	827.73
+300	39.600	1.3532	11.281	132.6119	263.11	87.27	577.56	7.43	1953.76
+212	82.200	1.8799	17.200	205.5752	194.91	88.44	1192.66	15.33	2988.68
+150	101.800	2.3808	22.700	306.7086	230.48	90.01	1478.44	19.01	4381.03
+106	108.800	2.1473	19.400	408.1419	278.59	93.00	1575.24	20.25	5642.21
+75	70.500	1.4678	14.856	438.4096	449.07	95.43	1023.01	13.15	5906.43
+53	53.900	2.0626	12.060	426.3656	582.32	93.53	782.83	10.06	5860.94
+44	22.800	1.7940	3.535	225.2786	761.38	89.78	329.58	4.24	3226.21
+38	9.685	3.3827	2.135	190.2534	1696.83	79.73	140.63	1.81	3067.98
-38	18.600	4.2786	2.000	266.8174	1223.98	81.35	267.98	3.45	4217.07
TOTAL	535.685	27.9054	117.651	2708.31	399.51	87.16	7777.95	100.00	39952.18

III-1 : SMD 1,3

MASS PPROCESSED = 8555 g

Size (um)	W (g) TL.	Au (mg)	W (g) CONC.	Au (mg)	Au (g/t) TOTAL	R %	MASS (g)	MASS %	UNITS
+1200	0.000	0.0000	0.000	0.0000	0.00	0.00	0.00	0.00	0.00
+850	1.042	0.3225	1.699	30.6402	1887.50	85.06	19.08	0.22	421.05
+600	2.285	0.1840	2.008	30.1642	828.14	90.76	40.13	0.47	388.48
+425	6.200	0.3406	3.745	69.0756	697.46	92.40	107.19	1.25	873.85
+300	20.700	1.2254	8.465	140.5740	455.08	87.30	353.83	4.14	1882.16
+212	55.400	1.9320	14.810	231.8385	281.19	87.79	939.11	10.98	3086.76
+150	84.800	1.4410	22.600	349.7034	260.01	93.57	1437.41	16.80	4368.74
+106	104.500	1.4969	26.400	507.5664	300.89	95.31	1769.89	20.69	6224.91
+75	72.200	2.1664	17.700	500.2208	438.82	93.26	1222.29	14.29	6269.61
+53	70.000	2.0874	12.793	529.2544	477.76	93.83	1180.68	13.80	6593.58
+44	21.300	1.1729	4.162	264.5293	790.19	93.11	359.53	4.20	3320.84
+38	9.591	0.6749	1.800	119.4878	808.00	91.39	161.82	1.89	1528.32
-38	57.500	5.0474	4.700	384.1197	485.80	82.02	964.04	11.27	5474.36
TOTAL	505.518	18.0914	120.882	3157.1743	404.33	91.27	8554.99	100.00	40432.67

III-2: SMD 2

MASS PROCESSED = 5540

Size (um)	W (g) TL.	Au (mg)	W (g) CONC.	Au (mg)	Au (g/t) TOTAL	R %	MASS (g)	MASS %	UNITS
+1200	0.588	0.0288	0.737	10.8711	1819.81	97.63	6.12	0.11	200.99
+850	1.253	0.0287	1.335	26.5542	2094.58	99.02	12.80	0.23	484.06
+600	2.626	0.1904	2.900	19.0790	773.05	91.63	26.93	0.49	375.84
+425	6.594	0.5077	5.192	45.8951	771.12	90.81	65.54	1.18	912.31
+300	24.310	0.8011	9.290	86.0750	402.99	92.15	231.78	4.18	1686.04
+212	63.400	1.3464	13.128	142.4635	260.85	92.04	593.39	10.71	2793.97
+150	97.100	1.4594	19.600	224.0098	261.33	94.37	908.30	16.40	4284.59
+106	120.640	2.2095	22.700	316.7013	299.00	94.00	1126.85	20.34	6081.64
+75	91.069	1.6680	20.100	333.3971	408.46	95.62	853.60	15.41	6293.55
+53	78.600	2.5013	17.200	329.2351	478.06	93.50	736.58	13.30	6356.09
+44	27.200	1.7733	5.070	158.5283	687.98	90.77	254.02	4.59	3154.48
+38	11.190	0.6933	4.600	175.0947	1695.46	96.50	107.02	1.93	3275.09
-38	66.800	6.6769	5.700	173.7436	380.59	73.98	617.08	11.14	4239.22
TOTAL	591.370	19.8848	127.552	2041.6478	401.38	91.82	5540.01	100.00	40137.88

IV: PCOF

MASS PROCESSED = 6043 g

Size (um)	W (g) TL.	Au (mg)	W (g) CONC.	Au (mg)	Au (g/t) TOTAL	R %	MASS (g)	MASS %	UNITS
+1200	0.000	0.0000	0.000	0.0000	0.00	0.00	0.00	0.00	0.00
+850	0.000	0.0000	0.000	0.0000	0.00	0.00	0.00	0.00	0.00
+600	0.000	0.0000	0.000	0.0000	0.00	0.00	0.00	0.00	0.00
+425	0.000	0.0000	0.000	0.0000	0.00	0.00	0.00	0.00	0.00
+300	0.000	0.0000	0.000	0.0000	0.00	0.00	0.00	0.00	0.00
+212	4.200	0.0121	2.787	9.0415	114.96	97.580	80.60	1.33	153.33
+150	15.500	0.0461	3.668	0.2142	3.67	20.050	290.84	4.81	17.68
+106	45.700	0.1441	8.883	0.5220	3.73	16.354	855.57	14.16	52.82
+75	44.600	0.1454	13.750	0.9814	4.37	26.703	840.05	13.90	60.82
+53	38.100	0.1387	26.200	2.6210	7.09	50.494	732.08	12.11	85.90
+44	28.800	0.1329	10.912	2.2389	8.63	47.624	544.49	9.01	77.79
+38	17.700	0.1565	8.664	3.6766	19.54	55.908	336.59	5.57	108.82
-38	126.900	2.3460	11.700	18.7474	26.33	30.134	2362.78	39.10	1029.49
TOTAL	321.500	3.1218	86.564	38.0430	15.87	39.677	6042.99	100.00	1586.64

V-I: SCUF 1

MASS PROCESSED = 5800 g

Size (um)	W (g) TL.	Au (mg)	W (g) CONC.	Au (mg)	Au (g/t) TOTAL	R %	MASS (g)	MASS %	UNITS
+1200	0.000	0.0000	0.000	0.0000	0.00	0.00	0.00	0.00	0.00
+850	0.000	0.0000	0.000	0.0000	0.00	0.00	0.00	0.00	0.00
+600	0.000	0.0000	0.000	0.0000	0.00	0.00	0.00	0.00	0.00
+425	0.000	0.0000	0.000	0.0000	0.00	0.00	0.00	0.00	0.00
+300	1.578	0.0330	0.000	0.0000	20.91	0.00	13.92	0.24	5.02
+212	12.599	0.1144	2.140	7.0503	71.13	87.48	113.31	1.95	138.96
+150	65.200	0.5783	3.743	2.2474	12.69	30.58	579.06	9.98	126.73
+106	179.700	1.0051	11.435	9.2454	11.24	51.04	1597.09	27.54	312.32
+75	164.200	1.9671	20.400	25.0062	28.83	59.03	1469.28	25.33	730.41
+53	63.800	1.7043	27.800	57.1824	122.25	79.18	590.76	10.19	1245.19
+44	52.600	2.0489	10.300	38.9096	120.12	68.28	474.44	8.18	932.57
+38	33.600	2.0686	8.121	63.4068	268.09	77.65	304.60	5.25	1407.93
-38	73.700	8.9577	7.200	161.5913	365.97	67.15	657.52	11.34	4148.85
TOTAL	646.977	18.4774	91.139	364.6394	90.98	69.102	5800.00	100.00	9087.97

V-2:SCUF 2

MASS PROCESSED = 6674 g

Size (um)	W (g) TL.	Au (mg)	W (g) CONC.	Au (mg)	Au (g/t) TOTAL	R %	MASS (g)	MASS %	UNITS
+1200	0.000	0.0000	0.000	0.0000	0.00	0.00	0.00	0.00	0.00
+850	0.000	0.0000	0.000	0.0000	0.00	0.00	0.00	0.00	0.00
+600	0.000	0.0000	0.000	0.0000	0.00	0.00	0.00	0.00	0.00
+425	0.000	0.0000	0.000	0.0000	0.00	0.00	0.00	0.00	0.00
+300	1.810	0.1405	0.000	0.0000	177.68	0.00	19.29	0.29	51.35
+212	11.378	0.1189	3.191	3.1768	51.72	71.49	124.43	1.86	96.42
+150	62.000	0.3321	3.500	3.0287	8.93	46.12	664.13	9.95	88.84
+106	166.500	0.8924	12.000	11.6089	8.20	54.97	1786.12	26.76	219.52
+75	130.500	0.9113	23.100	28.2388	21.92	74.41	1413.63	21.18	464.21
+53	56.400	0.6324	31.800	73.9256	121.43	91.65	632.76	9.48	1151.31
+44	70.700	1.7128	11.100	49.9356	68.20	73.23	764.44	11.45	781.13
+38	38.100	1.7182	8.806	73.6227	198.36	80.08	414.78	6.21	1232.78
-38	79.400	10.3744	8.400	200.2185	247.25	64.43	854.44	12.80	3165.36
TOTAL	616.788	16.8330	101.897	443.7556	72.51	71.22	6674.02	100.00	7250.91

VI: TMD

MASS PROCESSED = 10428 g

Size (um)	W (g) TL.	Au (mg)	W (g) CONC.	Au (mg)	Au (g/t) TOTAL	R %	MASS (g)	MASS %	UNITS
+1200	0.000	0.0000	0.000	0.0000	0.000	0.00	0.00	0.00	0.00
+850	0.000	0.0000	0.000	0.0000	0.000	0.00	0.00	0.00	0.00
+600	0.000	0.0000	0.000	0.0000	0.000	0.00	0.00	0.00	0.00
+425	0.000	0.0000	2.240	0.6807	303.88	100.00	2.24	0.02	6.53
+300	0.000	0.0000	0.518	0.3885	750.00	100.00	0.52	0.00	3.73
+212	4.066	0.0477	1.103	2.3768	28.79	59.58	138.57	1.33	38.26
+150	16.718	0.0835	3.737	6.8109	16.93	70.70	568.94	5.46	92.39
+106	52.000	0.2716	10.986	21.3369	17.25	69.91	1769.01	16.96	292.67
+75	61.200	0.4255	17.500	44.9590	28.44	75.76	2086.56	20.01	569.10
+53	55.900	0.7384	27.200	88.1819	59.02	77.94	1917.07	18.38	1085.05
+44	25.400	0.2737	17.600	91.5655	115.05	90.82	876.33	8.40	966.84
+38	20.700	1.0165	5.587	34.5946	97.76	50.17	705.41	6.76	661.32
-38	69.500	3.0130	13.400	76.0650	103.91	30.98	2363.06	22.66	2354.74
TOTAL	305.484	7.8699	99.871	366.9598	60.71	57.97	10427.70	100.00	6070.62

VII: SCOF

MASS PROCESSED = 3598 g

Size (um)	W (g) TL.	Au (mg)	W (g) CONC.	Au (mg)	Au (g/t) TOTAL	R %	MASS (g)	MASS %	UNITS
+1200	0.000	0.0000	0.000	0.0000	0.00	0.00	0.00	0.00	0.00
+850	0.000	0.0000	0.000	0.0000	0.00	0.00	0.00	0.00	0.00
+600	0.000	0.0000	0.000	0.0000	0.00	0.00	0.00	0.00	0.00
+425	0.000	0.0000	0.000	0.0000	0.00	0.00	0.00	0.00	0.00
+300	0.000	0.0000	0.000	0.0000	0.00	0.00	0.00	0.00	0.00
+212	0.000	0.0000	1.766	1.6441	930.97	100.00	1.77	0.05	45.69
+150	1.968	0.1544	2.283	2.5717	121.04	37.81	56.19	1.56	189.02
+106	6.418	0.5152	5.691	8.1036	122.41	36.48	181.49	5.04	617.44
+75	16.800	0.4318	8.225	7.8214	41.95	39.81	468.40	13.02	546.11
+53	17.900	0.7863	16.700	6.3489	55.00	22.77	507.00	14.09	775.06
+44	10.538	0.4667	15.300	3.3443	53.06	20.74	303.95	8.45	448.24
+38	7.200	0.3310	6.217	1.2973	50.94	12.52	203.43	5.65	288.04
-38	67.700	1.3621	21.400	18.0700	29.52	32.63	1875.78	52.13	1539.17
TOTAL	128.524	4.0475	77.582	49.2013	44.49	30.74	3598.00	100.00	4448.78

Appendix C.3: Size-by-size grade and overall grade of the streams of the secondary loop

Size (μm)	Grade (g/t)		
	SCUF	TMD	SCOF
+1200	0.00	0.00	0.00
+850	0.00	0.00	0.00
+600	0.00	0.00	0.00
+425	0.00	303.88	0.00
+300	99.30	750.00	0.00
+212	61.43	28.79	930.97
+150	10.81	16.93	121.04
+106	9.77	17.25	122.41
+75	25.38	28.44	41.95
+53	121.84	59.02	55.00
+44	94.16	115.05	53.06
+38	233.23	97.76	50.94
-38	306.61	103.91	29.52
Σ	81.75	60.71	44.49

Appendix C.4: Grade of the various streams estimated from sub-sieve analysis

Stream		Concentrate Weight (g)	Au (mg)	Total Au (mg)	Tails Weight (g)	Au (mg)	Total Au (mg)	Grand T.Au (mg)	Grade (g/t)
PMD 1,2	+25 um	0.19	0.3168	2.248	0.98	0.0365	9.744	11.992	45.604
	+15 um	0.44	0.1305	0.926	3.95	0.0286	7.635	8.561	8.095
	-15 um	0.30	1.2036	8.542	4.68	0.1067	28.484	37.025	29.586
	Total	0.93	1.6509	11.716	9.61	0.1718	45.862	57.578	22.387
PMD 3	+25 um	0.14	0.1315	0.664	1.02	0.0380	5.017	5.681	41.965
	+15 um	0.48	1.1432	5.773	5.01	0.0322	4.252	10.024	15.098
	-15 um	0.39	0.0719	0.363	3.63	0.0982	12.966	13.329	27.696
	Total	1.01	1.3466	6.800	9.66	0.1684	22.235	29.035	22.673
PCUF 1	+25 um	0.34	49.1036	130.529	0.16	0.4244	147.490	278.019	4919.985
	+15 um	0.24	15.8029	42.008	0.50	0.0574	19.948	61.956	355.248
	-15 um	0.21	49.5161	131.625	0.31	0.1197	41.599	173.224	1599.608
	Total	0.79	114.4226	304.161	0.97	0.6015	209.037	513.199	1512.963
PCUF 2	+25 um	0.15	23.1594	87.394	0.43	0.2163	18.499	105.893	2835.802
	+15 um	0.21	11.5241	43.487	1.28	0.1142	9.767	53.254	482.971
	-15 um	0.17	16.7335	63.145	1.40	0.3406	29.130	92.275	766.559
	Total	0.53	51.417	194.026	3.11	0.6711	57.395	251.422	938.210
SMD 1,3	+25 um	0.27	29.0565	132.588	1.60	0.2848	28.167	160.755	1008.038
	+15 um	0.43	14.4569	65.968	4.55	0.3542	35.031	100.999	223.469
	-15 um	0.33	25.2791	115.351	3.55	0.2087	20.641	135.992	385.680
	Total	1.03	68.7925	313.908	9.7	0.8477	83.838	397.746	412.584
SMD 2	+25 um	0.09	0.0585	1.450	0.93	0.2919	18.526	19.976	326.110
	+15 um	0.07	4.1765	103.505	3.67	0.2290	14.534	118.038	503.023
	-15 um	0.07	2.1136	52.381	5.02	0.7238	45.937	98.318	306.918
	Total	0.23	6.3486	157.335	9.62	1.2447	78.997	236.332	383.499
PCOF	+25 um	0.18	0.1874	2.088	1.82	0.0295	7.100	9.188	20.880
	+15 um	0.45	0.1526	1.700	3.68	0.0381	9.170	10.870	12.204
	-15 um	0.42	1.1238	12.522	4.27	0.1054	25.368	37.890	36.701
	Total	1.05	1.4638	16.311	9.77	0.1730	41.638	57.949	24.522
SCUF 1	+25 um	0.20	4.2901	29.701	2.15	0.3103	20.902	50.603	346.095
	+15 um	0.50	6.4618	44.736	4.67	0.3688	24.843	69.578	218.774
	-15 um	0.34	17.5482	121.488	2.83	0.4722	31.808	153.295	794.336
	Total	1.04	28.3001	195.924	9.65	1.1513	77.553	273.477	416.102
SCUF 2	+25 um	0.09	2.3285	150.457	0.78	0.0858	7.494	157.951	2136.009
	+15 um	0.03	0.5666	36.611	6.07	0.2977	26.004	62.615	117.665
	-15 um	0.01	0.3592	23.210	2.84	0.9309	81.312	104.522	420.249
	Total	0.13	3.2543	210.278	9.69	1.3144	114.810	325.088	380.307
TMD	+25 um	0.17	3.9603	104.055	1.41	0.1209	28.989	133.044	388.393
	+15 um	0.22	2.1018	55.224	4.63	0.2302	55.196	110.420	98.948
	-15 um	0.12	3.9127	102.804	3.76	0.3945	94.591	197.396	218.187
	Total	0.51	9.9748	262.083	9.8	0.7456	178.776	440.859	110.902
SCOF	+25 um	0.21	0.1475	2.147	0.83	0.0516	9.793	11.941	74.357
	+15 um	0.74	0.1900	2.766	3.94	0.0204	3.872	6.638	8.750
	-15 um	0.52	4.8202	70.172	5.00	0.1414	26.837	97.009	101.415
	Total	1.47	5.1577	75.085	9.77	0.2134	40.502	115.587	61.623

Appendix C.5: The balanced size distribution of the ore in sub-sieve ranges.

B

1	0	2.803	0	-1	0	-2.803	0
0	1	0	2.803	0	-1	0	-2.803

V

0.023	0	0	0	0	0	0	0
0	0.179	0	0	0	0	0	0
0	0	0.011	0	0	0	0	0
0	0	0	0.115	0	0	0	0
0	0	0	0	0.132	0	0	0
0	0	0	0	0	0.539	0	0
0	0	0	0	0	0	0.00003	0
0	0	0	0	0	0	0	0.0002

B*V

0.023	0	0.030833	0	-0.132	0	-0.00008	0
0	0.179	0	0.322345	0	-0.539	0	-0.000560

B transpose

1	0
0	1
2.803	0
0	2.803
-1	0
0	-1
-2.803	0
0	-2.803

(B*V*B(T))

0.241660	0
0	1.623104

(B*V*B(T)) INVERSE

4.138034	0
0	0.616103

V*B(T)

0.023	0
0	0.179
0.030833	0
0	0.322345
-0.132	0
0	-0.539
-0.000084	0
0	-0.000560

V*B(T)*(B*V*B(T))(INVERSE)

0.095174	0
0	0.110282
0.127588	0
0	0.198597
-0.54622	0
0	-0.33207
-0.00034	0
0	-0.00034

V*B(T)*(B*V*B(T))(INVERSE)*B

0.0951748	0	0.26677496	0	-0.09517	0	-0.26677
0	0.1102824	0	0.309121	0	-0.11028	0
0.1275880	0	0.35762924	0	-0.12758	0	-0.35762
0	0.1985978	0	0.556669	0	-0.19859	0
-0.546220	0	-1.5310563	0	0.546220	0	1.531056
0	-0.332079	0	-0.93081	0	0.332079	0
-0.000347	0	-0.0009753	0	0.000347	0	0.000975
0	-0.000345	0	-0.00096	0	0.000345	0

SIZE (um)	UNADJUSTED (%)	ADJUSTMENT (%)	ADJUSTED (%)			
+25(PMD)	1.89	0.273	2.16			(%)
+15	8.45	-0.352	8.10	PMD	-15 um=	7.93
+25(SMD)	1.44	0.366	1.81			
+15	4.69	-0.634	4.06	SMD	-15 um=	5.16
+25(PCOF)	7.28	-1.566	5.71			
+15	14.73	1.061	15.79	PCOF	-15 um=	17.59
+25(PCUF)	0.54	-0.001	0.54			
+15	1.31	0.001	1.31	PCUF	-15 um=	1.72

ORE TO UNDERFLOW

(um)	(%)
+25	20.95
+15	18.87
-15	21.15

Appendix C.6: The balanced size distribution of the gold in sub-sieve ranges.

B

2.16	0	0	5.07	0	0	-5.71	0	0	-1.51	0
0	8.1	0	0	11.38	0	0	-15.79	0	0	-3.67
0	0	7.93	0	0	14.46	0	0	-17.59	0	0
2.16	8.1	7.93	0	0	0	-5.71	-15.79	-17.59	0	0
0	0	0	5.07	11.38	14.46	0	0	0	-1.51	-3.67

V

15	0	0	0	0	0	0	0	0	0	0
0	7	0	0	0	0	0	0	0	0	0
0	0	9	0	0	0	0	0	0	0	0
0	0	0	96	0	0	0	0	0	0	0
0	0	0	0	228	0	0	0	0	0	0
0	0	0	0	0	85	0	0	0	0	0
0	0	0	0	0	0	3	0	0	0	0
0	0	0	0	0	0	0	1.5	0	0	0
0	0	0	0	0	0	0	0	3	0	0
0	0	0	0	0	0	0	0	0	804	0
0	0	0	0	0	0	0	0	0	0	200
0	0	0	0	0	0	0	0	0	0	0

B*V

32.4	0	0	486.72	0	0	-17.13	0	0	-1214.04	0
0	56.7	0	0	2594.64	0	0	-23.685	0	0	-734
0	0	71.37	0	0	1229.1	0	0	-52.77	0	0
32.4	56.7	71.37	0	0	0	-17.13	-23.685	-52.77	0	0
0	0	0	486.72	2594.64	1229.1	0	0	0	-1214.04	-734

B transpose

2.16	0	0	2.16	0
0	8.1	0	8.1	0
0	0	7.93	7.93	0
5.07	0	0	0	5.07
0	11.38	0	0	11.38
0	0	14.46	0	14.46
-5.71	0	0	-5.71	0
0	-15.79	0	-15.79	0
0	0	-17.59	-17.59	0
-1.51	0	0	0	-1.51
0	-3.67	0	0	-3.67
0	0	-4.82	0	-4.82

(B*V*B(T))

4468.6672	0	0	167.7963	4300.870
0	33054.039	0	833.25615	32220.78
0	0	25075.074	1494.1884	23580.88
167.7963	833.25615	1494.1884	2495.2408	0
4300.8708	32220.783	23580.886	0	60102.54

(B*V*B(T)) INVERSE

9999.9998	9999.9998	9999.9998	-9999.999	-9999.99
9999.9998	10000.000	10000.000	-10000.00	-10000.0
9999.9998	10000.000	10000.000	-10000.00	-10000.0
-9999.999	-10000.00	-10000.00	10000.000	10000.00
-9999.999	-10000.00	-10000.00	10000.000	10000.00

V*B(T)

32.4	0	0	32.4	0
0	56.7	0	56.7	0
0	0	71.37	71.37	0
486.72	0	0	0	486.72
0	2594.64	0	0	2594.64
0	0	1229.1	0	1229.1
-17.13	0	0	-17.13	0
0	-23.685	0	-23.685	0
0	0	-52.77	-52.77	0
-1214.04	0	0	0	-1214.04
0	-734	0	0	-734
0	0	-1205	0	-1205

V*B(T)*(B*V*B(T))(INVERSE)

1.18E-10	-0.007088	-0.007539	0.0198666	0.006758
0	0.0020020	-0.000512	0.0223613	-0.00087
0	0.0003481	0.0022244	0.0271541	-0.00105
0.0000000	-0.109013	-0.108749	0.1015242	0.109206
0	0.0781576	0.0006059	-0.026462	0.001032
0	-0.000379	0.0496953	-0.029631	0.001156
-6.23E-11	0.0037478	0.0039860	-0.010503	-0.00357
0	-0.000836	0.0002138	-0.009340	0.000364
0	-0.000257	-0.001644	-0.020077	0.000783
-0.000000	0.2719148	0.2712559	-0.253234	-0.27239
0	-0.022110	-0.000171	0.0074860	-0.00029
0	0.0003724	-0.048720	0.0290504	-0.00113

V*B(T)*(B*V*B(T))(INVERSE)*B

0.0429118 0.1035009 0.0977549 0.0342644 -0.00376 -0.01129 -0.113438 -0.2017628 -0.21683595 -0.01020 0.001212 0.003764
0.0483004 0.1973435 0.1732646 -0.004423 0.012855 -0.02001 -0.127683 -0.3846980 -0.38432841 0.001317 -0.00414 0.006673
0.0586529 0.2227687 0.2329722 -0.005371 -0.00809 0.016846 -0.155050 -0.4342615 -0.51676952 0.001599 0.002610 -0.00561
0.2192924 -0.060660 -0.057292 0.5536787 0.002203 0.006619 -0.579703 0.11825006 0.127084164 -0.16490 -0.00071 -0.00220
-0.057159 0.4187289 -0.205043 0.0052344 0.901182 0.023691 0.1511018 -0.8162629 0.454819404 -0.00155 -0.29062 -0.00789
-0.064003 -0.243092 0.1591065 0.0058611 0.008832 0.735311 0.1691955 0.47387980 -0.35292364 -0.00174 -0.00284 -0.24510
-0.022687 -0.054721 -0.051683 -0.018115 0.001988 0.005971 0.0599752 0.10667277 0.114641970 0.005395 -0.00064 -0.00199
-0.020176 -0.082435 -0.072376 0.0018476 -0.00537 0.008362 0.0533363 0.16069793 0.160543537 -0.00055 0.001731 -0.00278
-0.043367 -0.164712 -0.172256 0.0039713 0.005984 -0.01245 0.1146419 0.32108707 0.382092307 -0.00118 -0.00192 0.004152
-0.546987 0.1513066 0.1429066 -1.381057 -0.00549 -0.01651 1.4459716 -0.2949546 -0.31698976 0.411320 0.001772 0.005503
0.0161698 -0.118454 0.0580049 -0.001480 -0.25493 -0.00670 -0.042745 0.23091335 -0.12866426 0.000441 0.082215 0.002234
0.0627489 0.2383257 -0.155986 -0.005746 -0.00865 -0.72089 -0.165878 -0.4645880 0.346003578 0.001711 0.002792 0.240297

UNADJUSTED GRADE	SIZE (um)	ADJUSTMENT	ADJUSTED GRADE	MASS(%)	UNITS			
41.965	+25 (PMD)	26.370	68.335	2.16	147.603	GOLD IN - GOLD OUT	(38/25 um)=	0.000
15.098	+15	5.932	21.030	8.10	170.345	GOLD IN - GOLD OUT	(25/15 um)=	0.000
27.696	-15	14.386	42.082	7.93	333.710	GOLD IN - GOLD OUT	(-15 um)=	0.000
326.11	+25 (SMD)	285.262	611.372	5.07	3099.654			
503.023	+15	-319.585	183.438	11.38	2087.527	GRADE	PMD (g/t)=	35.825
306.918	-15	-32.236	274.682	14.46	3971.904	GRADE	SMD (g/t)=	296.315
20.88	+25(PCOF)	-13.942	6.938	5.71	39.617	GRADE	PCOF (g/t)=	16.671
12.204	+15	-2.478	9.726	15.79	153.573	GRADE	PCUF (g/t)=	700.995
36.701	-15	-10.637	26.064	17.59	458.469			
2835.802	+25(PCUF)	-711.536	2124.266	1.51	3207.641		GOLD TO UNDERFLOW	
482.971	+15	90.408	573.379	3.67	2104.299	(um)		(%)
766.559	-15	31.604	798.163	4.82	3847.145	+25		98.78
						+15		93.20
						-15		89.35

Appendix C.7: Estimated recovery of sub-sieve ranges of the various streams

Stream		Concentrate			Tails				
		Weight (g)	Au (mg)	Total Au (mg)	Weight (g)	Au (mg)	Total Au (mg)	Grand T.Au (mg)	Au Reco. (%)
PMD 1,2	+25 um	0.19	0.3168	2.248	0.98	0.0365	9.744	11.992	18.75
	+15 um	0.44	0.1305	0.926	3.95	0.0286	7.635	8.561	10.82
	-15 um	0.30	1.2036	8.542	4.68	0.1067	28.484	37.025	23.07
	Total	0.93	1.6509	11.716	9.61	0.1718	45.862	57.578	20.35
PMD 3	+25 um	0.14	0.1315	0.664	1.02	0.0380	16.150	16.814	3.95
	+15 um	0.48	1.1432	5.773	5.01	0.0322	13.685	19.458	29.67
	-15 um	0.39	0.0719	0.363	3.63	0.0982	41.735	42.098	0.86
	Total	1.01	1.3466	6.800	9.66	0.1684	71.570	78.370	8.68
PCUF 1	+25 um	0.34	49.1036	130.529	0.16	0.4244	145.843	276.372	47.23
	+15 um	0.24	15.8029	42.008	0.50	0.0574	19.725	61.733	68.05
	-15 um	0.21	49.5161	131.625	0.31	0.1197	41.134	172.759	76.19
	Total	0.79	114.4226	304.161	0.97	0.6015	206.703	510.864	59.54
PCUF 2	+25 um	0.15	23.1594	87.394	0.43	0.2163	18.499	105.893	82.53
	+15 um	0.21	11.5241	43.487	1.28	0.1142	9.767	53.254	81.66
	-15 um	0.17	16.7335	63.145	1.40	0.3406	29.130	92.275	68.43
	Total	0.53	51.417	194.026	3.11	0.6711	57.395	251.422	77.17
SMD 1,3	+25 um	0.33	29.0565	132.588	1.60	0.2848	28.167	160.755	82.48
	+15 um	0.43	14.4569	65.968	4.55	0.3542	35.031	100.999	65.32
	-15 um	0.27	25.2791	115.351	3.55	0.2087	20.641	135.992	84.82
	Total	1.03	68.7925	313.908	9.7	0.8477	83.838	397.746	78.92
SMD 2	+25 um	0.09	0.0585	1.450	0.93	0.2919	18.526	19.976	7.26
	+15 um	0.07	4.1765	103.505	3.67	0.2290	14.534	118.038	87.69
	-15 um	0.07	2.1136	52.381	5.02	0.7238	45.937	98.318	53.28
	Total	0.23	6.3486	157.335	9.62	1.2447	78.997	236.332	66.57
PCOF	+25 um	0.18	0.1874	2.088	1.82	0.0295	7.100	9.188	22.73
	+15 um	0.45	0.1526	1.700	3.68	0.0381	9.170	10.870	15.64
	-15 um	0.42	1.1238	12.522	4.27	0.1054	25.368	37.890	33.05
	Total	1.05	1.4638	16.311	9.77	0.1730	41.638	57.949	28.15
SCUF 1	+25 um	0.20	4.2901	29.701	2.15	0.3103	20.902	50.603	58.69
	+15 um	0.50	6.4618	44.736	4.67	0.3688	24.843	69.578	64.30
	-15 um	0.34	17.5482	121.488	2.83	0.4722	31.808	153.295	79.25
	Total	1.04	28.3001	195.924	9.65	1.1513	77.553	273.477	71.64
TMD	+25 um	0.17	3.9603	104.055	1.41	0.1209	28.989	133.044	78.21
	+15 um	0.22	2.1018	55.224	4.63	0.2302	55.196	110.420	50.01
	-15 um	0.12	3.9127	102.804	3.76	0.3945	94.591	197.396	52.08
	Total	0.51	9.9748	262.083	9.8	0.7456	178.776	440.859	59.45

Appendix C.8: Results of calculation of the selection function of the gold and ore.

1) GOLD

TAU PLUG FLOW = 0.10 TAU SMALL = 0.10 TAU = 0.70

BREAKAGE FUNCTION

0.46
0.17 0.46
0.12 0.17 0.46
0.08 0.12 0.17 0.46
0.05 0.08 0.12 0.17 0.46
0.04 0.05 0.08 0.12 0.17 0.46
0.02 0.04 0.05 0.08 0.12 0.17 0.46
0.01 0.02 0.04 0.05 0.08 0.12 0.17 0.46
0.01 0.01 0.02 0.04 0.05 0.08 0.12 0.17 0.46

SIZE CLASS	FEED %	MEASURED PRODUCT (%)	CALCULATED PRODUCT (%)	SELECTION FUNCTION
1	1.18	0.29	O.29	1.9352
2	1.46	0.47	0.47	2.0764
3	2.71	1.24	1.24	1.4409
4	6.89	4.32	4.32	0.8014
5	14.63	11.23	11.23	0.4833
6	18.72	16.10	16.10	0.3810
7	20.67	20.48	20.48	0.2359
8	13.80	14.59	14.59	0.2558
9	11.65	12.80	12.80	0.2293
10	4.53	7.11	7.11	0.1427